INTEGRATION OF SIGMA IMPROVEMENT FOR PSHA AND SENSIBILITY STUDIES (INTERMEDIATE RESULTS)

AUTHORS			REVIEW			APPROVAL		
NOM	DATE	VISA	NOM	DATE	VISA	NOM	DATE	VISA
G. Ameri GEOTER			E. Faccioli			JM Thiry G. Senfaute		
			G. Woo					

***DISSEMINATION**: Authors; Steering Committee; Work Package leaders, Scientific Committee, Archiving.*

GEOTER SAS. Fugro Group
POLE GEO-ENVIRONNEMENT
3, rue Jean Monnet
34 830 Clapiers - France
Tel: + 33 (0)4 67 59 18 11
Fax: + 33 (0)4 67 59 18 24
Email: geoter@geoter.fr
Website: http://www.geoter.fr

SIGMA PROJECT (WP4)

Sensitivity analysis of the SIGMA PSHA model (intermediate results)

Document type:	**Identification:**
Final Report	Report GTR/ARE/0214-1150

Revisions

Ind.	Date	Modifications
0	20 October 2014	First emission of the final report
1	30 July 2015	Final emission of the report including comments from SIGMA reviewers and from the Client

Client:	Document type:	Identification:	
AREVA	**final REPORT**	GTR/ARE/0214-1150	
Recipient: **Jean-Michel THIRY**	*GEOTER archive (text and figures):* Serveur\affaire\2013\4013	*Date of origin:* 20/10/2014	*Number of pages:* 79 p.

REPORT TITLE:

SIGMA PROJECT (WP4)

Sensitivity analysis the SIGMA PSHA model (intermediate results)

Realization:

GEOTER

Pole Geo-environnement
3, rue Jean Monnet
34 830 Clapiers

Tel.: 04 67 59 18 11
Fax: 04 67 59 18 24
Email: geoter@geoter.fr
Website: www.geoter.fr

Command: n° FC01/1013055023 dated 26 July 2013

Client approval:
Monsieur Jean-Michel THIRY
AREVA
69456 LYON Cedex 06
Email : jeanmichel.thiry@areva.com
Tel : +33 4 72 74 87 84

Date	Written by	Reviewed by	Approved by
30 July 2015	G. AMERI C. GOMES	R. SECANELL	Ch. MARTIN
Visas			

Executive Summary

Within the framework of the WP4 of the SIGMA Project a PSHA model has been developed in 2012 (SIGMA-2012-D4-24) for the France southeastern ¼. The 2012 model aimed to represent a state-of-the-art PSHA at the beginning of the SIGMA project and was intended to define a reference point in order to evaluate the improvements, in various aspects of SHA, achieved through the course of the Project.

The 2012 PSHA model for the France southeastern ¼ has been proposed by the technical integration team, composed by engineers and scientists from GEOTER. Two intermediate reports were also produced during the task WP4-1:

- The models and parameters proposed for building a preliminary "classical" hazard map for France's southeast ¼ were detailed in the SIGMA report SIGMA-2011-D4-08 and discussed during the first scientific committee (Ref: SIGMA-2011-CR11) ;
- Refinements of the model were discussed in the SIGMA report SIGMA-2011-D4-18, to consider the action items and recommendations issued by the SIGMA scientific committee.

At the beginning of 2013, a Working Group of Integration (WGI) was formed to propose concrete actions to improve the integration of results across all the SIGMA WPs. During the March 8, 2013 meeting the WGI recommended to perform a detailed and carefully constructed sensitivity analysis in order to identify the PSHA input parameters that contribute the most to the uncertainty in hazard estimation.

In this context, we performed a sensitivity analysis of the SIGMA PSHA model in order to investigate the origins of uncertainties and to better guide the improvement of this model in the course of the Project. The conceived sensitivity analysis has three main objectives:

1. to measure the sensitivity of the seismic hazard to the different parameters/inputs (i.e., which one affects most the results);
2. to evaluate the contribution of the uncertainties in the input parameters to the total hazard uncertainties;
3. to quantify the reduction of uncertainties before and after SIGMA project (long term objective).

The objective 3) will be accomplished when all contributions from the other WPs will be available. In particular, the SIGMA earthquake catalogue, which is expected to be a major source of improvement, is not available and its impact of the SIGMA PSHA model cannot be assessed in the present report.

The sensitivity analysis is performed for three different sites in the French area of interest, characterized by different levels of seismicity and/or location at boundaries of seismic sources. According to the scope of work the sensitivity analysis will only focus on the French area of interest and the Italian area of interest (Po Plain) will be out of concern.

It appears useful to remind that in probabilistic seismic hazard analysis it is common practice to distinguish and separately process uncertainties of two different types: aleatory and epistemic.

Aleatory uncertainties reflect the random nature of the earthquake process and associated ground motions. Examples include the location, size and time of future earthquakes as well as the standard deviation of the GMPEs. Aleatory uncertainty generally does not depend on the amount of available information, although the increasing knowledge and acquisition of additional data can lead to a refinement of the aleatory uncertainty. Aleatory uncertainties are directly included in the hazard integral.

Epistemic uncertainties reflect the lack of knowledge on the earthquake process. Examples include the seismotectonic model (location and size of seismic zones), the Mmax, the earthquake catalogue (magnitude and locations), the GMPEs to be used. Epistemic uncertainties are incorporated into the seismic hazard using logic trees (leading to alternative hazard curves). Depending on the available information, epistemic uncertainty can be reduced by collecting data and hence it can evolve through time.

The proposed sensitivity analysis will apply mainly to epistemic uncertainties. Aleatory uncertainties will be considered in terms of distributions of focal depths within the seismogenic layer of a source zone as well as in terms of standard deviation of the GMPEs.

The present report illustrates the results of the sensitivity analysis and it discusses the following points:

- Definition of the metrics that are used to quantify the uncertainties and to express the sensitivity of the hazard to the considered parameters;
- Exploitation of the results of the 2012 SIGMA PSHA model (SIGMA Deliverable D4-24). Discussion on the considered uncertainties in terms of seismotectonic model, synthetic earthquake catalogue and GMPEs, and on their impact on the mean hazard and contribution to the hazard uncertainties;
- Deaggregation of seismic hazard in order to identify the sources that mostly contribute to the hazard at different return periods and for different sites;
- Sensitivity to an alternative instrumental catalogue (Si-Hex);
- Sensitivity to alternative models to define magnitude-frequency distributions (MFDs) and their uncertainties;
- Sensitivity to alternative models to define maximum magnitude distributions;
- Sensitivity to alternative aleatory distributions of earthquake focal depths;
- Consideration of recently developed GMPEs in the PSHA model and test of their impact on the mean hazard uncertainties;
- Sensitivity to the single station-sigma approach;
- Consideration of the smoothed-seismicity approach (Woo, 1996) for hazard calculation.

The results of the sensitivity analysis on the 2012 PSHA model show that:

- The uncertainties in the estimation of GR parameters are a major contribution to the uncertainties in the final hazard;
- The mean hazard is controlled by the choice of the GMPE and of the seismotectonic model.

The results on the alternative hypotheses considered for several elements of the SIGMA PSHA model show that:

- Alternative hypotheses on depth aleatory distribution and on the instrumental earthquake catalogue have minor impact on the hazard;
- Alternative hypotheses on the Mmax distribution, on the set of considered GMPEs and on the use of areal source zones (smoothed seismicity approach) have a moderate-to-major impact on the hazard.

Beside the main report, a number of analyses and results are reported in the following Annexes:

- Annex 1: deaggregation by source for the three sites at three spectral periods (PGA, PSA at T=0.2s and PSA at T=1s) considering three seismotectonic models.
- Annex 2: comparison between the SIGMA 2012 earthquake catalogue and Si-Hex catalogue.
- Annex 3: analysis of earthquake depths distribution in Si-Hex catalogue.
- Annex 4: application of the EPRI (1994) Bayesian technique for the determination of Mmax to European stable continental regions.
- Annex 5: application of the smoothed-seismicity approach.
- Annex 6: hazard curves at the three sites obtained considering alternative GMPEs.

TABLE OF CONTENTS

TABLE OF ILLUSTRATIONS

1. METHODOLOGY USED FOR THE SENSITIVITY ANALYSIS

Three sites are selected for the sensitivity analysis (Figure 1). The aim was to selected sites in different tectonic contexts and with different seismic activity rates. The three sites are:

- **Grenoble**, located in an active zone;
- **Valence**, located near a limit of active zone;
- **Marseille**, located in a low seismicity zone.

The ground motion is calculated at a **reference rock site condition characterized by a Vs30=800 m/s**.

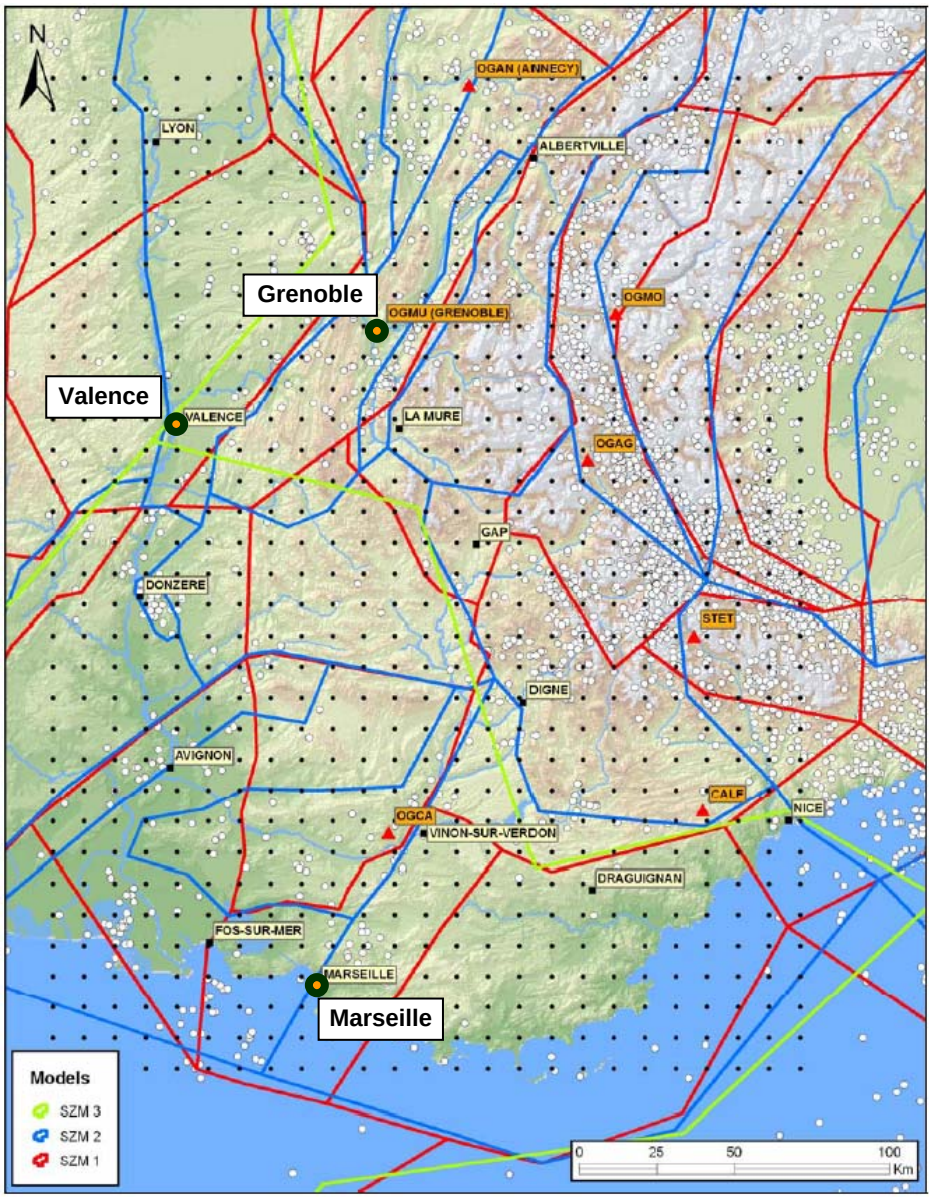

Figure 1 : Location of the three selected sites in the three seismotectonic zonations.

1.1 METRICS

The uncertainties in the seismic hazard and the sensitivity of the hazard to the different parameters of the model will be measured using two metrics:

- **distance between percentiles hazard curves (e.g., 16-84 %):** this can be the case, for instance, for the final hazard from the total logic tree, but also for hazard from a single seismotectonic model considering uncertainties in all the other parameters (e.g., GMPEs, Mmax). An example of this distance for 10,000 yrs return period is presented in Figure 2a;
- **distance between mean hazard curves:** this can be the case, for instance, for the mean hazard curves obtained for different GMPEs. For each GMPE, the mean hazard curve over the other model parameters (e.g., seismotectonic model, Mmax) is calculated. An example of this distance for 10,000 yrs return period is presented in Figure 2b.

The sensitivity analysis is conducted for 3 return periods (475 yrs, 10,000 yrs and 100,000 yrs) in order to investigate the variation of hazard uncertainties as a function of the return period. This is done because typically the parameters that contribute to the hazard uncertainties are not the same for short and long return periods. Note that results for the three return periods will not be showed for all the tests, if judged not useful.

In terms of spectral frequencies, the sensitivity analysis will be performed as a minimum for 3 spectral periods (PGA, 0.2 s, 1 s) in order to assess the variation of uncertainties as a function of frequency. Several figures contain more frequencies for graphical reasons.

As graphical representation of the two metrics, we used Tornado diagrams (Figure 2c) that allow to represent in the same figure several metrics and to compare the uncertainties in the different model parameters. The Tornado diagram is constructed by fixing the return period of interest (e.g., 10,000 years) and finding in the hazard curves the mean acceleration corresponding to that return period. Then, the median and percentiles Annual Frequency of Exceedance (AFE) that acceleration value are selected and reported in the Tornado plot (Figure 2). The same approach is followed for the two distance metrics.

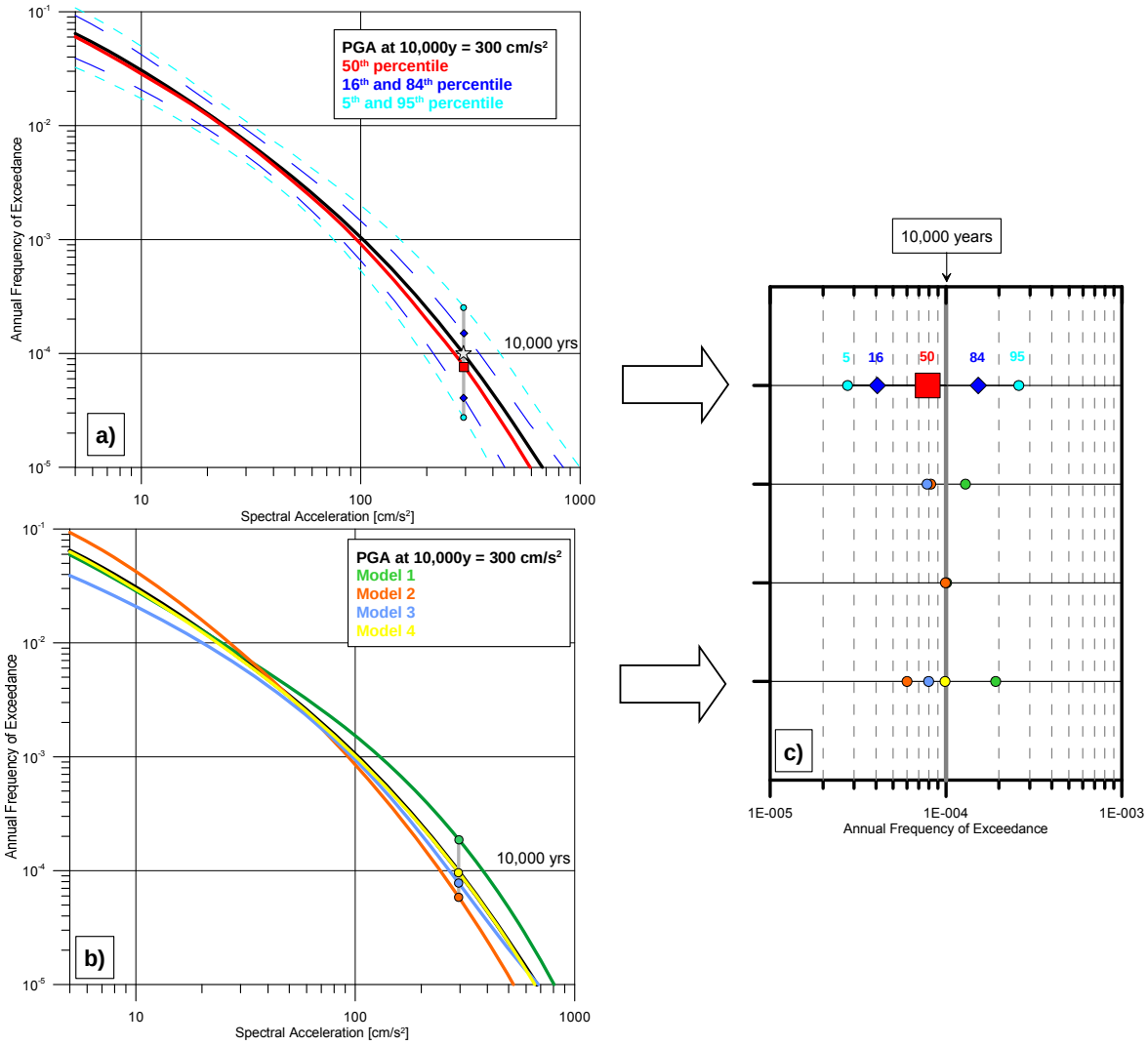

Figure 2: Example illustration of the development of a tornado diagram. a) hazard curves in terms of mean and 5th, 16th, 50th, 84th and 95th percentiles (total hazard for the logic tree). b) mean hazard curves for different models (e.g., different GMPEs). c) Tornado diagram for mean PGA with 10,000 yrs return period.

2. EXPLOITATION OF THE 2012 SIGMA PSHA MODEL

In this section, a sensitivity analysis of the 2012 SIGMA PSHA model is performed in order to assess the influence of the considered model parameters. We refer to the SIGMA Deliverable D4-24 for details of the 2012 model. We first recall the logic tree used in the preliminary PSHA (Figure 3). The logic tree is composed as follows:

- 3 seismotectonic models based on areal sources:
  - Areal sources based on a previous GEOTER model;
  - Model based on the identification of fault systems (Belledone Fault, Nîme fault, Provence faults system and the specific cluster of Tricastin);
  - Areal sources based on a previous IRSN model;
- 2 catalogues of seismicity with associated completeness periods :

- SIGMA 2012 catalogue (homogenized in Mw using the original instrumental catalog and macroseismic database available for France);
- A synthetic catalogue that considers variability on the estimation of earthquake magnitude and location (one single realization);

- 4 ground motion prediction equations :
  - Akkar and Bommer (2010), AB10;
  - Berge-Thierry et al. (2003), BT03;
  - Boore and Atkinson (2008, 2011), BA08;
  - Zhao et al. (2006), Zhao06;
- 100 combinations of maximum magnitude and recurrence parameters for each seismic source of 1 model.

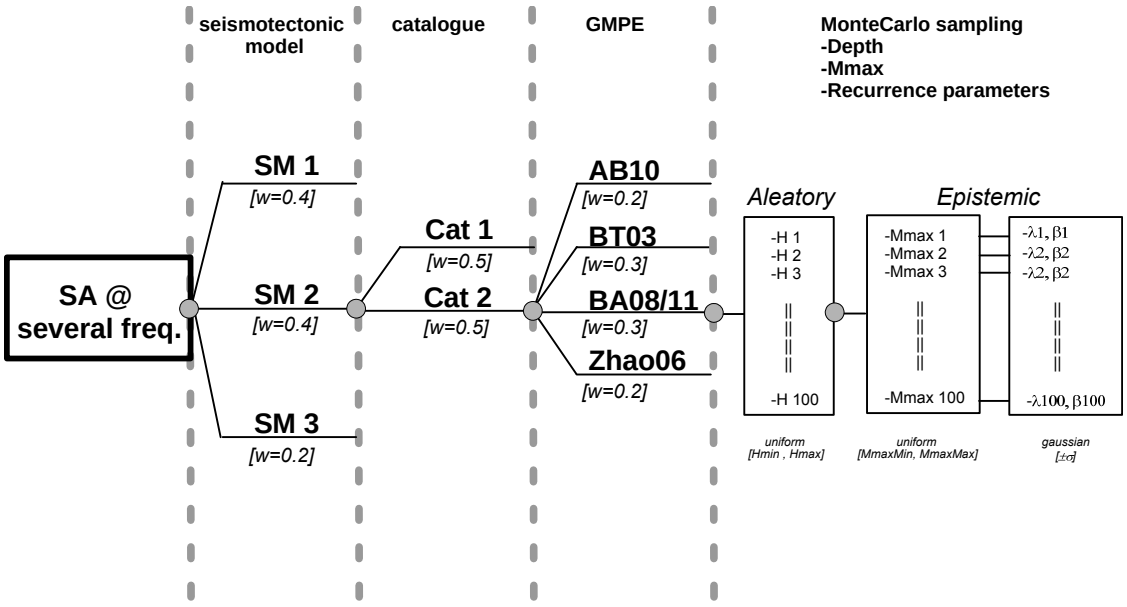

Figure 3 : Schematic logic tree used in the initial SIGMA PSHA model.

2.1 UNCERTAINTIES IN TOTAL HAZARD

As a first step, we recall in Figure 4 the hazard curves obtained in the 2012 PSHA study for the three sites. The mean and percentiles hazard curves are reported for the three spectral periods selected for the sensitivity analysis. Focusing on the uncertainties, the tornado diagrams in Figure 5 and Figure 6 compare the total seismic hazard uncertainties at the three sites at different spectral periods for return periods of 475 years and 10,000 years, respectively. The tornado diagrams represent the distance between percentiles in terms of AFE.

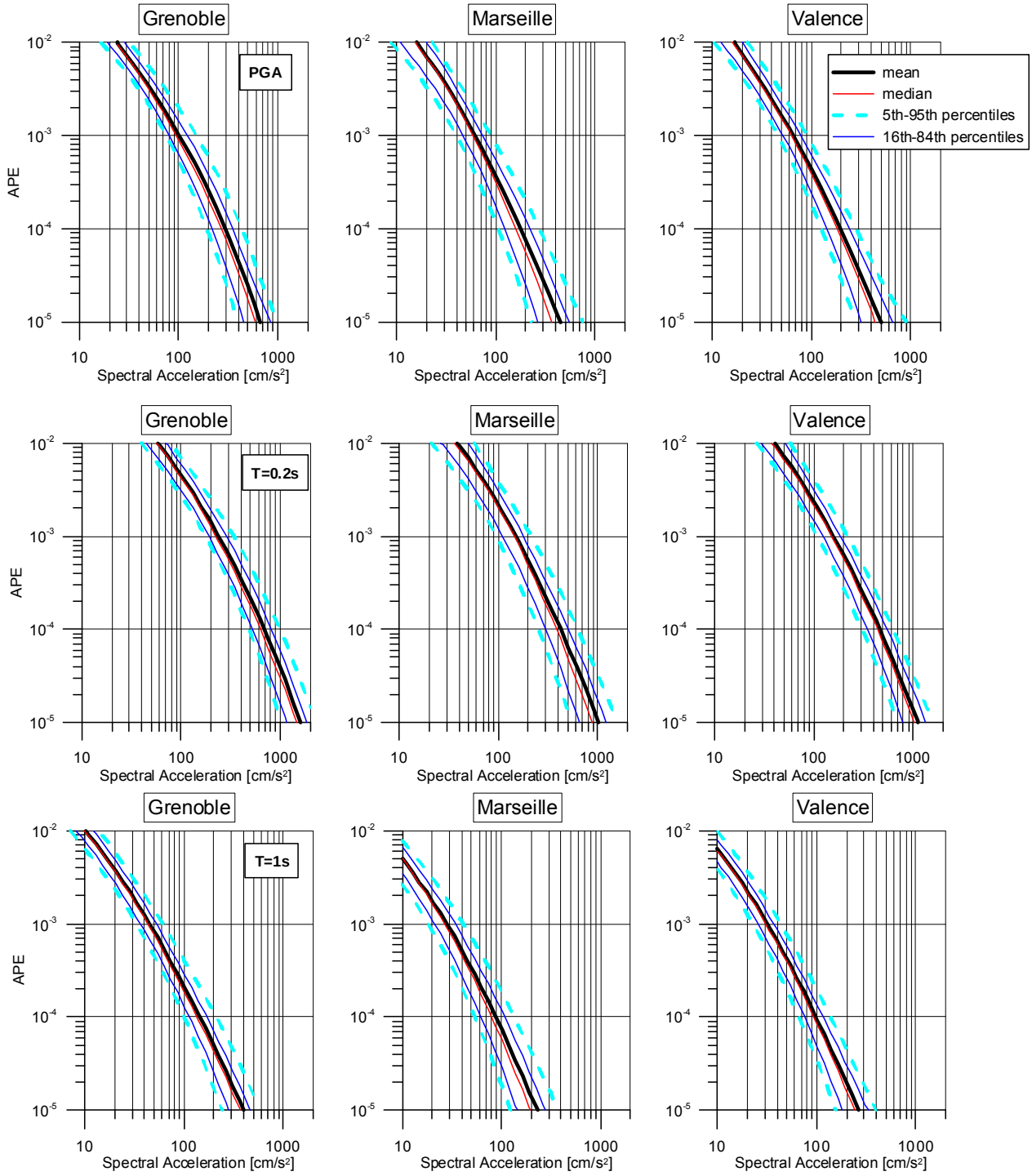

Figure 4 : Hazard curves calculate using the 2012 PSHA model at the three sites and considering three spectral periods.

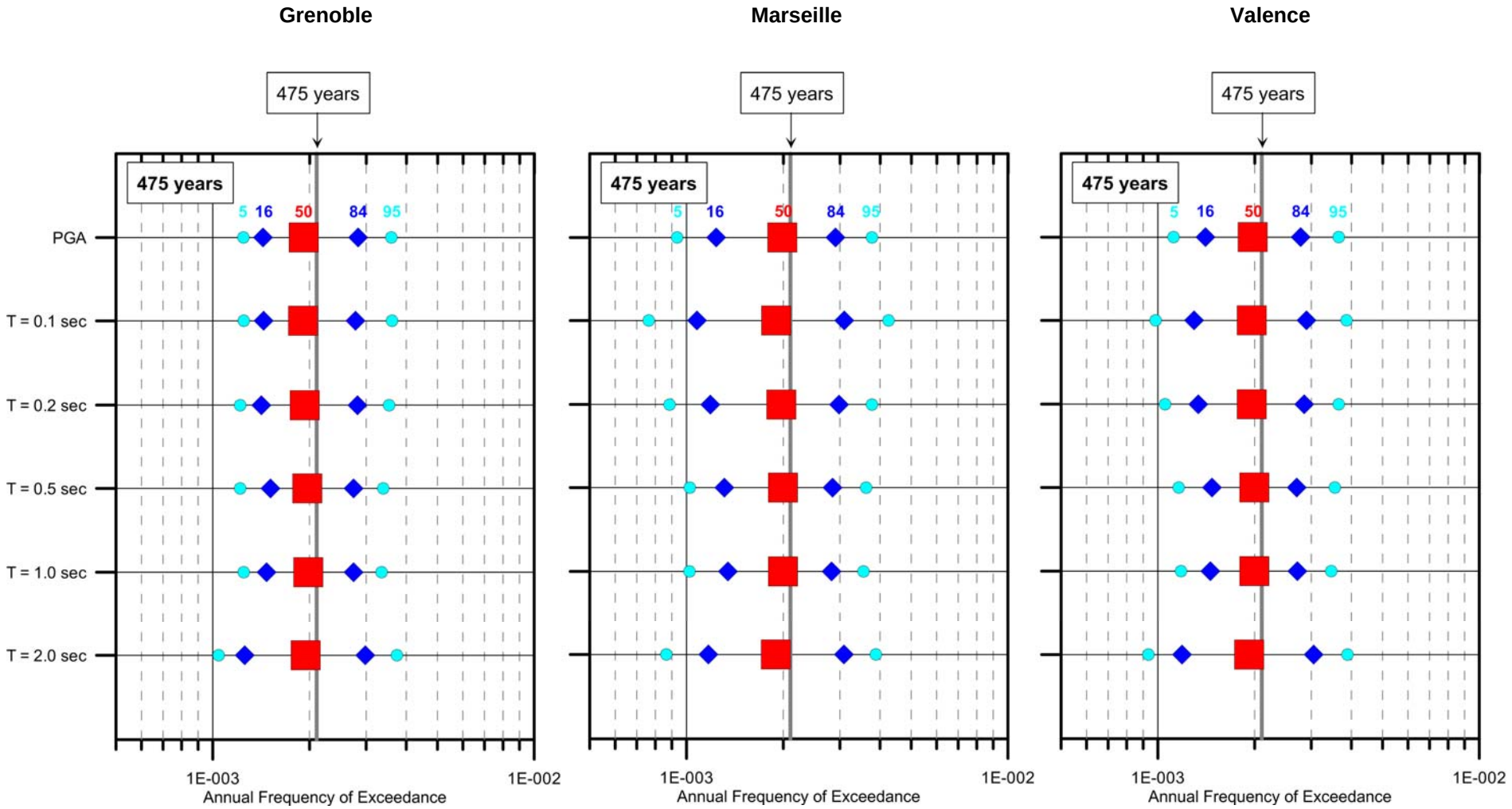

Figure 5 : Tornado diagrams at 475 years return period for the three sites showing the uncertainties in the total hazard for several spectral periods.

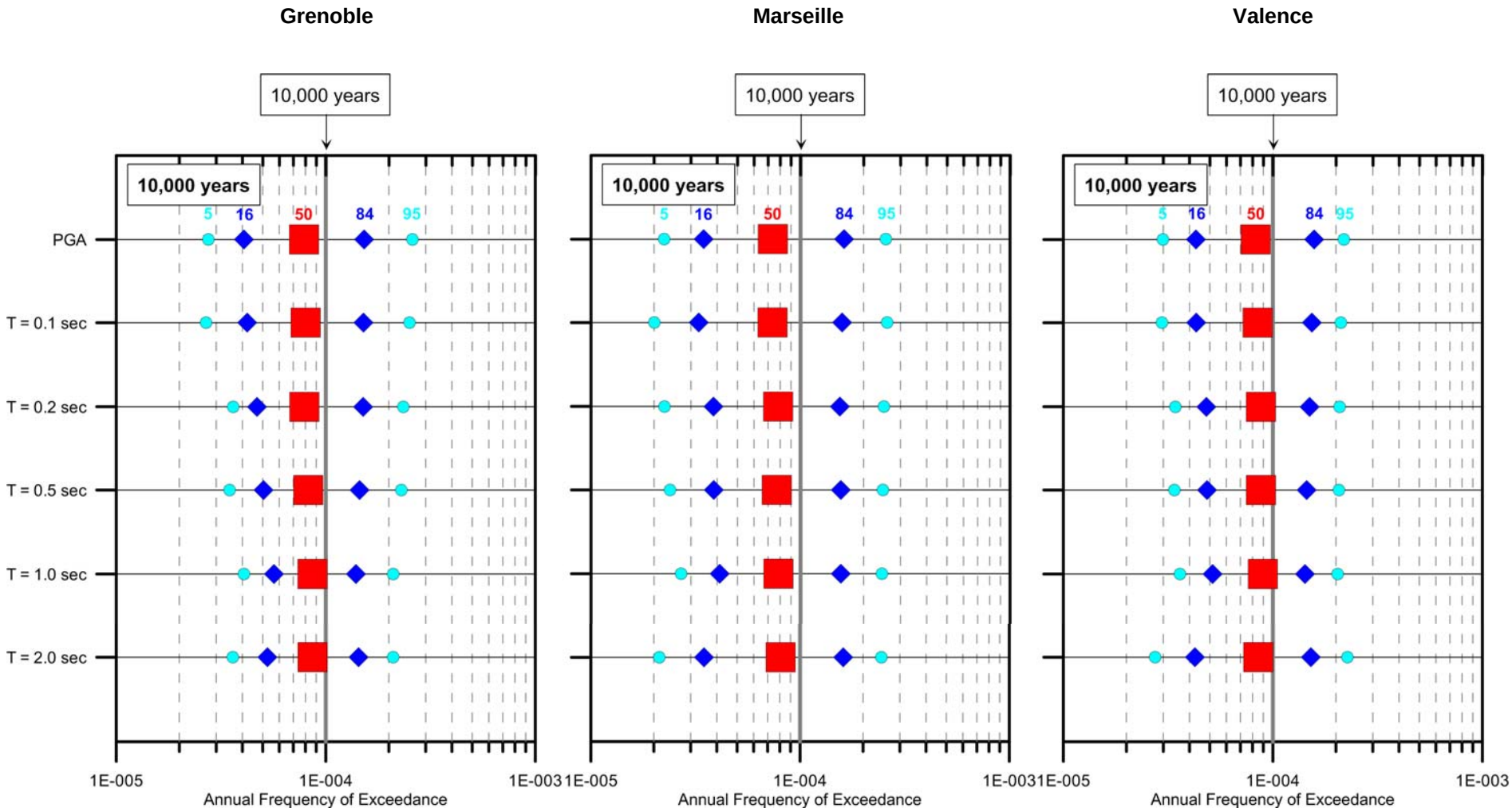

Figure 6 : Tornado diagrams at 10,000 years return period for the three sites showing the uncertainties in the total hazard for several spectral periods.

The comparison between uncertainties (distance between 84th and 16th percentiles) in total hazard at 475, 10,000 and 100,000 years return periods for the three sites as a function of spectral period is presented in Figure 7. This figure shows essentially the same as the Tornado diagrams presented in Figure 5 and Figure 6, but allows a better comparison between the return periods.

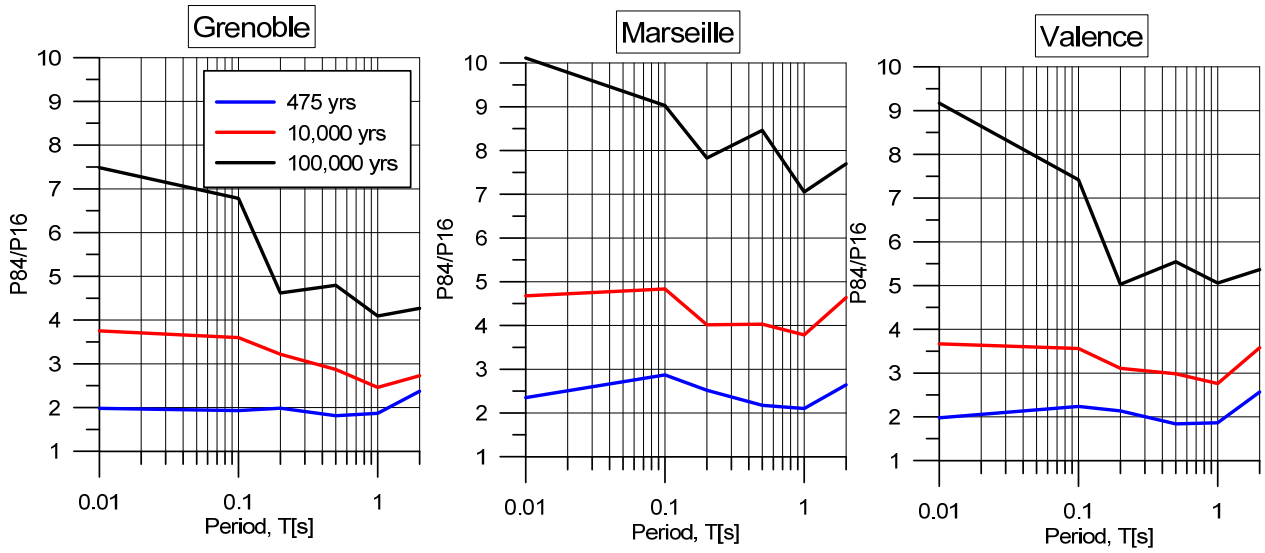

Figure 7 : Ratio between the 84th and 16th percentile hazard curves at 475y (blue), 10,000y (red) and 100,000y (black) return periods as a function of spectral period for the three sites.

The results show that:

- The uncertainties in the total hazard increase with increasing return period. This is expected because the uncertainties in the Mmax for each zone do not affected significantly the hazard at short return periods. Moreover, uncertainties in the activity rates increase with increasing magnitude and thus affect more the long return periods than the short ones;
- The uncertainties in the total hazard for the Grenoble and Valence sites are comparable, whereas they are larger for Marseille. This is related to the fact that Marseille is located in a low seismicity zone, where the data to constrain the Gutenberg-Richter (G-R) model are scarce. As a consequence, the uncertainties in the G-R are significant and cause a larger uncertainty in the final hazard when compared to the other two sites.

2.2 GMPEs EXPLORATION

The uncertainties related to the GMPEs used in the PSHA are investigated in this section. The hazard curves for each GMPEs, exploring all the other branches of the logic tree, are selected. Then the mean and percentiles are calculated for each GMPE and for the 3 selected spectral periods and are reported in the tornado diagrams. The results for the three sites and for 475 and 10,000 years return periods are presented in Figure 8 and Figure 9, respectively. The uncertainties within each GMPE for different spectral periods are also compared to the uncertainties in the total hazard (i.e., the hazard from the whole logic tree).

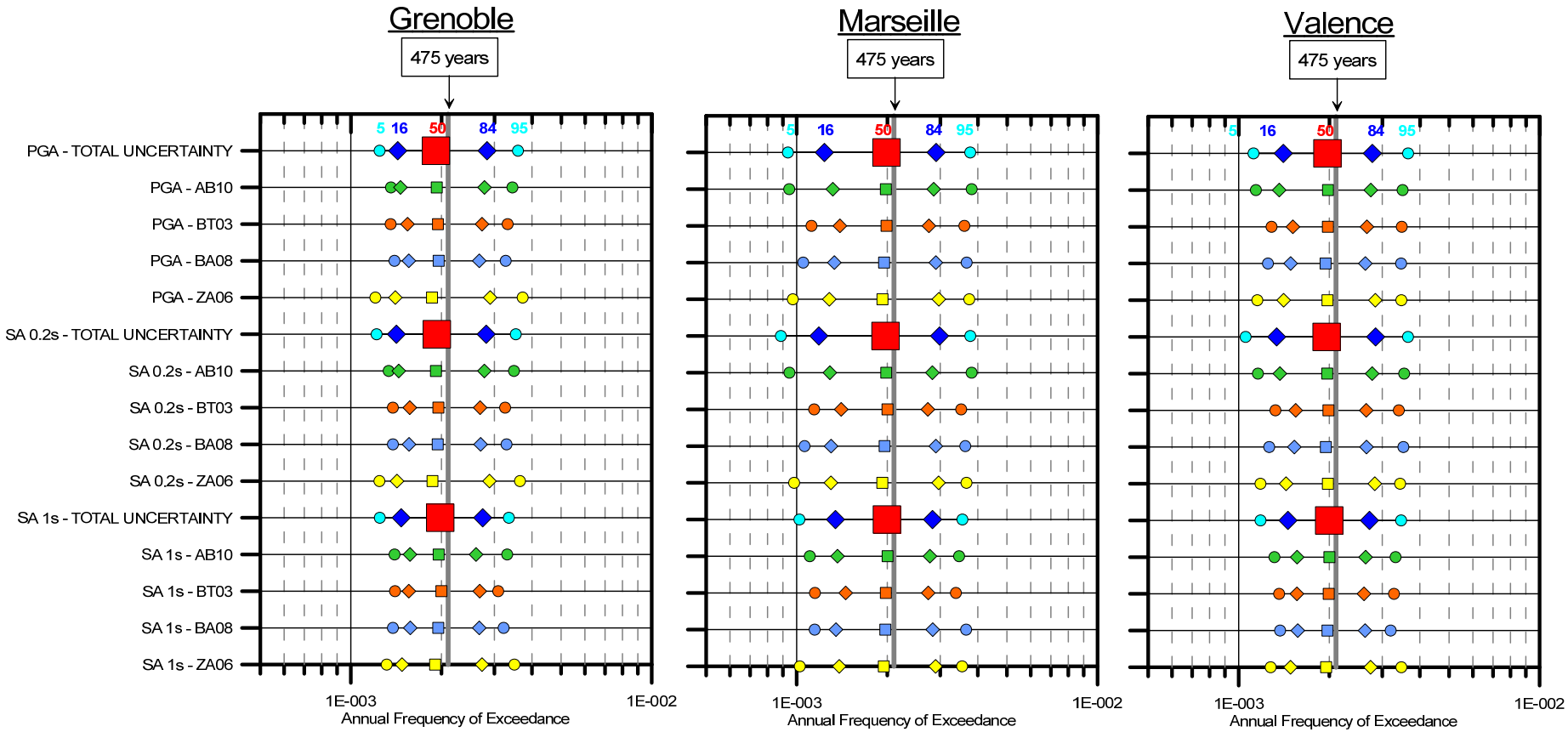

Figure 8 : Tornado diagrams at 475 years return period for the three sites showing the within GMPE uncertainties for the four considered GMPEs and three spectral periods (PGA, 0.2s and 1s).

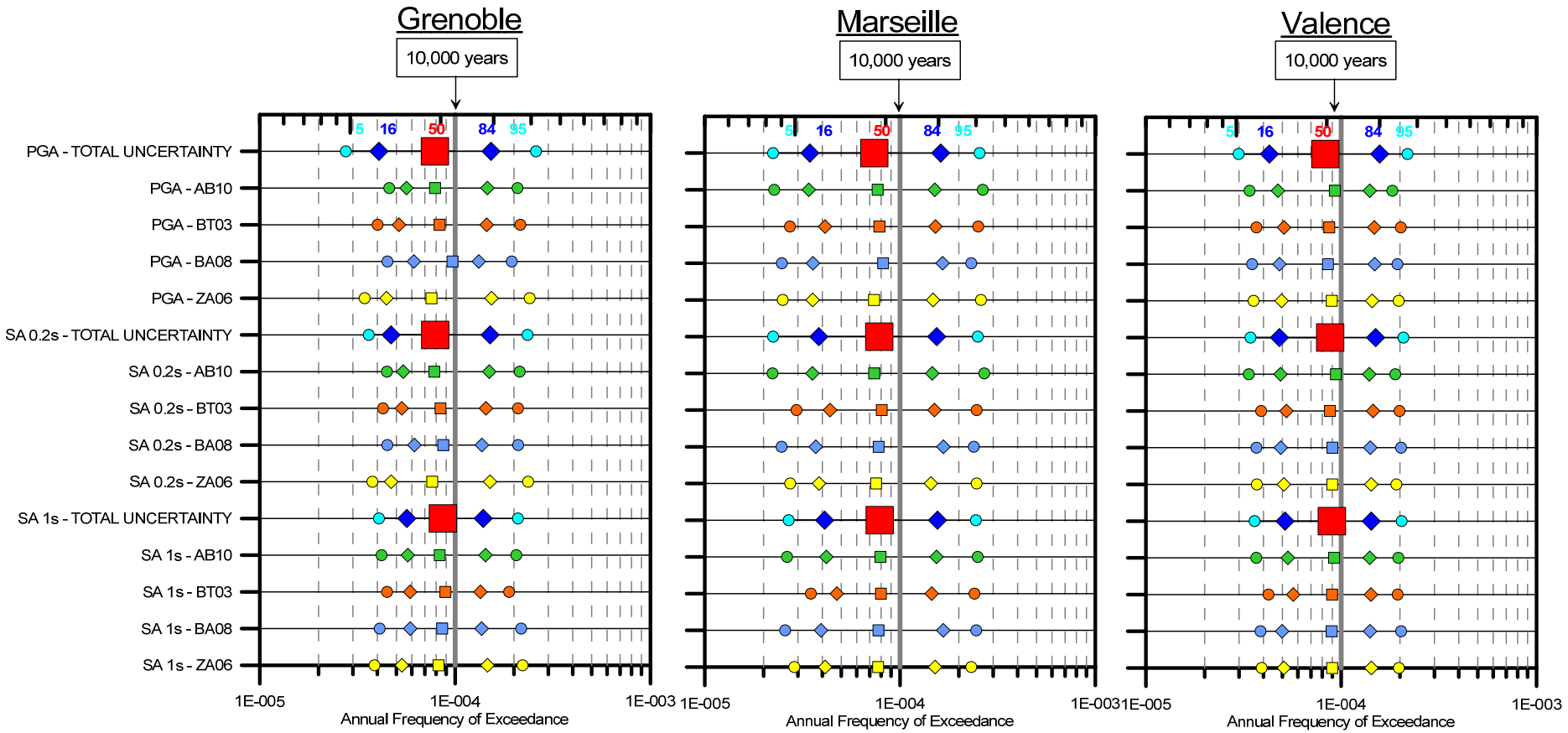

Figure 9 : Tornado diagrams at 10,000 years return period for the three sites showing the within GMPE uncertainties for the four considered GMPEs and three spectral periods (PGA, 0.2s and 1s).

The main results can be summarized as follows:

- The uncertainty within GMPE is slightly higher in ZA06 and AB10, lowest in BA08 but fairly consistent over all models. This mean that all the selected GMPEs produce the about same uncertainties and that the contribution of each GMPE to the total hazard uncertainties is almost the same;
- The uncertainties in the total hazard (i.e., the percentiles distribution) are very similar among the 4 GMPEs. In other words, the uncertainties in the total hazard would not be significantly different using one single GMPE instead of four models, even if the mean hazard is different when using each individual GMPE.

2.3 SEISMOTECTONIC MODEL EXPLORATION

The uncertainties related to the seismotectonic models used in the PSHA are investigated in this section. The hazard curves for each seismotectonic model, exploring all the other branches of the logic tree, are selected. Then, the mean and percentiles are calculated for each seismotectonic model and for the 3 selected spectral periods and are reported in the tornado diagrams. The results for the three sites and for 475, 10,000 and 100,000 years return periods are presented in Figure 10, Figure 11 and Figure 12, respectively. The uncertainties within each seismotectonic model for different spectral periods are also compared to the uncertainties in the total hazard.

The uncertainties within each seismotectonic model are clearly different for the three zonations. In particular:

- The uncertainties within seismotectonic model is generally highest for SM1 and lowest for SM3. The smaller uncertainties of SM3 compared to the other seismotectonic models are mostly related to the fact that, because SM3 uses very large seismic zones, the sample of seismicity within each zone is quite large and, as the consequence, the uncertainties in the G-R parameters are smaller (see next section).
- The result illustrated in the previous point is consistent over the 3 sites, spectral periods and return periods. The only exception is for Marseille at 475 y where SM2 provides uncertainties larger than SM1.

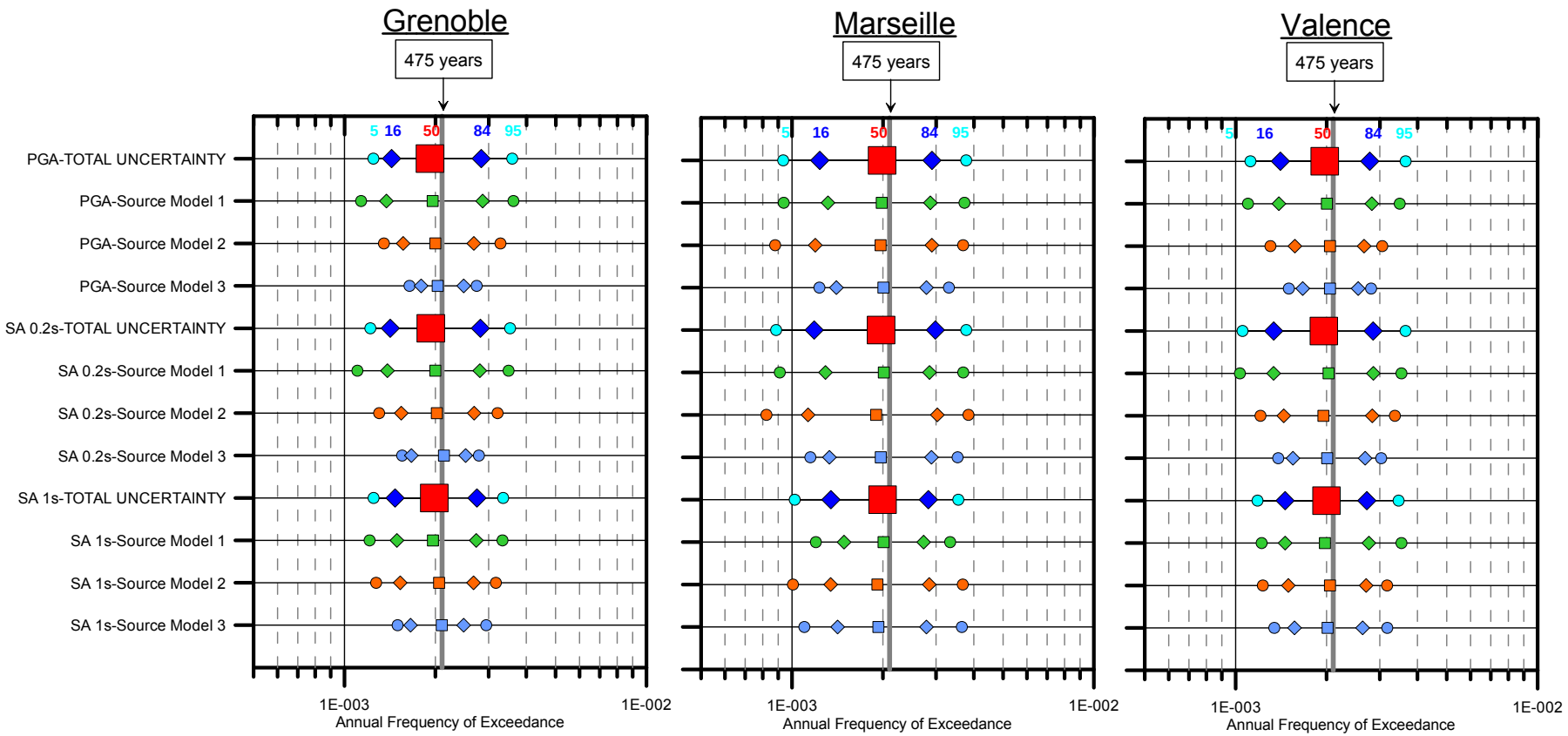

Figure 10 : Tornado diagrams at 475 years return period for the three sites showing the within Seismotectonic Model uncertainties for the three considered models (SM1, SM2 and SM3) and three spectral periods (PGA, 0.2s and 1s).

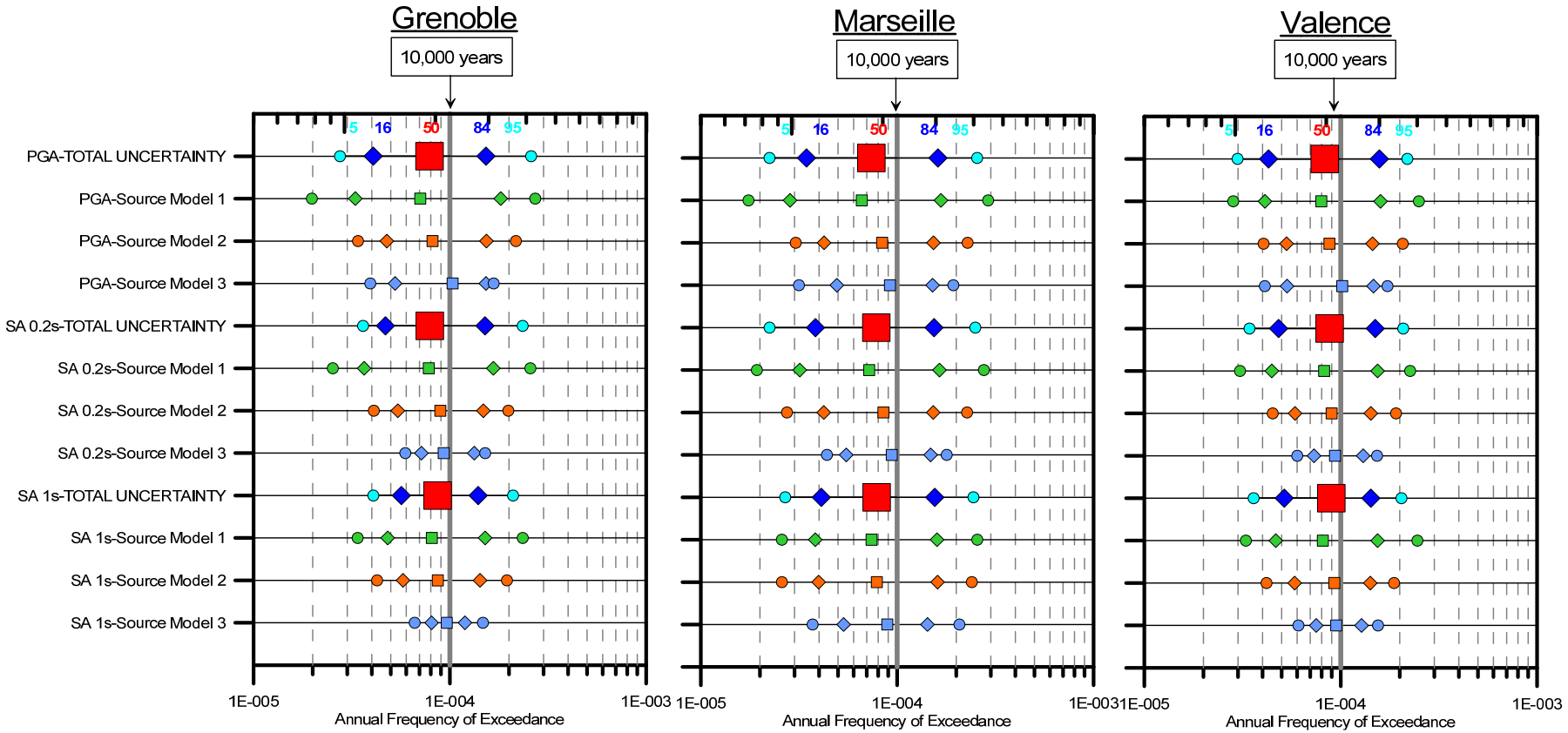

Figure 11 : Tornado diagrams at 10,000 years return period for the three sites showing the within Seismotectonic Model uncertainties for the three considered models (SM1, SM2 and SM3) and three spectral periods (PGA, 0.2s and 1s).

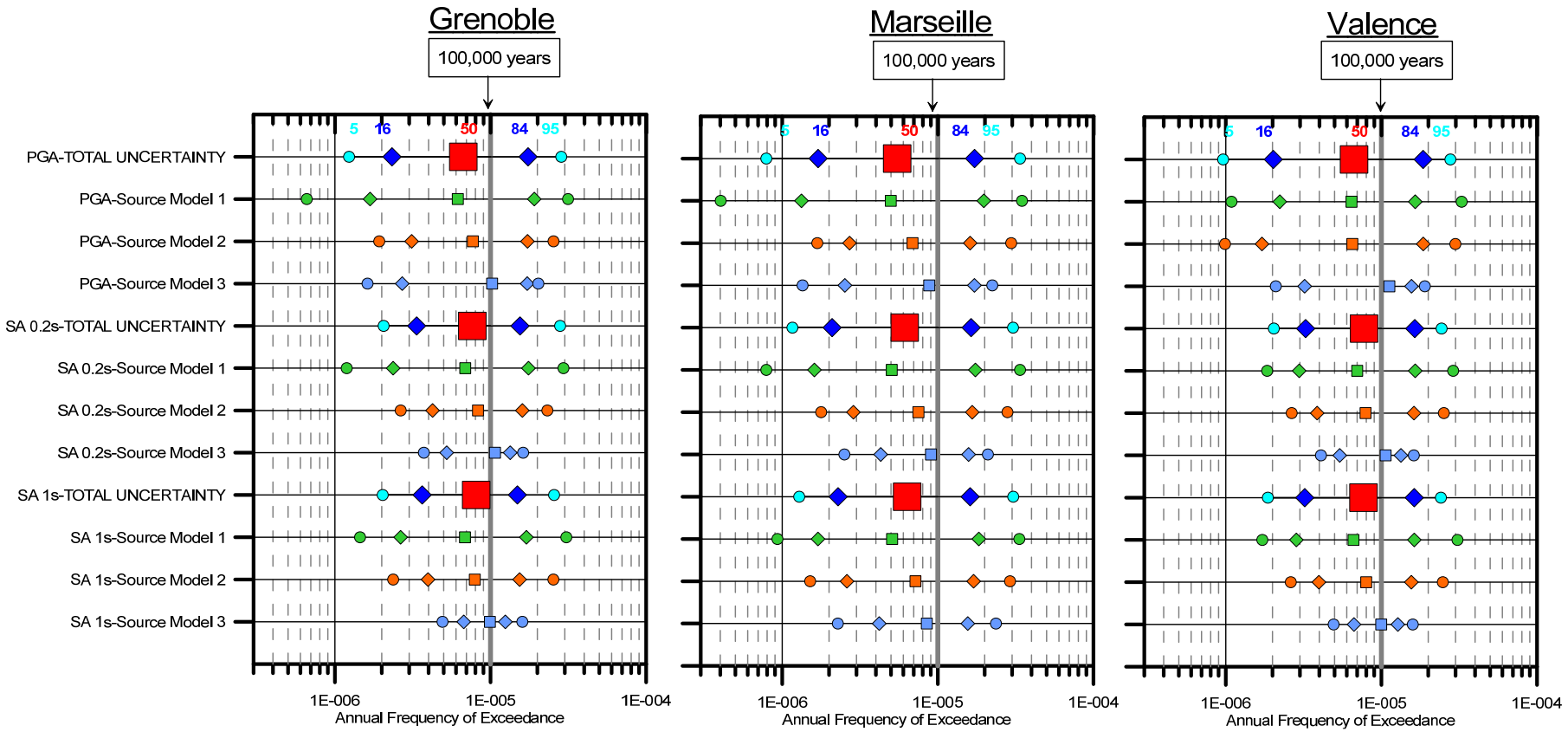

Figure 12 : Tornado diagrams at 100,000 years return period for the three sites showing the within Seismotectonic Model uncertainties for the three considered models (SM1, SM2 and SM3) and three spectral periods (PGA, 0.2s and 1s).

2.3.1 Breakdown of source model uncertainties

In order to further investigate the reason of the different uncertainties generated using the 3 seismotectonic models, we separate the contribution of uncertainties related the considered distribution of Mmax and those related to the lambda and beta parameters of the G-R relations.

To this aim, we calculate the hazard at the three sites for each seismotectonic model and one single GMPE (we used the BA08 in this test), considering the following cases:

- For each seismic source, we fixed the Mmax to its mean value and we considered only the variations of the 100 values of λ, β using the Monte-Carlo random sampling process.
- For each seismic source, we fixed λ, β to the mean values and we considered only the variations of the 100 values of Mmax using the Monte-Carlo random sampling process.

Then, for the two cases, the mean and percentiles are calculated, for each seismotectonic model for 2 selected spectral periods (PGA and 1 s). Finally, they are reported in the tornado diagrams for 10,000 years return period (Figure 13). In Figure 13, the total uncertainties of the logic tree are compared with uncertainties using one single seismotectonic model, with uncertainties only considering Mmax variations and with uncertainties only considering Lambda and Beta variations. This is repeated for the 3 seismotectonic models and 2 spectral periods. The analysis of the uncertainties presented in these figures shows that:

- The largest contribution to the uncertainties comes from the uncertainties in the activity rates parameters Lambda and Beta. The uncertainties related to the Mmax show a much smaller contribution.
- As supposed in the previous section, the uncertainties are smaller in SM3 because of the smaller uncertainties in the activity rates (due to the use of large zones). The uncertainties on the Mmax are also smaller but much more comparable to those of other seismotectonic models.

Figure 13 reports the results for 10,000 yrs return periods but we expect that the same conclusions hold for 475 and 100,000 years return periods.

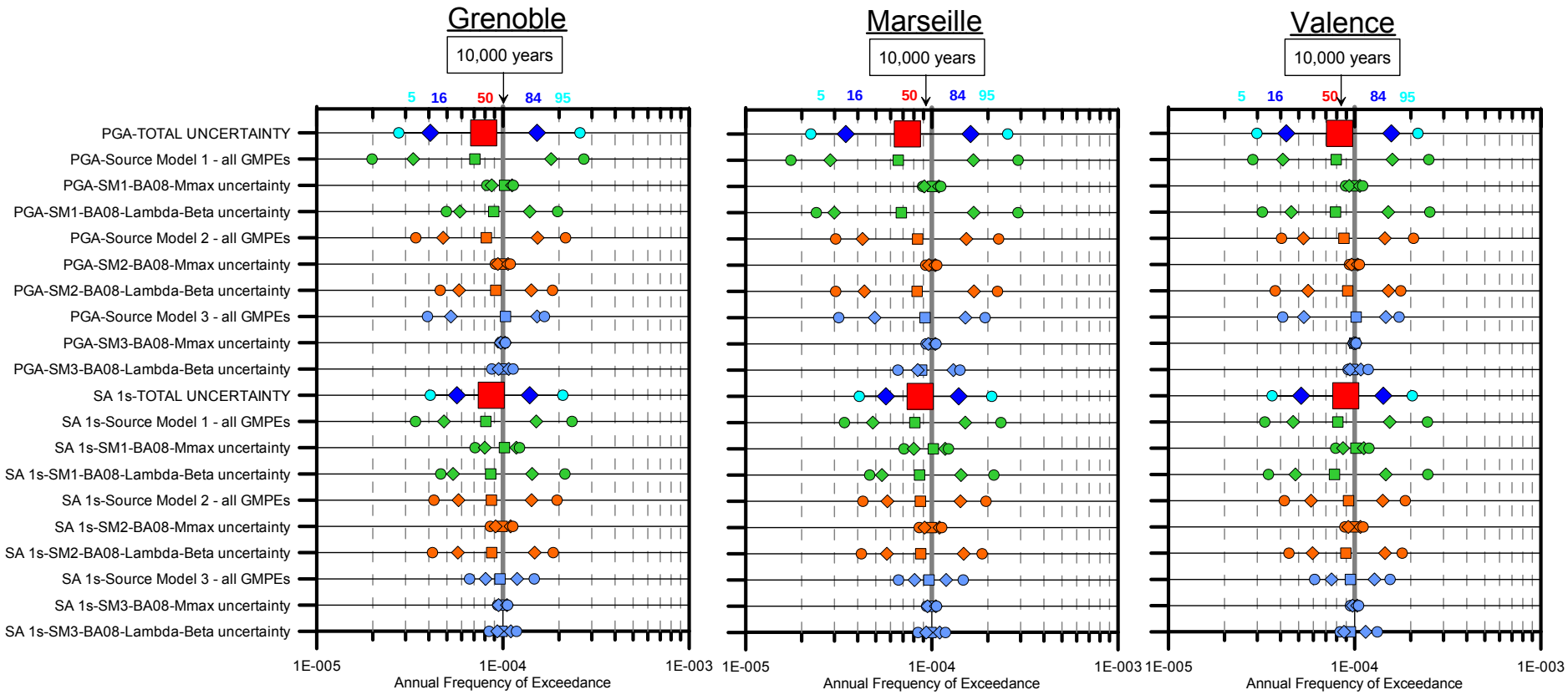

Figure 13 : Tornado diagrams at 10,000 years return period for the three sites showing, for each Seismotectonic Model (SM1, SM2 and SM3), the uncertainties due to Mmax and activity rates parameters. The results are for two spectral periods (PGA and 1s).

2.4 SYNTHETIC SEISMIC CATALOGUE EXPLORATION

In the 2012 PSHA an alternative synthetic catalogue was considered in order to assess the uncertainties related to the SIGMA catalogue. The synthetic catalogue was built by assigning to each earthquake in the catalogue an alternative magnitude and location based on one single random sampling of the original catalogue and related uncertainties (see SIGMA-2012-D4-24 for details). The uncertainties related to the earthquake catalogues used in the 2012 PSHA are investigated in this section. The hazard curves for each catalogue, exploring all the other branches of the logic tree, are selected. Then, the mean and percentiles are calculated for each catalogue and for PGA (the results are the same for the other spectral periods) and are reported in the tornado diagrams. The results for the three sites and for 475 and 10,000 years return periods are presented in Figure 14 and Figure 15, respectively. The uncertainties within each catalogue are also compared to the uncertainties in the total hazard.

The within seismic catalogue uncertainty in roughly the same for the two catalogues. This holds for both 475 and 10,000 years return periods. As already observed for GMPEs, the uncertainties obtained using one seismic catalogue are of the same order of the uncertainties of the whole logic tree (i.e., using two catalogues).

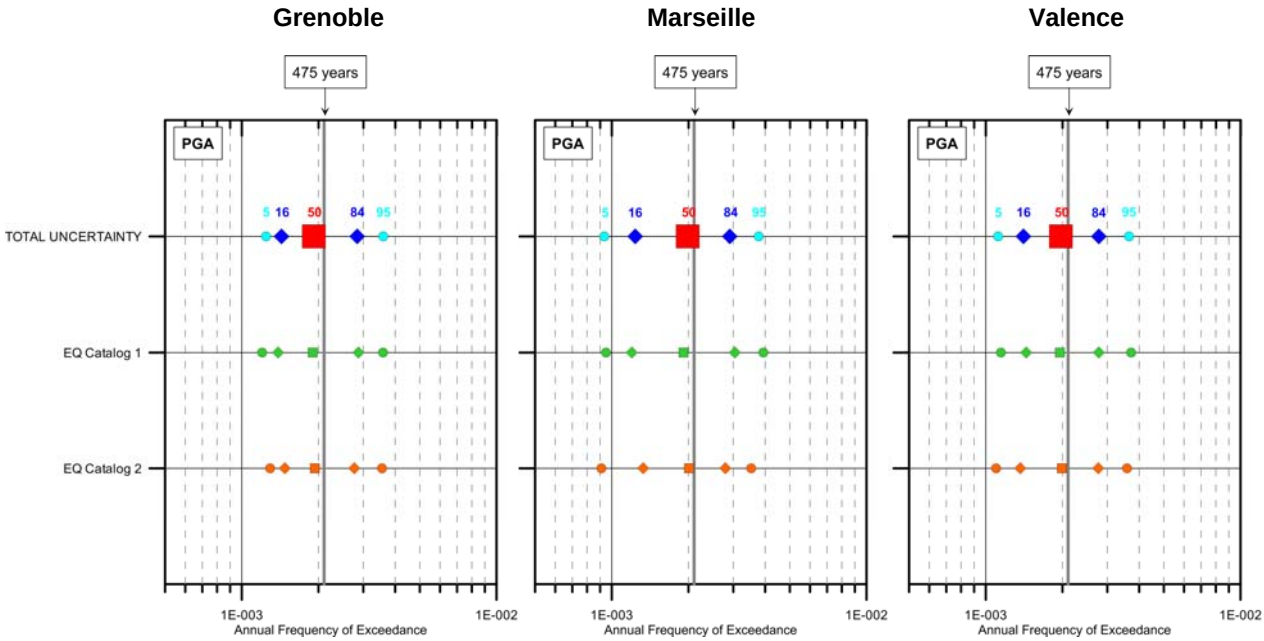

Figure 14 : Tornado diagrams at 475 years return period for the three sites showing the within earthquake catalogue uncertainties for the two considered catalogues and for PGA.

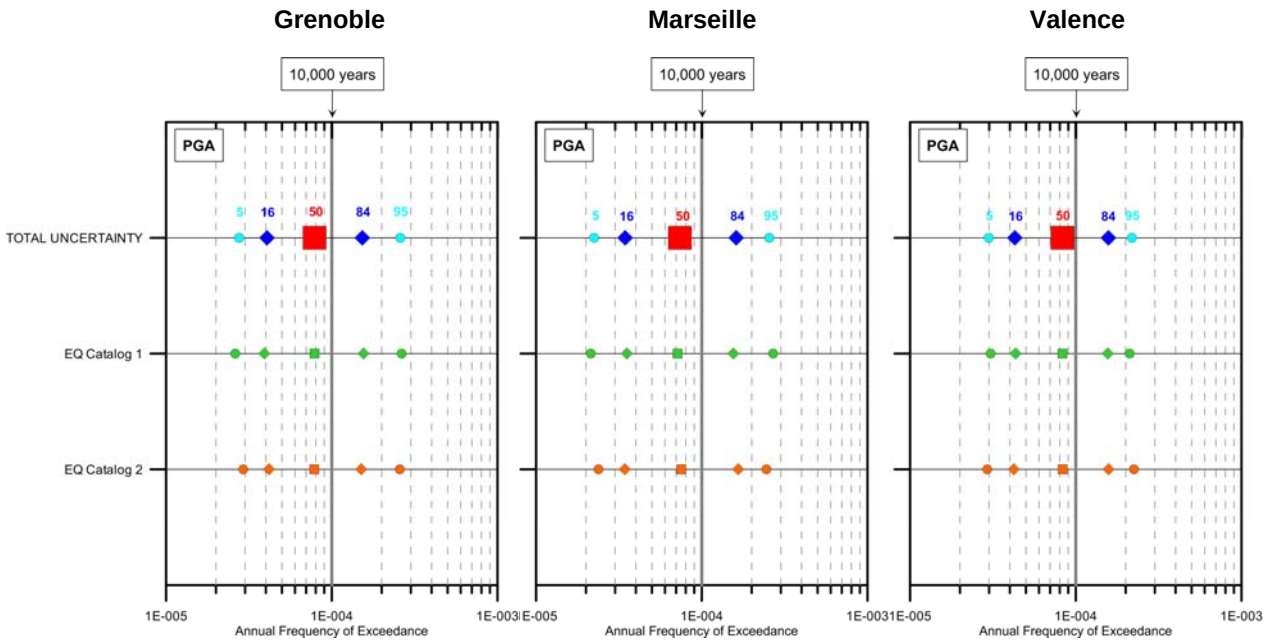

Figure 15 : Tornado diagrams at 10,000 years return period for the three sites showing the within earthquake catalogue uncertainties for the two considered catalogues and for PGA.

2.5 OVERALL UNCERTAINTIES CONTRIBUTION TO MEAN HAZARD

In this section, the sensitivity of the mean hazard to the different parameters of the PSHA model (seismotectonic model, earthquake catalogue, GMPE) is discussed. For example, considering the seismotectonic model, the mean hazard curve from the logic tree branches that consider SM1 is calculated, the same is done for the other two seismotectonic models. The AFE for the three mean hazard curves are reported in the tornado diagram as explained in Figure 2b. The same process is followed for the GMPEs and earthquake catalogues. The results for the three sites, the three spectral periods and for 475, 10,000 and 100,000 years return periods are presented in Figure 16, Figure 17 and Figure 18, respectively. The uncertainties in the mean hazard are also compared to the uncertainties in the total hazard.

The main results are:

- The mean hazard uncertainty is controlled by Source Model and GMPE. The uncertainties due to seismic catalogue have a negligible impact on the mean hazard;
- The Source Model and GMPEs contribute almost equally to mean hazard uncertainty. Only at long return periods and for PGA, the GMPE uncertainty is higher;
- SM1 usually provide larger mean hazard than the other seismotectonic models;
- The AB10 GMPE provide larger mean hazard than the other GMPEs at the three sites for long return periods and for PGA and 0.2s.

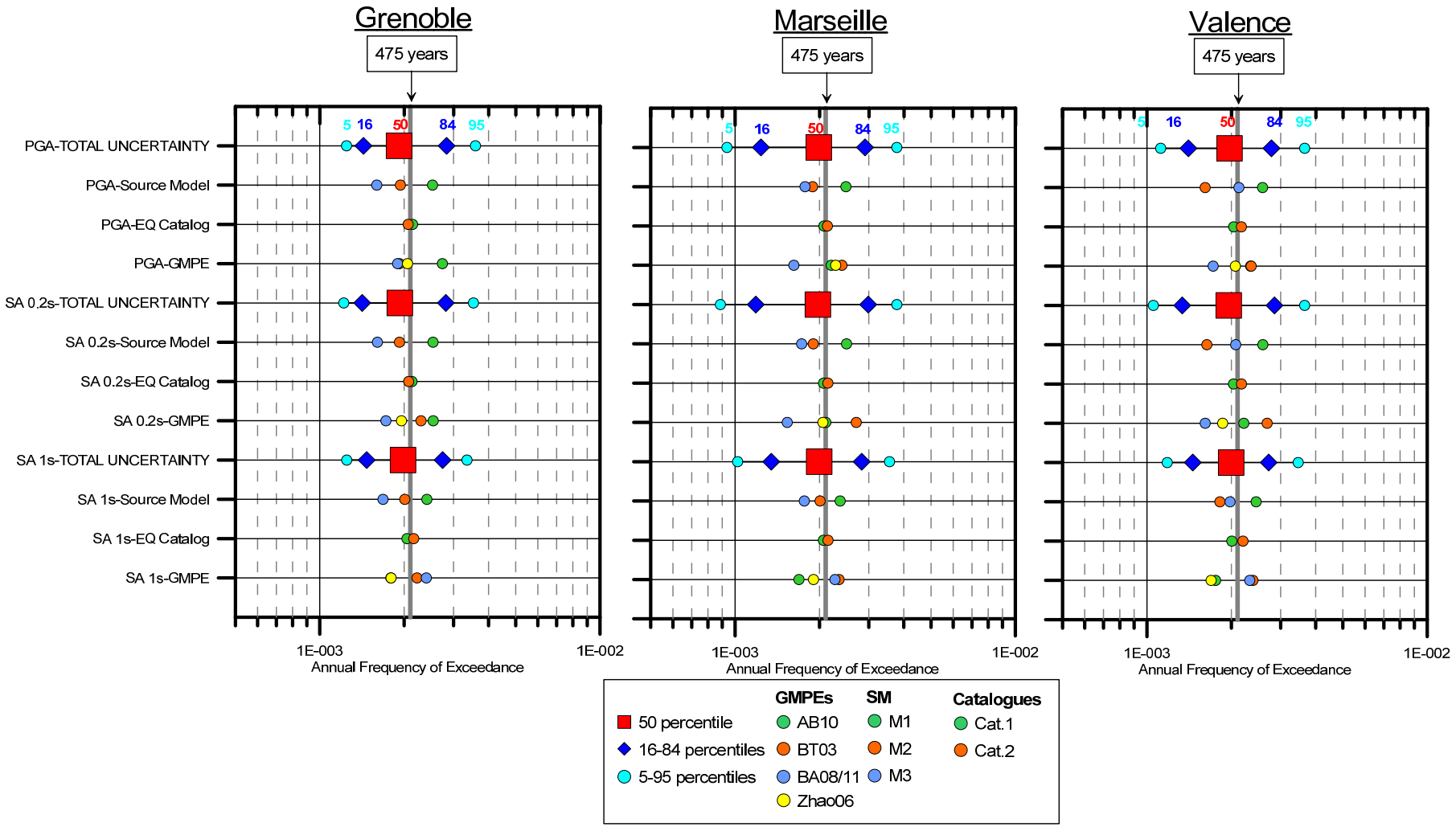

Figure 16 : Tornado diagrams at 475 years return period for the three sites showing the sensitivity of mean hazard to Source Model, Earthquake Catalogue and GMPE at three spectral periods (PGA, 0.2s and 1s).

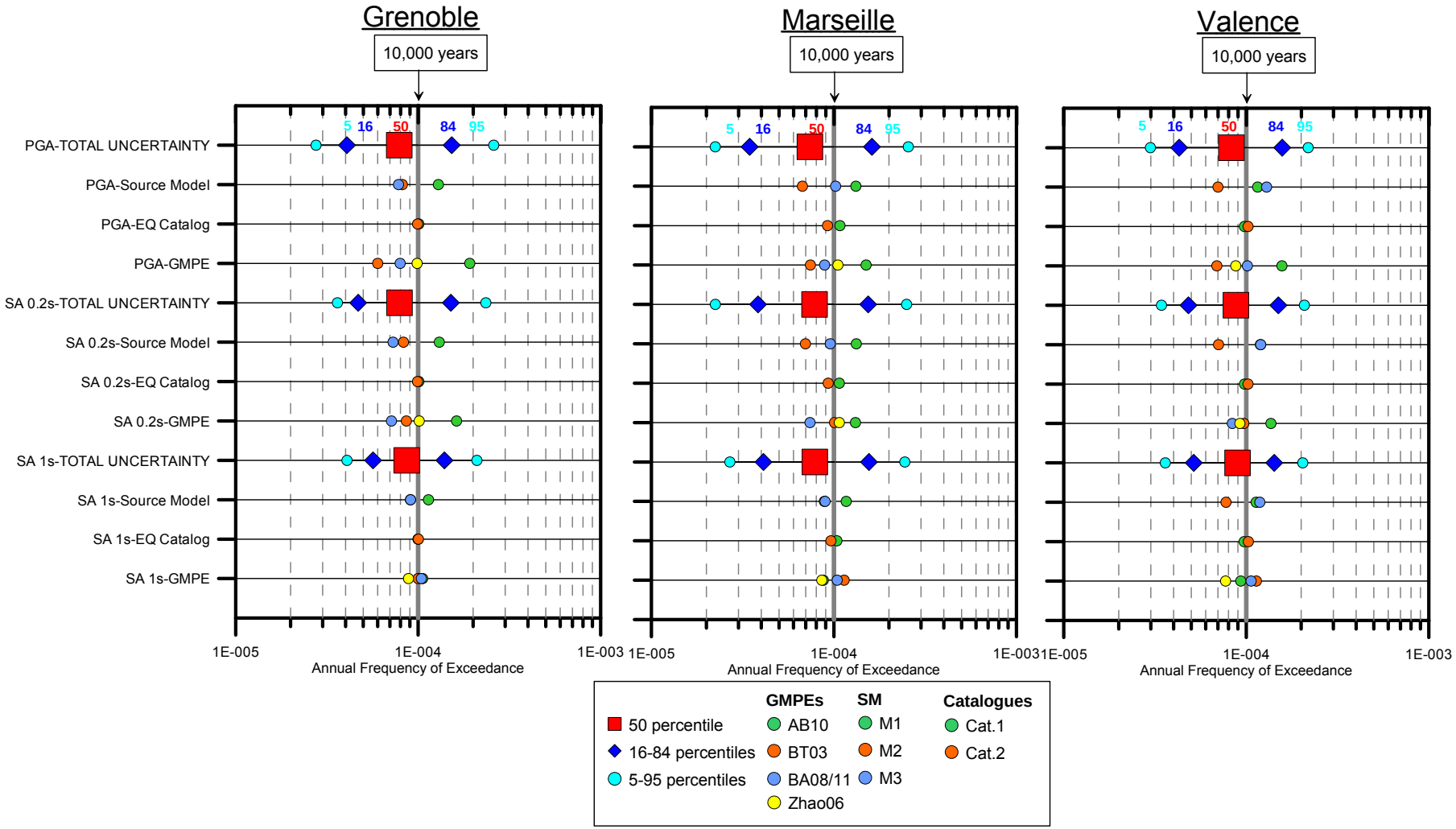

Figure 17 : Tornado diagrams at 10,000 years return period for the three sites showing the sensitivity of mean hazard to Source Model, Earthquake Catalogue and GMPE at three spectral periods (PGA, 0.2s and 1s).

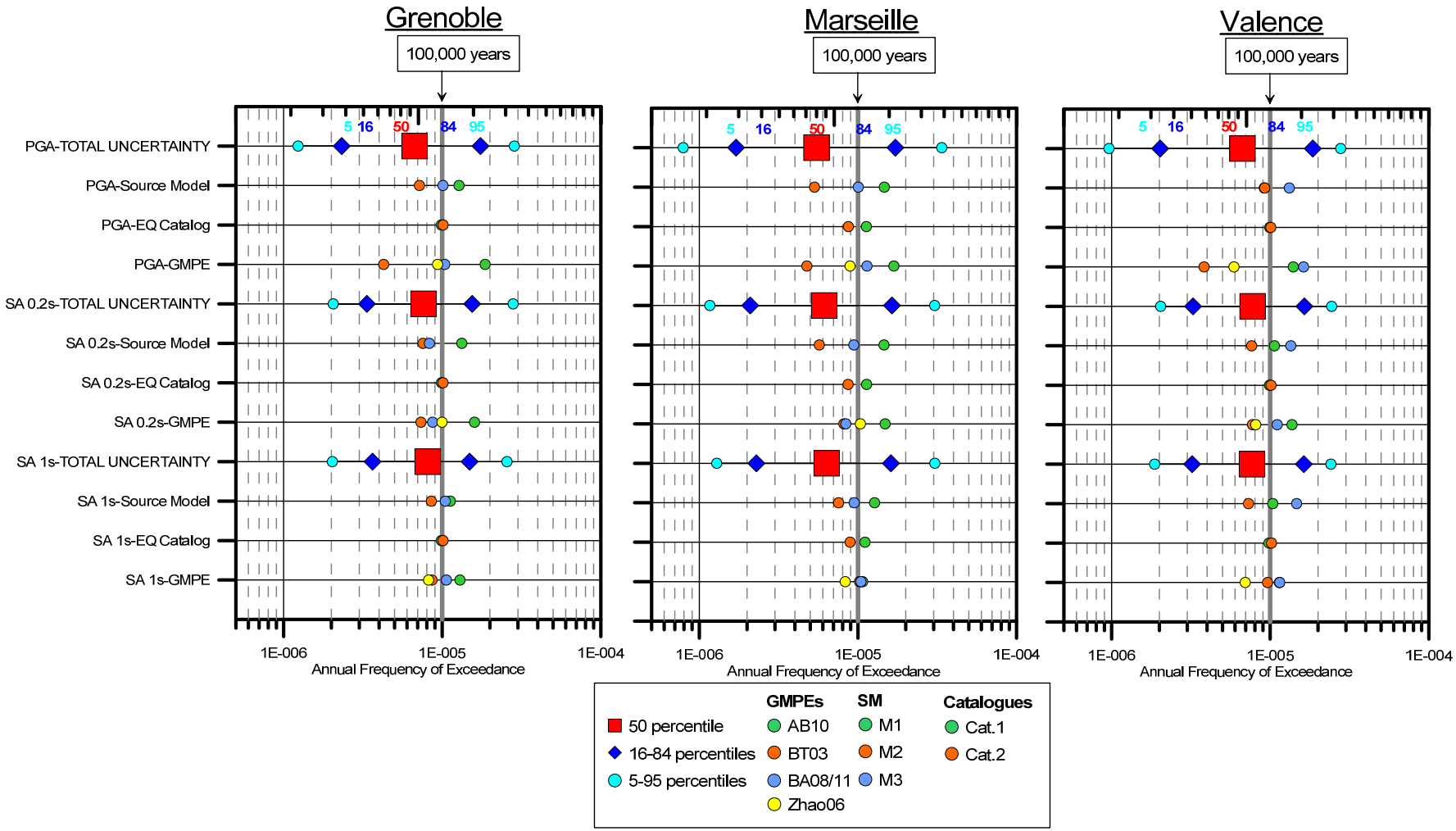

Figure 18 : Tornado diagrams at 100,000 years return period for the three sites showing the sensitivity of mean hazard to Source Model, Earthquake Catalogue and GMPE at three spectral periods (PGA, 0.2s and 1s).

2.6 SOURCES CONTRIBUTION (DEAGGREGATION)

In order to track the origin of uncertainties in the source characterization of the 2012 PSHA model, it is important to assess which seismic sources contribute most to the hazard at the three sites (Grenoble, Marseille and Valence). A deaggregation of the hazard by seismic sources is performed at the three sites, for the three considering seismotectonic models, at two return periods (475y and 10,000y) and two spectral periods (PGA and T=1s). The hazard curves and the percentage contribution to the total hazard for each seismic source are reported in the Annex 1.

Table 1 summarizes the main results of the deaggregation, reporting only the seismic sources that contribute for more than 10% to the total hazard at the site. The table also reports the uncertainties in the maximum magnitude (Mmax) and depth for each of the contributing seismic sources. In this way, the uncertainties considered in these parameters can be easily identified and compared among the different seismotectonic models and sites.

Return period	Site	Seismotectonic Model 1				Seismotectonic Model 2				Seismotectonic Model 3			
		Contributing Sources (>10%)		Mmax	Depth	Contributing Sources (>10%)		Mmax	Depth	Contributing Sources (>10%)		Mmax	Depth
		PGA	*T=1s*	*min,max*	*min,max*	*PGA*	*T=1s*	*min,max*	*min,max*	*PGA*	*T=1s*	*min,max*	*min,max*
475 yrs	Grenoble	ALS	ALS	6.3,7.3	3,15	CSS	CSS	6.5,7.2	3,15	ALP	ALP	7.2,7.6	5,15
			OBM	6.3,7.3	5,15	BEL	BEL	6.5,7.2	3,20				
							MEX	6.5,7.2	3,20				
	Marseille	MPR	MPR	6.3,7.0	3,8	PRO	PRO	6.5,7.0	5,15	RIF	RIF	7.2,7.6	5,15
		PCP	PCP	6.3,7.0	3,8	SFP	SFP	6.5,7.2	3,10		ALP	7.2,7.6	5,15
			ACC	6.3,7.0	3,15								
			NDC	6.3,7.3	5,15								
	Valence	ALS	ALS	6.3,7.3	3,15	CSS	CSS	6.5,7.2	3,15	ALP	ALP	7.2,7.6	5,15
		CBD	CBD	6.3,7.0	5,15	BRE	BRE	6.5,7.0	3,15	SFR	SFR	6.5,7.0	5,15
			LAN	6.3,7.0	3,15	DIO	DIO	6.5,7.0	3,15	RIF	RIF	7.2,7.6	5,15
10,000 yrs	Grenoble	ALS	ALS	6.3,7.3	3,15	CSS	CSS	6.5,7.2	3,15	ALP	ALP	7.2,7.6	5,15
						BEL	BEL	6.5,7.2	3,20				
	Marseille	MPR	MPR	6.3,7.0	3,8	PRO	PRO	6.5,7.0	5,15	RIF	RIF	7.2,7.6	5,15
			PCP	6.3,7.0	3,8	SFP	SFP	6.5,7.2	3,10				
	Valence	ALS	ALS	6.3,7.3	3,15	CSS	CSS	6.5,7.2	3,15	ALP	ALP	7.2,7.6	5,15
		CBD	CBD	6.3,7.0	5,15	BRE	BRE	6.5,7.0	3,15	SFR	SFR	6.5,7.0	5,15
							DIO	6.5,7.0	3,15		RIF	7.2,7.6	5,15

Table 1 : Deaggregation by source for the three seismotectonic models and three sites at two spectral periods and two return periods. Only the sources contributing by more than 10% to the total hazard are reported.

3. SENSITIVITY TO SI-HEX INSTRUMENTAL EARTHQUAKE CATALOGUE

The compilation of the new SIGMA earthquake catalogue is in progress by WP1 and should be finalized at the beginning of 2015. In this section, we present a first attempt to compare the SIGMA 2012 catalogue and the new one (SIGMA 2015) in terms of impact on the seismic hazard. In order to do this, we consider the latest version of the Si-Hex catalogue (http://www.franceseisme.fr/sismicite.html) that will be the base for the instrumental part of the SIGMA 2015 earthquake catalogue.

In Annex 2, we present first a comparison between the 2012 SIGMA earthquake catalogue and the Si-Hex catalogue in terms of Mw and epicentral locations. The common events identified in the two catalogues reveal sometimes quite significant differences in terms of Mw of location. Then, we constructed a new earthquake catalogue by replacing the instrumental part of the SIGMA catalogue with the Si-Hex catalogue. The new catalogue is then used to calculate the activity rates and to compare the hazard levels with the ones obtained in the 2012 model. A detailed description of the analyses is reported in Annex 2, here we briefly present the results.

Figure 19, Figure 20 and Figure 21 show a comparison between the mean uniform hazard spectra (UHS) obtained using the hybrid SIGMA/SiHex and the SIGMA 2012 catalogues. The UHS are shown at 475 years, 10’000 years and 100’000 years return period at the three considered sites.

The results clearly show that the impact of using the SiHex catalogue in the hazard calculation is relatively small at the three sites. This suggests, as also shown in Annex 2, that the activity rates in the magnitude range considered for estimating the lambda and beta parameters of the G-R are controlled by the pre-instrumental earthquakes.

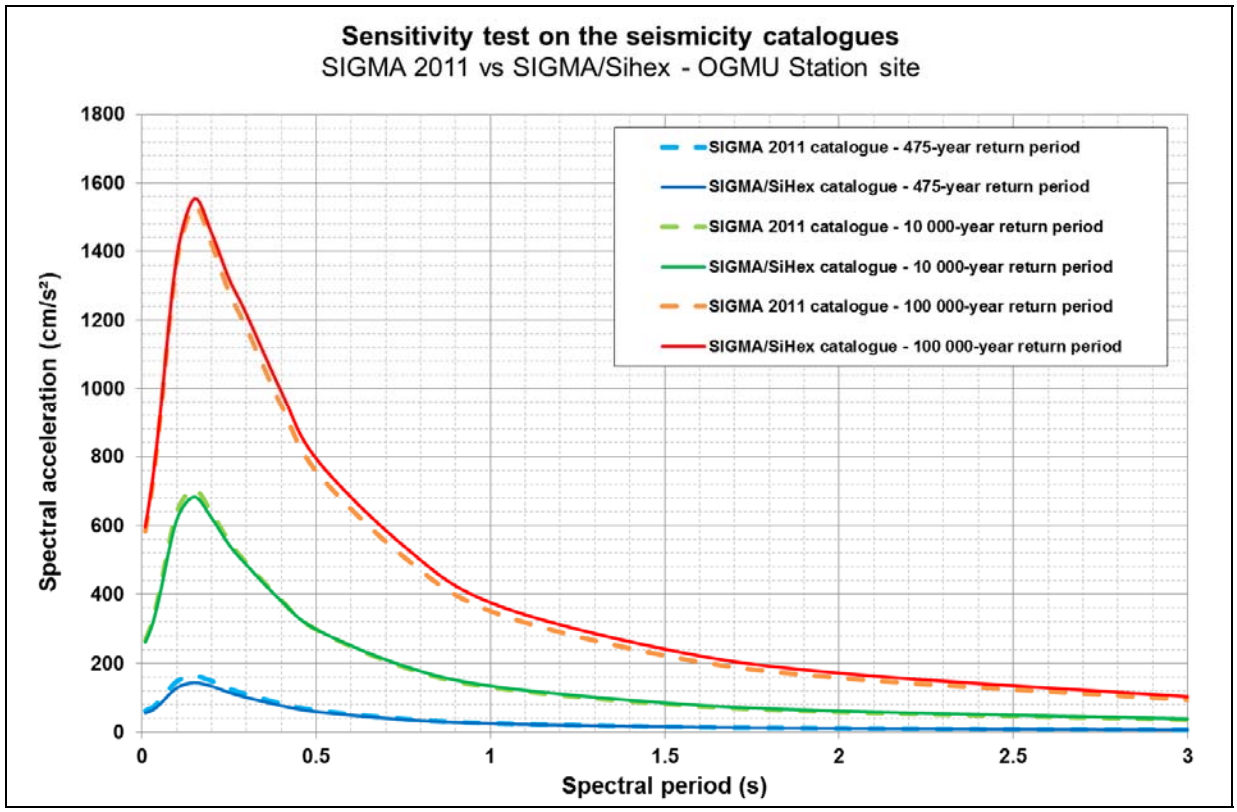

Figure 19 : Grenoble Site (OGMU RAP Station) – Comparison between the mean UHS spectra calculated with the two considered catalogues for 475-, 10 000- and 100 000-year return period – Horizontal component, 5% damping

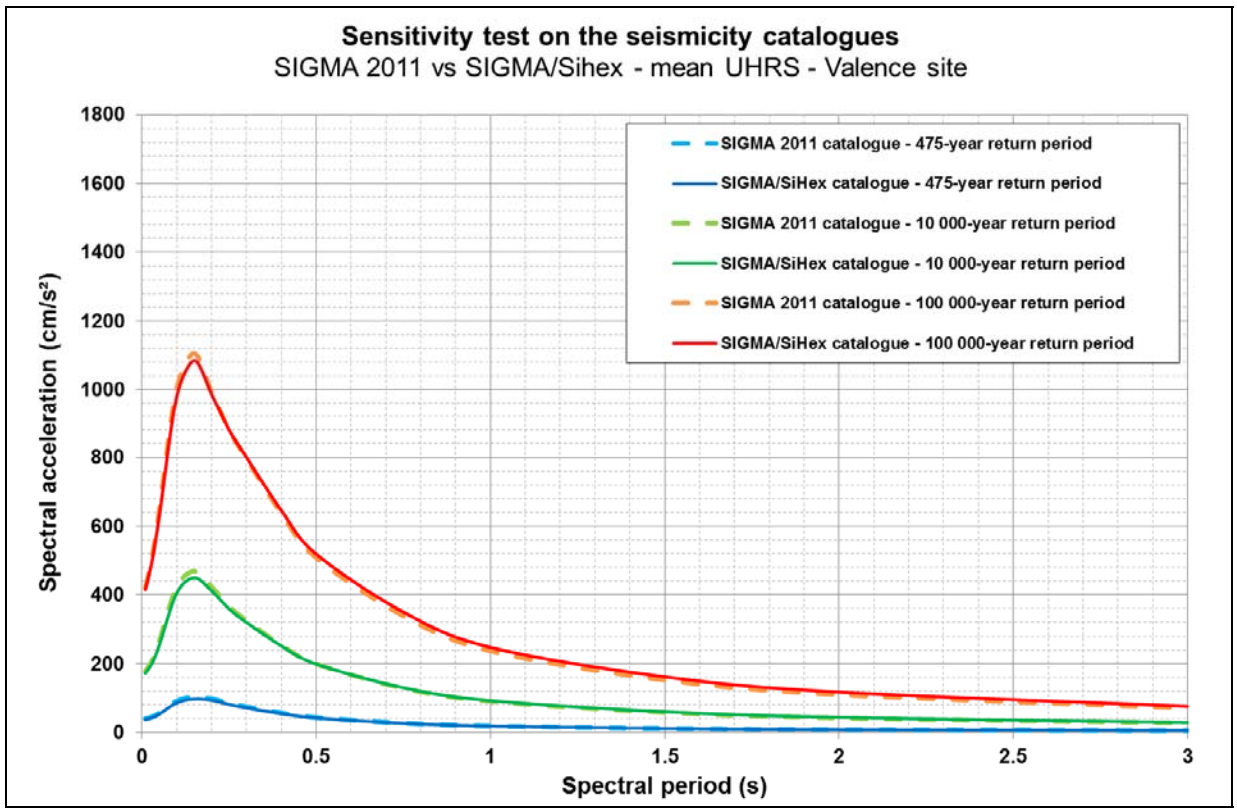

Figure 20 : Valence Site – Comparison between the mean UHS spectra calculated with the two considered catalogues for 475-, 10 000- and 100 000-year return period – Horizontal component, 5% damping

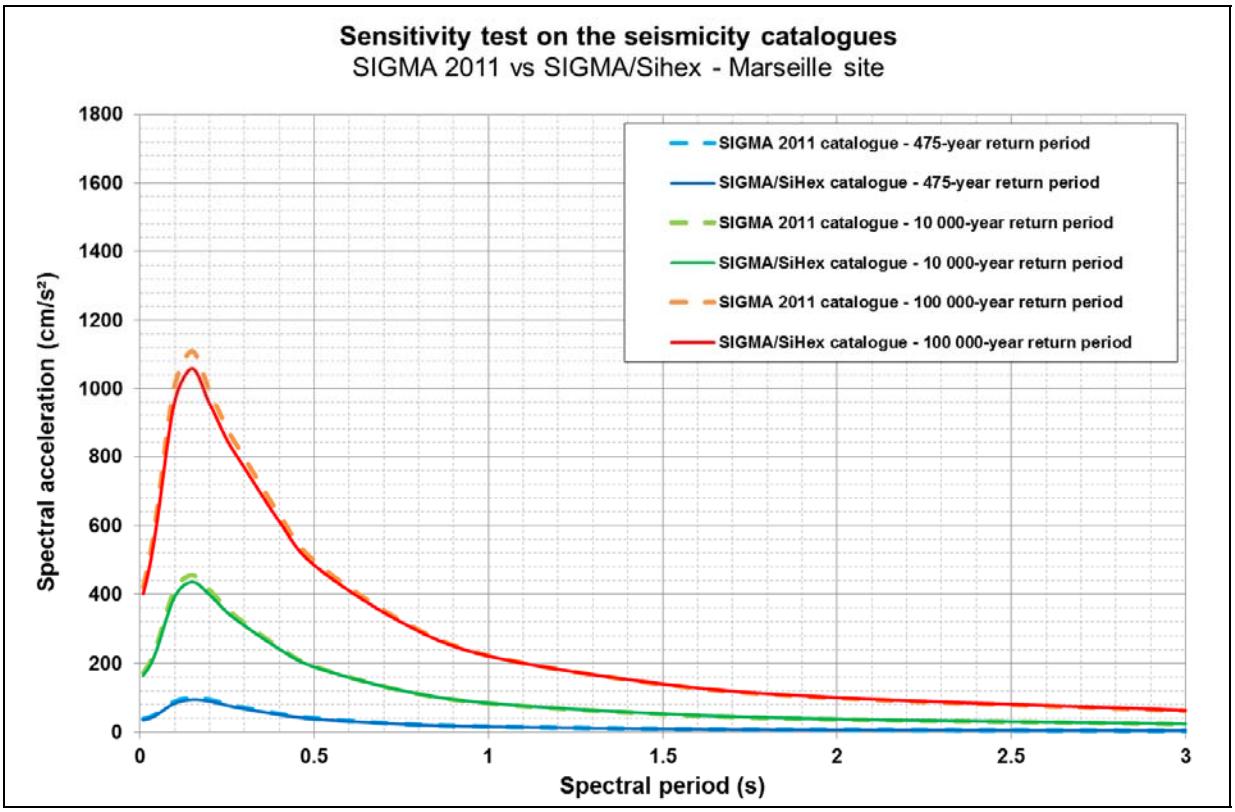

Figure 21 : Marseille Site – Comparison between the mean UHS spectra calculated with the two considered catalogues for 475-, 10 000- and 100 000-year return period – Horizontal component, 5% damping

4. SENSITIVITY TO METHODS FOR EVALUATING THE ACTIVITY RATES

In this section, we test alternative methods to determine the a and b (or lambda and beta) parameters of the Gutenberg-Richter model. We first focus on the impact of the use of different methods on the mean hazard at the three sites. Then, we considered alternative approaches to propagate the uncertainties in the G-R parameters throughout the PSHA calculation.

4.1 ALTERNATIVE METHODS TO DETERMINE G-R

In this section, we test the sensitivity to the method used to estimate lambda and beta parameters for the G-R. In the 2012 SIGMA PSHA model these parameters were estimated using the Weichert (1980) maximum likelihood approach which is widely known and it used in a number of PSHA projects worldwide. The alternative methods considered are:

- Least-squares;
- Weighted Least-Squares (weight by the inverse of the errors estimated for the activity rates);

- Maximum likelihood with prior b-value (e.g., EPRI 1994, PEGASOS 2004). The prior b value is calculated using the whole catalogue and is b = 1.03.

In order to compare only the effect of fitting method we decided to fix the other relevant parameters (i.e., the minimum magnitude of the fit considered for each zone and the magnitude discretization step) to the reference value used in the 2012 study. This choice need to be taken into account in order to give an interpretation to the results because the parameters in the 2012 study have been selected for the application of the Weichert (1980) approach and thus we can expect that they may not be fully appropriate for other methods (e.g. least squares).

Figure 22 shows the G-R relations derived, using the alternative methods, for some of the zones of SM1 that mostly contributing to hazard at the three sites. The obtained Lambda (M≥4.5) and b values are reported in Table 2. We may note that some of the obtained b values are rather unrealistic (e.g., b=-0.41 for zone CBD) and normally should not be considered in the PSHA. In such cases, a different selection of the minimum magnitude of the fit would likely provide more realistic b values. For the sensitivity purpose, we decided to keep these values in the hazard calculation but the results of such low b values should be interpreted with care.

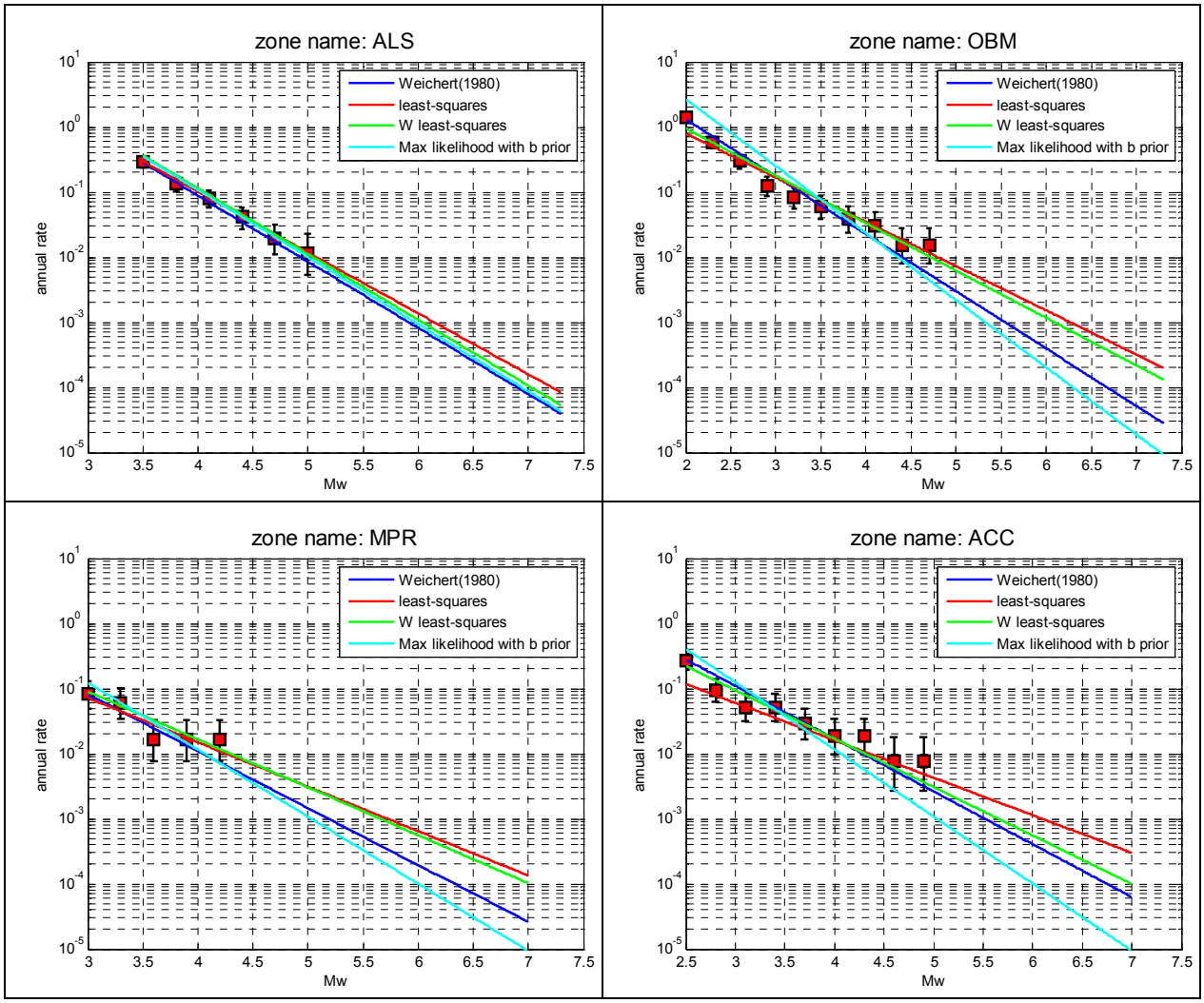

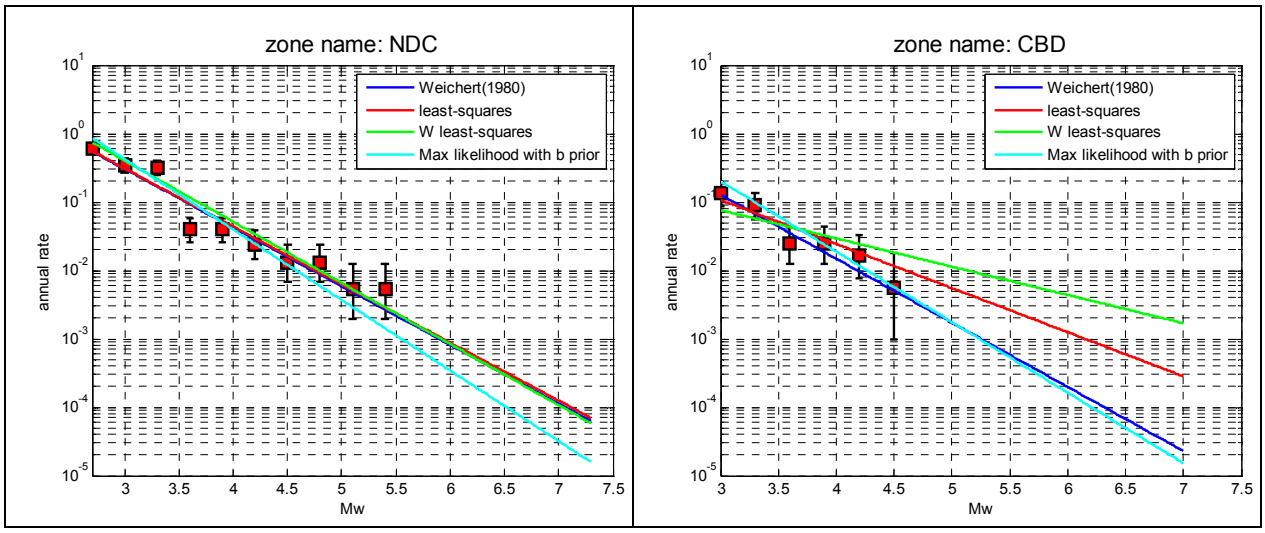

Figure 22 : Examples of G-R relations derived using different methods for several zones of SM1. The red symbols show the observed activity rates with associated uncertainties.

		Weichert(1980)	least-squares	weigthed least-squares	maximum likelihood with prior b
ALS	***b***	-1.02	-0.94	-1.01	-1.03
	λ(M≥4.5)	0.0275	0.0346	0.0358	0.0329
OBM	***b***	-0.88	-0.68	-0.73	-1.03
	λ(M≥4.5)	0.0083	0.0160	0.0144	0.0071
MPR	***b***	-0.87	-0.68	-0.74	-1.03
	λ(M≥4.5)	0.0040	0.0068	0.0071	0.0035
PCP	***b***	-1.12	-0.73	-1.02	-1.03
	λ(M≥4.5)	0.0284	0.0283	0.0500	0.0472
ACC	***b***	-0.81	-0.58	-0.74	-1.03
	λ(M≥4.5)	0.0067	0.0083	0.0073	0.0036
NDC	***b***	-0.86	-0.85	-0.89	-1.03
	λ(M≥4.5)	0.0158	0.0165	0.0183	0.0121
CBD	***b***	-0.94	-0.65	-0.41	-1.03
	λ(M≥4.5)	0.0050	0.0116	0.0183	0.0057
LAN	***b***	-0.98	-0.83	-0.69	-1.03
	λ(M≥4.5)	0.0220	0.0304	0.0399	0.0274

Table 2 : Lambda and -b values obtained using different fitting methods for several zones of SM1.

Figure 23, Figure 24 and Figure 25 show the hazard curves obtained at the three sites by using the alternative methods to estimate the G-R relations. The hazard curves for each site are the mean of the hazard curves obtained by exploiting the logic tree for SM1 (i.e., considering all the GMPEs).

The hazard curves at Grenoble are quite consistent using the different methods. Considering Valence and Marseille, the hazard curved calculated using G-R relations derived by least-squares or weighted least-squares provide larger hazard. However, the results for these two sites are largely affected by the low b values obtained for MPR and CBD zones that cannot be considered realistic. The maximum likelihood method with prior b value provide results that are close to the standard Weichert (1980) method, at least in this test.

The only general conclusion that we can draw from this test is that for sites controlled by zones where the sample of observed seismicity is large enough the choice of the fitting method has a limited impact on the hazard results. Vice

versa, for low-seismicity zones with a limited earthquake sample, the impact may be important. However, we stress again that the differences are likely exaggerated by the fact that some of the fitting parameters are fixed at the reference value determined for the Weichert (1980) method. A more complete comparison would be to use the four fitting method but exploring a range of minimum Mw and magnitude step for each fit, and then compare the obtained mean values of lambda and beta parameters.

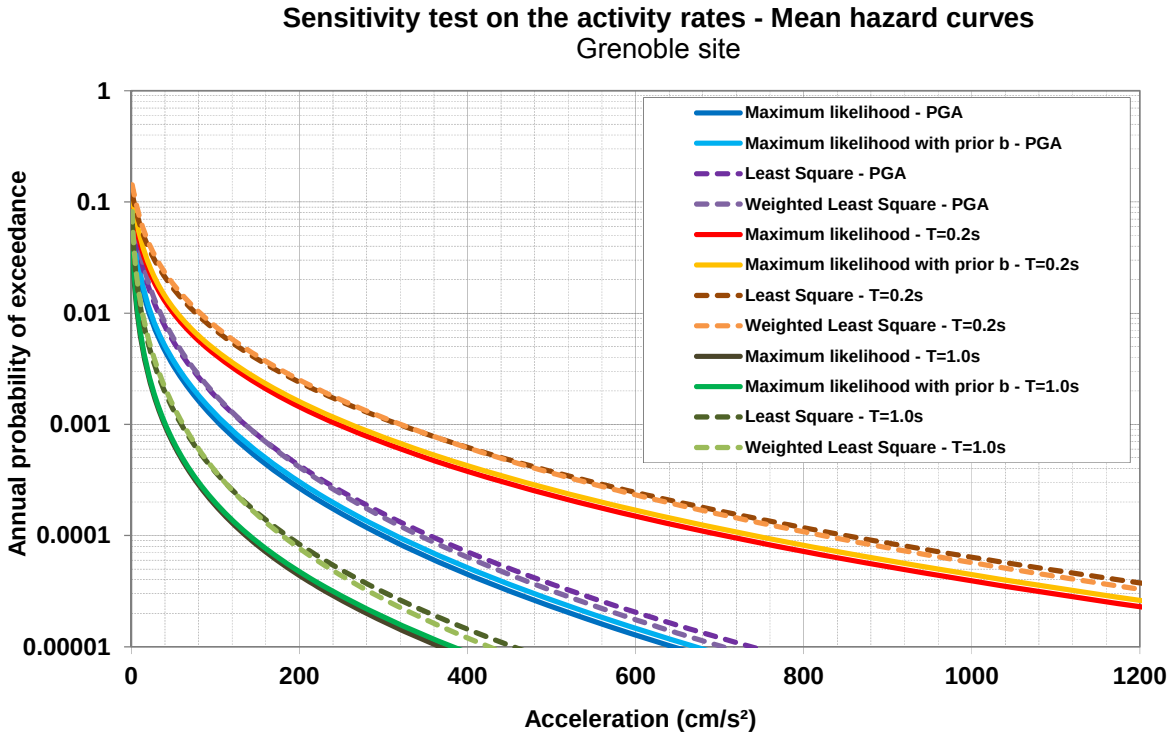

Figure 23 : Grenoble site - Impact of the alternative methods for determination of Gutenberg-Richter parameters in terms of mean hazard curves at three specific spectral periods (PGA, 0.2s and 1.0s).

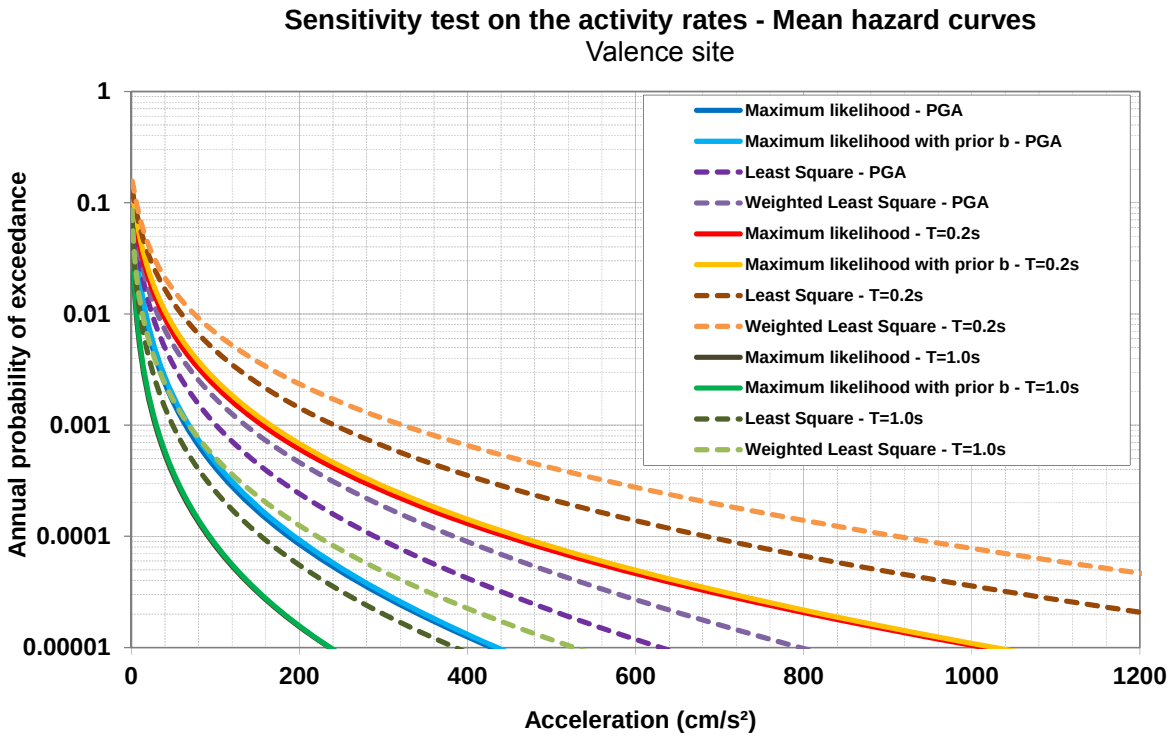

Figure 24 : Valence site - Impact of the alternative methods for determination of Gutenberg-Richter parameters in terms of mean hazard curves at three specific spectral periods (PGA, 0.2s and 1.0s).

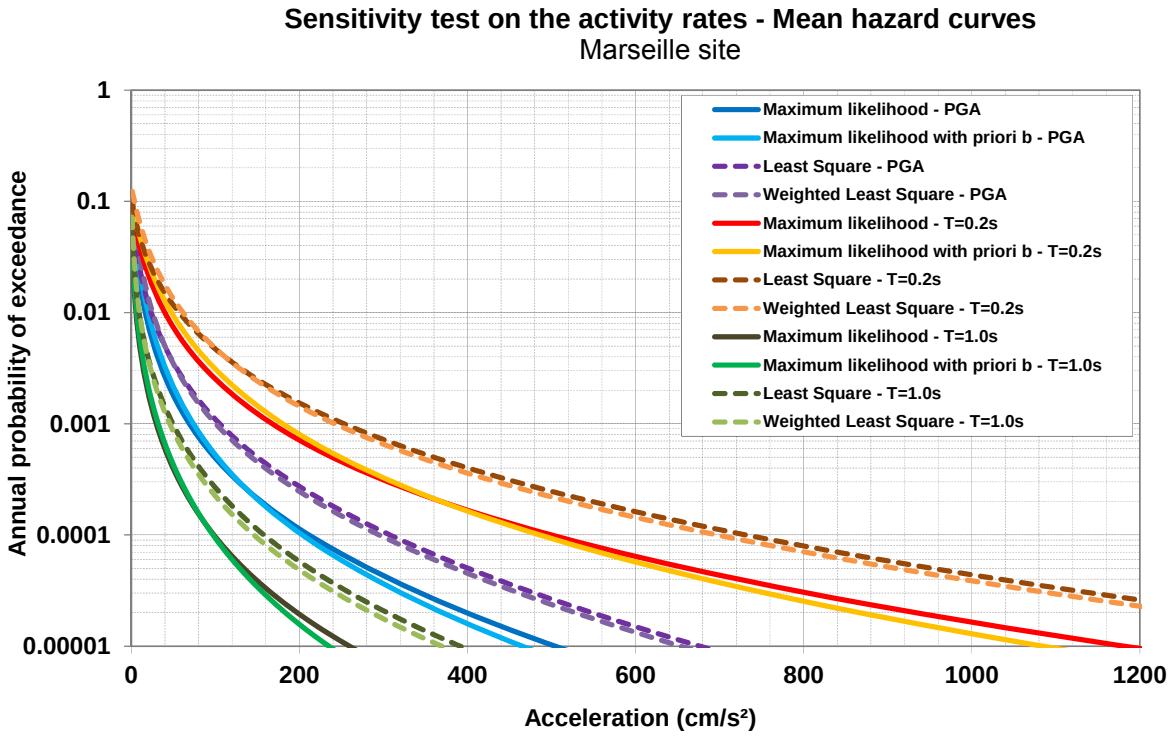

Figure 25 : Marseille site - Impact of the alternative methods for determination of Gutenberg-Richter parameters in terms of mean hazard curves at three specific spectral periods (PGA, 0.2s and 1.0s).

4.2 ALTERNATIVE METHODS TO PROPAGATE UNCERTAINTIES ON ACTIVITY RATES

In section 2.3.1, we showed that the largest contribution to the uncertainties within each source model comes from the uncertainties in the activity rates (Lambda and Beta values) propagated through the logic tree. Here, we test two alternative methods to propagate the uncertainties in the activity rates and evaluate the impact with respect to the method used in the SIGMA 2012 model.

4.2.1 Method 1 – Used in SIGMA 2012 model

We recall that in the SIGMA 2012 model we considered the standard deviation (sigma) of the a and b (or lambda and beta) values issued by the Weichert (1980) maximum likelihood method. Using such sigma values, we propagated the uncertainties via Monte Carlo approach by random sampling the normal distribution of lambda and beta truncated and 1 sigma. In order to consider the correlation between lambda and beta parameters we calculated the lambda values from the sampled beta distribution for 50% of the total samples. For the other 50% we calculated beta based on sampled lambda distribution fitting a linear model (by least-squares) to the activity rates data with the assumed lambda value.

Figure 26 shows an example of this approach for the zone ALS, which is the zone that largely contributes to the hazard at Grenoble and Valence (considering seismotectonic model 1). Figure 27 shows an example for zone MPR, which is the zone dominating the hazard for Marseille. We selected these two zones because they are characterized by different uncertainties in the estimated activity rates. Within ALS zone there is a larger number of events in the magnitude range of interest and, as a consequence, the uncertainties in the Gutenberg-Richter estimation (represented by the dashed MFDs) is lower than for zone MPR. Note that a single Mmax is considered in these examples in order to do not mix uncertainties due to Mmax and activity rates (although in the final calculations also Mmax uncertainties are considered). Figure 26 and Figure 27 also show the lambda and beta values obtained through correlated and uncorrelated (for comparison only) random sampling. The MFDs reported in gray in Figure 26 and Figure 27 are calculated using correlated lambda and beta values.

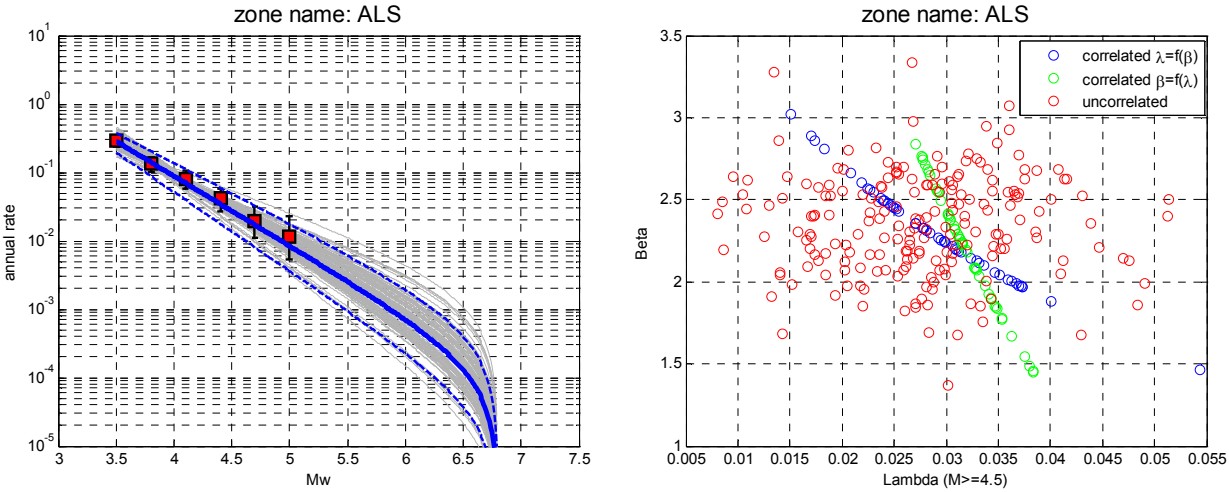

Figure 26 : Left: magnitude-frequency distributions (MFD) for zone ALS considering a fixed Mmax=6.7. The red symbols represent the calculated activity rates with associated uncertainties (±1sigma). The blue curves are the MFD (mean ± 1 sigma) obtained the Weichert (1980) method. Gray MFDs are obtained by 100 MC samples of the Lambda and Beta distributions as described in the text. Right: Lambda and Beta values obtained for 100 MC samples considering of not correlation (see text for explanation).

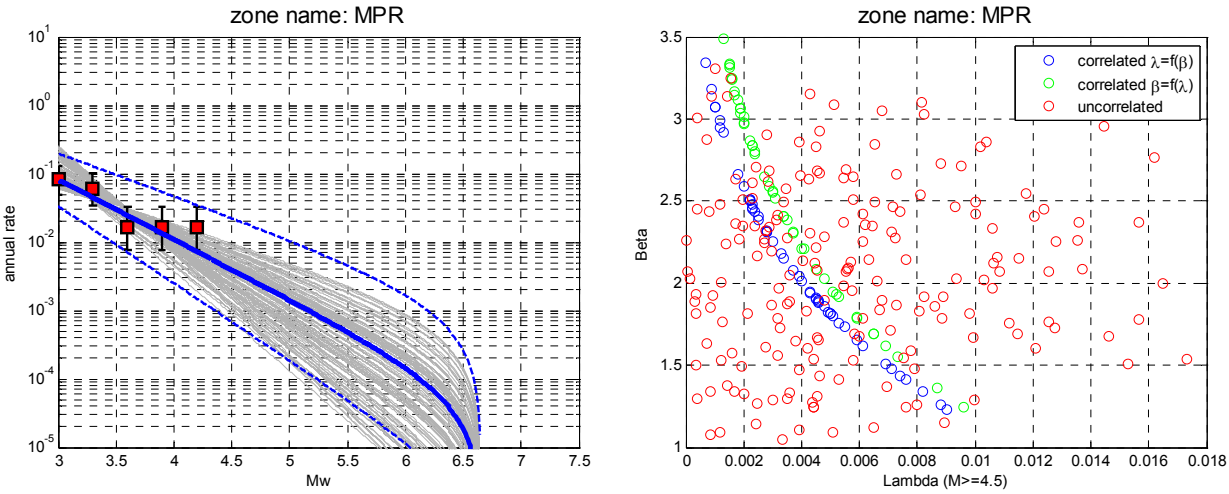

Figure 27 : Left: magnitude-frequency distributions (MFDs) for zone MPR considering a fixed Mmax=6.65. The red symbols represent the calculated activity rates with associated uncertainties (±1sigma). The blue curves are the MFD (mean ± 1 sigma) obtained the Weichert (1980) method. Gray MFDs are obtained by 100 MC samples of the Lambda and Beta distributions as described in the text. Right: Lambda and Beta values obtained for 100 MC samples considering of not correlation (see text for explanation).

4.2.2 Method 2 – Bootstrap resampling

In the second method, we use bootstrap resampling (Efron 1979), where the original earthquake catalogue for the considered zone is replaced with bootstrap catalogues obtained by randomly resampling N times, with replacement, the original catalogue. The sampling method used consists on generating a new catalogue, with the same number of earthquakes than the original, where each earthquake is chosen randomly from the original catalogue. Therefore, each earthquake of the new catalogue corresponds exactly (same location, occurrence date, magnitude) to an earthquake of the original one selected randomly. In this test, we considered N=200.

Figure 28 and Figure 29 show the cumulative annual rate obtained for ALS and MPR zones using the bootstrap resampling as well as the MFDs calculated using the Weichert method. For comparison, the annual rates and the MFDs (mean ± 1sigma) for the original catalogue are also reported.

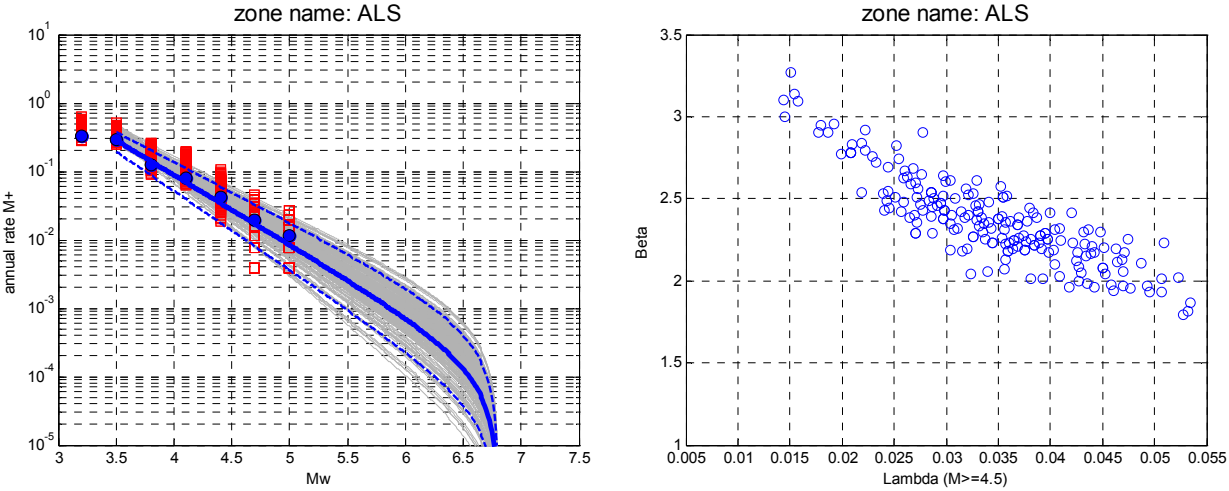

Figure 28 : Left: magnitude-frequency distributions (MFDs) for zone ALS considering method 2 and a fixed Mmax=6.7. The blue symbols represent the activity rates calculated using the original catalogue. The red symbols are the activity rates calculated using the N catalogues generated by bootstrap resampling. The blue curves are the MFD (mean ± 1sigma) obtained by Weichert (1980) method for the original catalogue. Gray MFDs are obtained by

Weichert (1980) method on the N bootstrap catalogues. Right: Lambda and Beta values obtained for the N bootstrap catalogues.

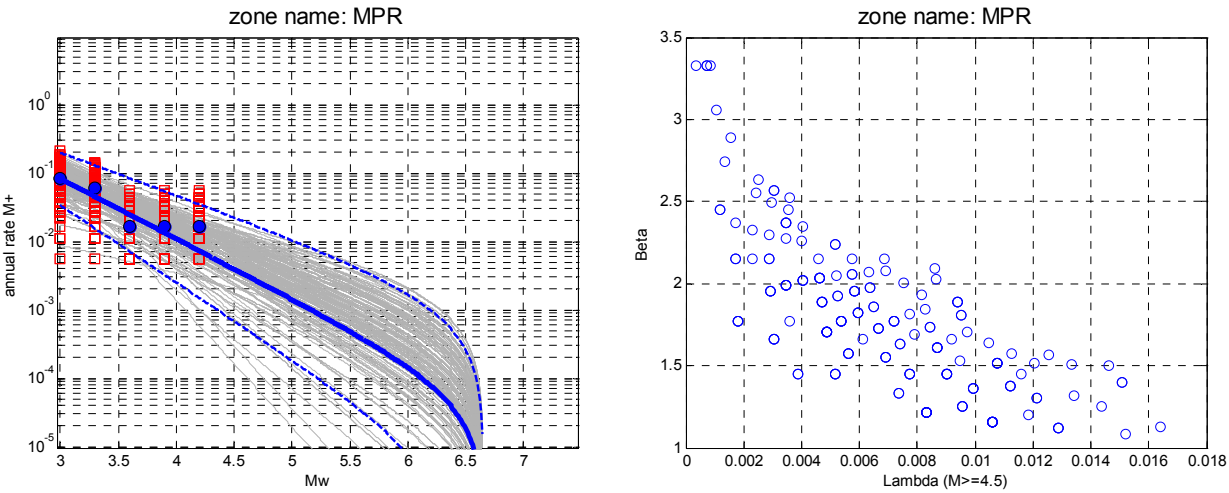

Figure 29 : Left: magnitude-frequency distributions (MFDs) for zone MPR considering method 2 and a fixed Mmax=6.65. The blue symbols represent the activity rates calculated using the original catalogue. The red symbols are the activity rates calculated using the N catalogues generated by bootstrap resampling. The blue curves are the MFD (mean ± 1sigma) obtained by Weichert (1980) method for the original catalogue. Gray MFDs are obtained by Weichert (1980) method on the N bootstrap catalogues. Right: Lambda and Beta values obtained for the N bootstrap catalogues.

4.2.3 Method 3 – Propagation of earthquake catalogue uncertainties

In the third method, we focus on the origins of the uncertainties in the observed activity rates. The uncertainties in the activity rates are caused by uncertainties in the earthquake magnitudes, in the completeness periods and in the earthquake locations. In this test, we consider uncertainties in the earthquake magnitudes and completeness periods and propagate them to the calculation of activity rates. Starting from the original catalogue and the completeness periods estimated in the 2012 study, we generate alternative catalogues by Monte Carlo sampling of the relative uncertainty distributions. For each alternative catalogue, we calculate the activity rates for fixed magnitude bins.

The uncertainties in Mw are defined considering a normal distribution (truncated at 2 sigma) as follows:

- σ(Mw)=0.2 for events after 1960
- σ(Mw)=0.3 for events before 1960

The uncertainties in the completeness periods (Tc) for different magnitude ranges are defined considering a normal distribution (truncated at 1 sigma) as follows:

- σ(Tc)=5 years for events with Mw<3.5
- σ(Tc)=25 years for events with 3.5<=Mw<=5
- σ(Tc)=50 years for events with Mw>5

Figure 30 shows the completeness periods and considered uncertainties for different magnitudes. Note that in this test the values of uncertainties assigned to Mw and completeness periods are based on expert judgment. In the following of the SIGMA project, the SIGMA earthquake catalogue, in preparation by the WP1, will include an evaluation of uncertainties on Mw.

For each cumulative distribution of the annual activity rate generated by the described random sampling, we used the Weichert (1980) method to calculate the Gutenberg-Richter MFDs. The results for ALS and MPR zones are presented in Figure 31 and Figure 32.

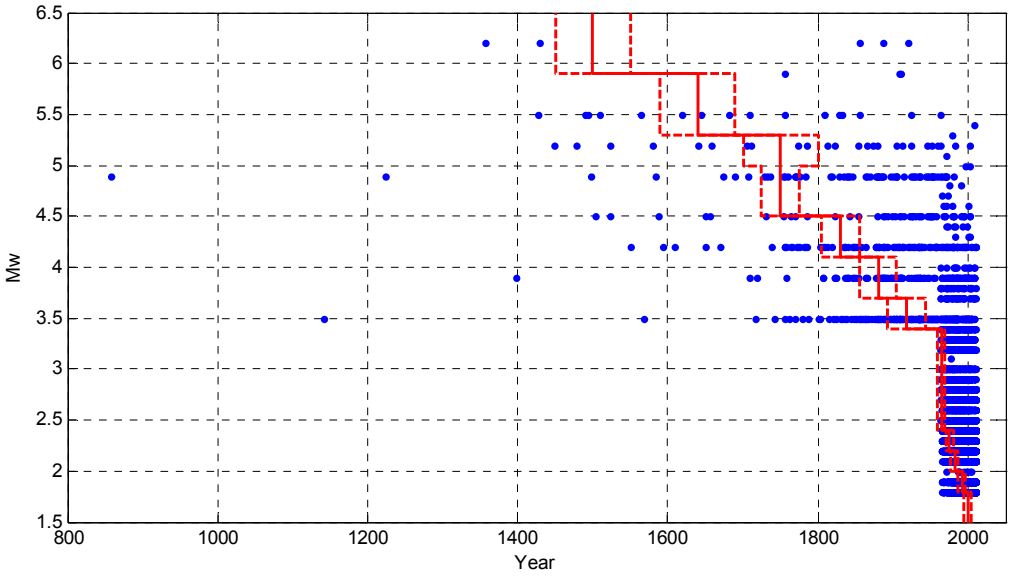

Figure 30 : Year versus Mw scatter plot of the SIGMA 2012 earthquake catalogue. The blue dots represent each earthquake of the SIGMA catalogue. The red lines show the completeness period for each Mw and associated uncertainties (dashed lines).

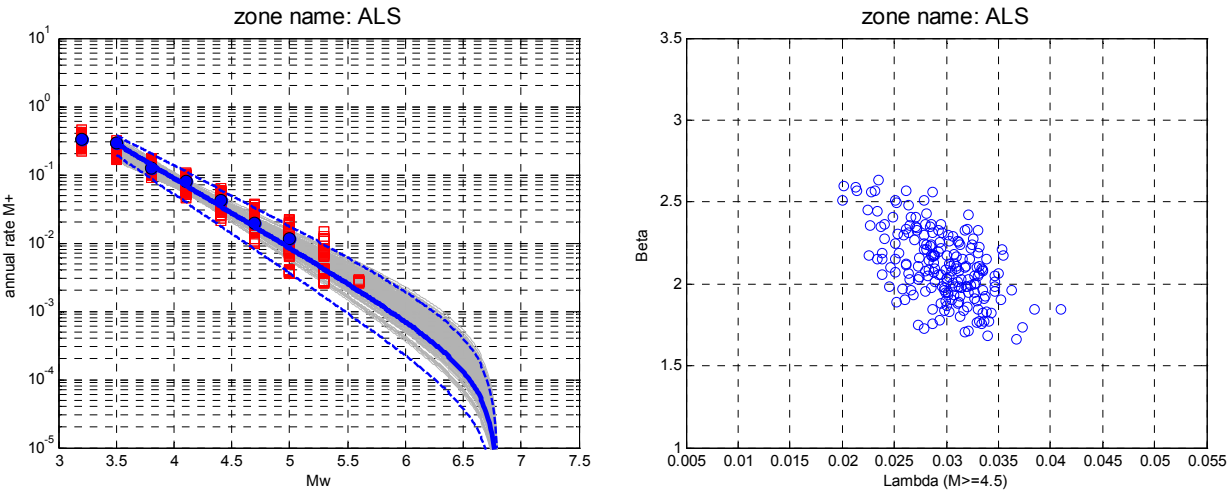

Figure 31 : Left: magnitude-frequency distributions (MFDs) for zone ALS considering Method 3 and fixed Mmax=6.7. The red symbols represent the calculated activity rates obtained by random sampling the catalogue uncertainties (Mw and completeness periods). The blue symbols represent the activity rates calculated using the original catalogue. The blue curves are the MFDs (mean ± 1sigma) obtained by Weichert (1980) method for the original catalogue. Gray MFDs are obtained by Weichert (1980) method on the catalogue generated using the synthetic activity rates (red symbols) Right: Lambda and Beta values obtained for the 200 MC generation of the synthetic catalogue (see text for explanation).

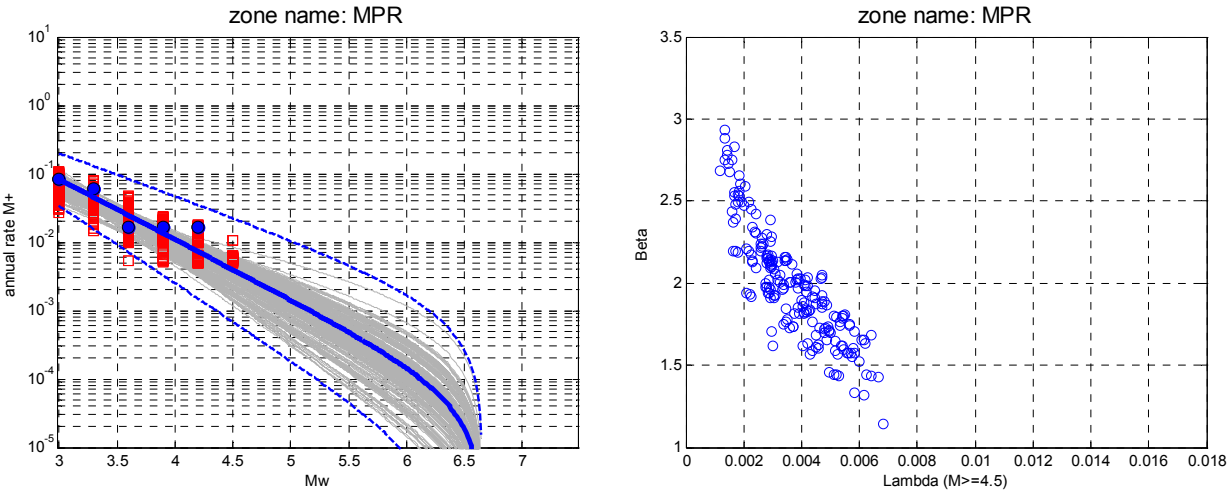

Figure 32 : Left: magnitude-frequency distributions (MFDs) for zone MPR considering Method 3 and fixed Mmax=6.65. The red symbols represent the calculated activity rates obtained by random sampling the catalogue uncertainties (Mw and completeness periods). The blue symbols represent the activity rates calculated using the original catalogue. The blue curves are the MFDs (mean ± 1sigma) obtained by Weichert (1980) method for the original catalogue. Gray MFDs are obtained by Weichert (1980) method on the catalogue generated using the synthetic activity rates (red symbols) Right: Lambda and Beta values obtained for the 200 MC generation of the synthetic catalogue (see text for explanation).

4.2.4 Comparison of hazard uncertainties using the three methods

Figure 33 shows the results of the three methods used to propagate uncertainties in the MFD parameters (Lambda and Beta). The results are expressed in terms of uncertainties in the hazard considering only one seismotectonic model (SM1) and one GMPE (BA08). Moreover, the Mmax is fixed to the mean value of the distribution for each areal zource zone. In this way the uncertainties in the hazard calculated at the site is only related to the uncertainty in the Lambda and Beta parameters. We may observe that method 1 and method 2 provide almost the same uncertainties in the calculated hazard, though method 2 provides slightly larger uncertainties at Grenoble site. Method 3 provides the smallest uncertainties at the three sites. Method 3 may be considered more adequate to propagate uncertainties in MFDs for zone of low seismicity where purely statistical methods may provide too large uncertainties, possibly generating activity rates that are not consistent with seismotectonic context of the considered zone.

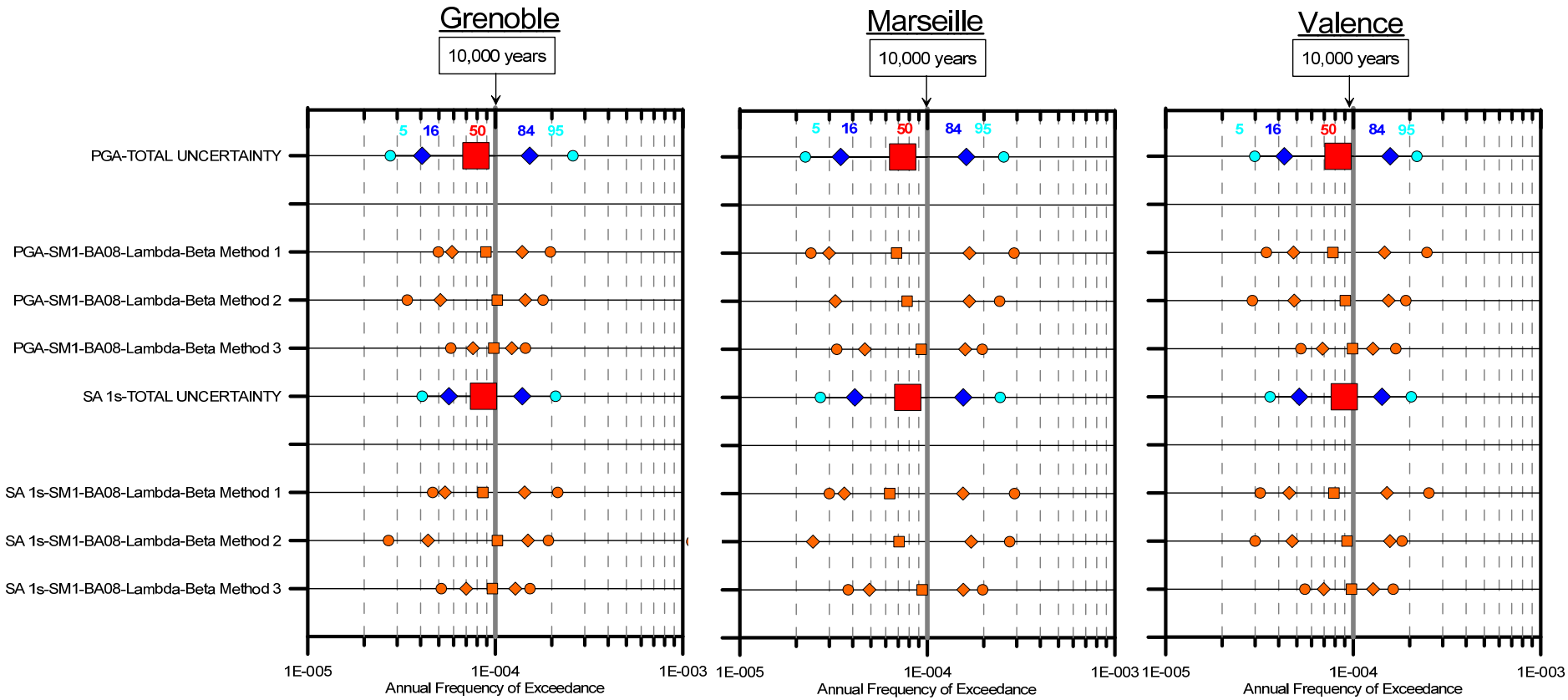

Figure 33 : Tornado diagrams at 10,000 years return period for the three sites showing, for each Seismotectonic Model (SM1, SM2 and SM3), the uncertainties due to Mmax and activity rates parameters. The results are for two spectral periods (PGA and 1s).

5. SENSITIVITY TO MAXIMUM MAGNITUDE (MMAX)

The maximum magnitude (Mmax) corresponds to the strongest earthquake able to occur in a given seismicity zone. This parameter is required in probabilistic evaluations of seismic hazard to avoid including in hazard calculations earthquakes that would be unrealistic, given the seismotectonic context. Different methodologies may be applied to assess the Mmax (see Wheeler, 2009) but regardless of the different available approaches, the determination of maximum earthquake magnitude remains significantly uncertain, and the uncertainty needs to be addressed.

In this section, we compare the Mmax distributions adopted in the 2012 study (detailed description of the determination of Mmax is reported in SIGMA-2012-D4-24) with distributions obtained using alternative models or methodologies.

This test is performed considering only one seismotectonic model (SM1).The results may be slightly different considering the other seismotectonic models but the general conclusion on the relative hazard values provided by each method would not change.

5.1.1 Model 1 – SHARE Mmax distributions

The first alternative model for Mmax that we tested comes from the results of the SHARE project (http://www.share-eu.org/). The approach followed by SHARE is illustrated in Figure 34 and it is different according to the tectonic domain under consideration (SCR, Active regions, Oceanic crust). For SCRs, SHARE followed the EPRI (1994) Bayesian approach by using the Mmax Prior distributions for non-extended and extended crust developed for Eastern US (see Annex 4 for further details on the EPRI 1994 approach). The Mmax distributions finally considered for the different regions are reported in Figure 34. For the seismotectonic zones covering the SIGMA area of interest we are mostly interested in Mmax distributions for SCRs extended crust and for active regions. Table 3 reports, for each of the source zone of SM1, the Mmax distribution assigned based on SHARE approach.

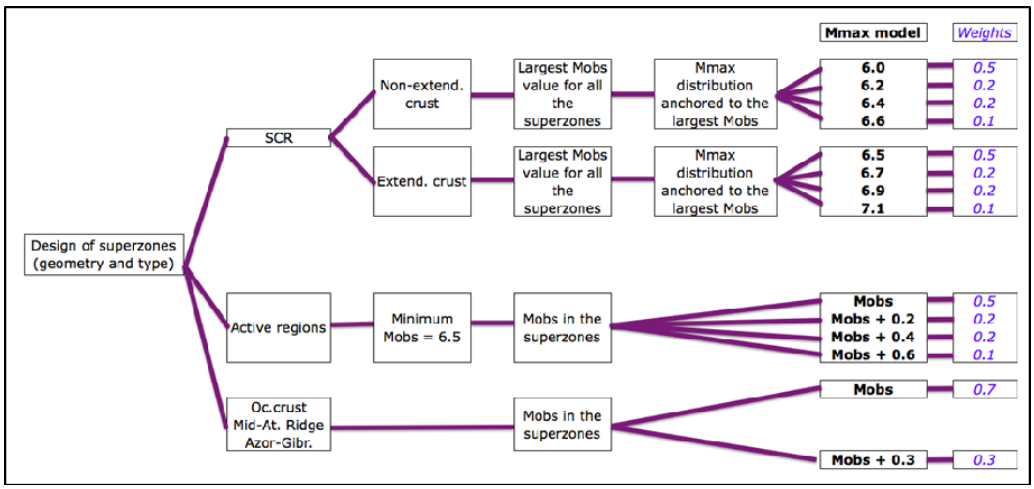

Figure 34 : Approach followed by SHARE for Mmax estimation for different tectonic regions (Woessner et al. 2012).

Zone name	Mmax SHARE	Weigths
LAN, CBD, MPR, ACC, PCP	6.5, 6.7, 6.9, 7.1	0.5, 0.2, 0.2, 0.1
ALS, NDC, OBM	6.9, 7.1, 7.3, 7.5	0.5, 0.2, 0.2, 0.1

Table 3 : Mmax distribution assigned to the zone of SM1 contributing to the hazard following the SHARE approach. Blue color identifies the zones classified as SCRs and red color identifies the zones classified as active.

5.1.2 Model 2 – EPRI (1994) Bayesian with European prior

The second alternative model for the Mmax distributions is developed by applying the EPRI (1994) Bayesian methodology to a new prior Mmax distribution for European stable continental regions (ESCRs). Annex 4 provides a brief description of the EPRI (1994) approach and illustrates the process followed to develop the new prior distribution for ESCRs. The posterior Mmax distributions for each of the zones contributing to the hazard for SM1 are calculated as follows:

- For zones ascribed to SCR (see Table 3). the European Prior Mmax distribution is considered (i.e., normal distribution with μ=6.2, σ=0.5)
- For the other zones, the EPRI(1994) extended crust prior Mmax distribution is considered (i.e., normal distribution with μ=6.4, σ=0.85)

Following the Bayesian approach, the likelihood function is calculated for each zone using the 2012 SIGMA catalogue (see Annex 4). The likelihood function is then used to update the prior distribution and to obtain the posterior Mmax distributions (Figure 35).

The posterior Mmax distributions finally are truncated as follows:

- Minimum Mmax ≥ 5.5. Because we believe that we cannot exclude a Mw=5.5 anywhere in the SIGMA region;
- Maximum Mmax = 7.5 for ALS, OBM and NDC zones, which corresponds to the upper bound defined by potential fault lengths and scaling laws.
- Maximum Mmax = 7.3 for the remaining zones.

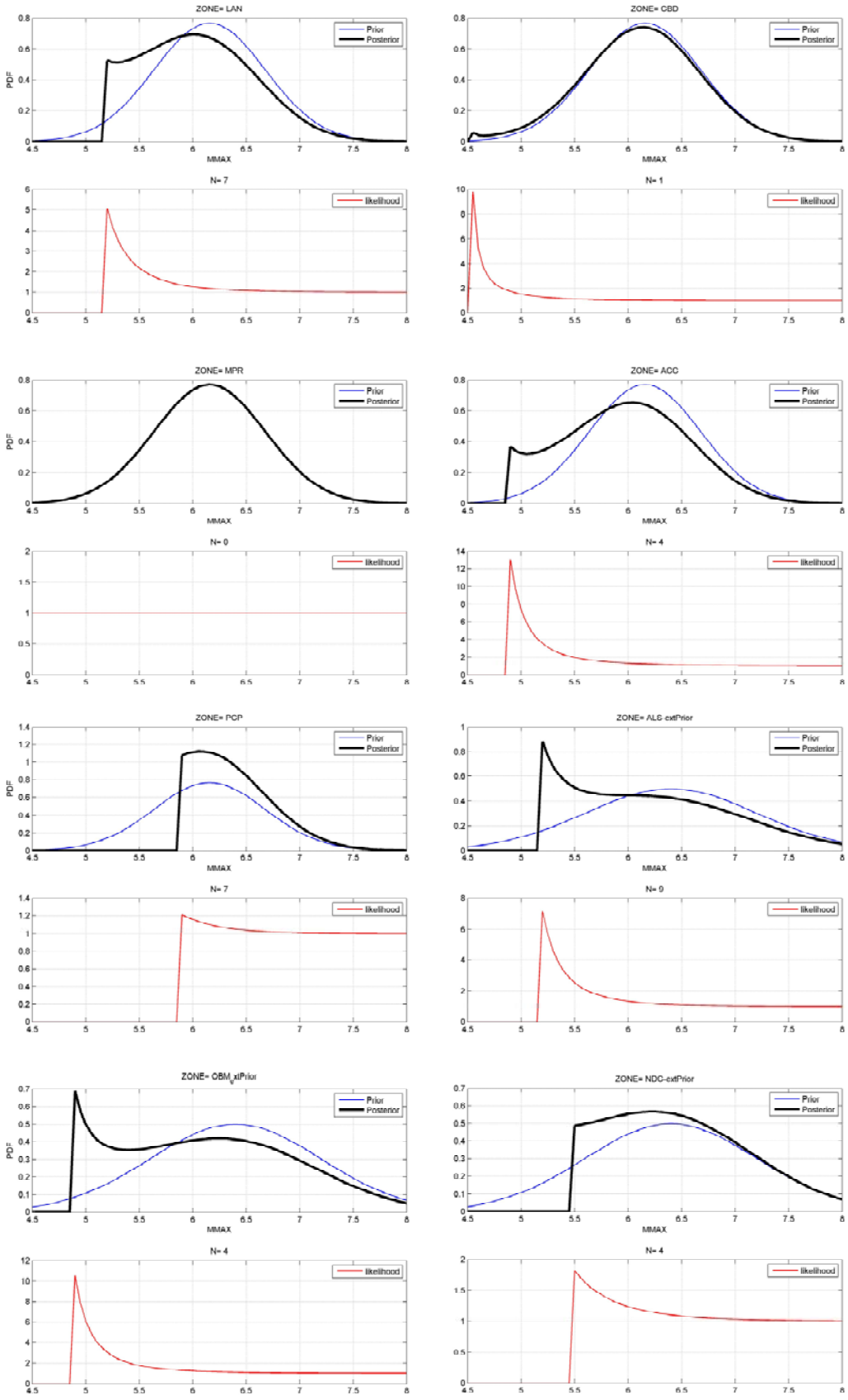

Figure 35 : Prior Mmax distribution (blue), likelihood functions (red) and posterior Mmax distributions (black) obtained for the considered zones.

5.1.3 Model 3 – Increment and scaling laws based method.

5.1.3.1 Definition of Mmax lower and upper bounds.

In this third approach, the maximum magnitude is derived from the combined analysis of the seismological database (earthquake catalog) and of the geological database used to develop the seismic sources models.

For a given source belonging to a given seismotectonic domain, the values of Mmax are distributed between a lower and an upper bound. The analysis has been conducted at the scale of the French territory and adjacent areas as it requires aggregating the seismic sources in the seven identified seismotectonic domains.

The SIGMA region of interest is covered mainly by three of them: the Alps, the rifting domain including the Upper Rhine Graben and the Limagnes d'Allier and a transition domain which encompasses Provence and Jura.

In each zone, the lower bound is determined as the maximum observed magnitude incremented by 0.3. Exception is applied to zones characterized by very low seismicity, adopting as basic rule, that the lower bound can never be lower than Mw 5.5, arguing that we do not have the appropriate data and geological arguments to exclude the occurrence of magnitudes lower than Mw 5.5. An exception is also applied to zones where paleoseismic evidence exists. If the paleoseismic magnitude is above the incremented magnitude the lower bound takes its value.

The upper bound is determined for each of the three seismic sources aggregations considering seismological scale laws (Léonard (2010), Papazachos et al. (2004) and Wesnousky (2008)) applied to the maximum fault dimensions identified in the geological database.

In such way:

- The lower bound obey to the arguable possibility that the maximum magnitude is close and slightly above the maximum observed magnitude, the increment of 0.3 corresponding approximately to one standard deviation of the magnitude estimate, or if any to the paleoearthquake ;
- The upper bound is more representative of the maximum potential of the largest faults derived from the geological state of knowledge.

Within the SIGMA region of interest, the lower and upper bounds of Mmax for the zone of SM1 contributing to the hazard are reported on Table 4.

5.1.3.2 Distribution of the Mmax values

An irregular trapezoidal distribution is adopted to generate the maximum magnitude values. The number of values is increasing regularly between the lower bound and a quarter of the magnitude range, constant between this value and the mean Mmax and decreasing towards the upper bound, as in the example of Figure 36.

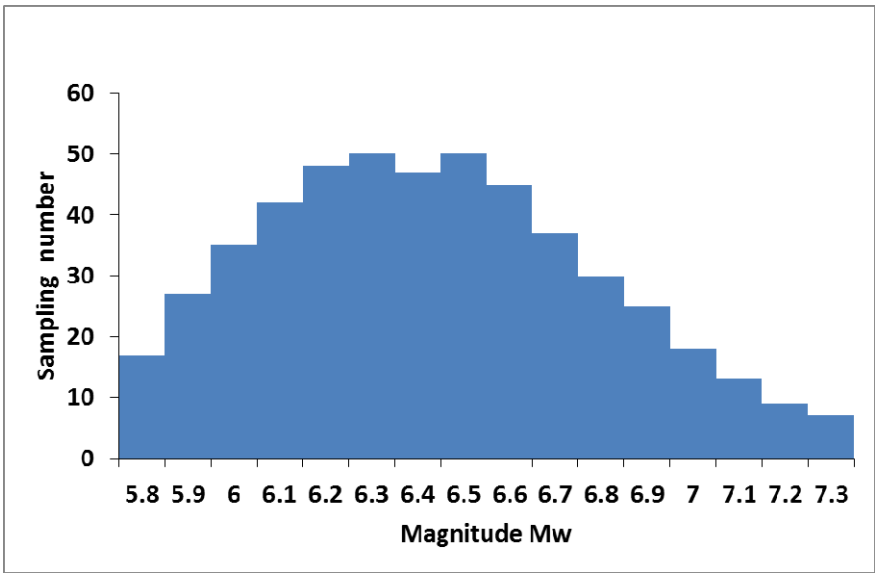

Figure 36 : Example of irregular trapezoidal distribution to generate the maximum magnitude sample.

5.1.4 Comparison in terms of hazard results

The lower and upper bounds of the Mmax distributions obtained for the three models illustrated above are compared in Table 4. Note that the simple comparison of lower and upper bounds is not fully representative of the actual differences in the distributions of Mmax between the two limits.

In terms of lower bound, we note that the values for model 2 and model 3 are quite similar because they are both based on observed seismicity. Model 1 provides the largest lower bounds based on conservative hypotheses.

Considering the upper bounds, model 1 and model 2 provide similar values that are also similar to values used in the 2012 model, whereas model 3 provides the slightly lower values.

	SIGMA 2012		Model 1		Model 2		Model 3	
	min	*max*	*min*	*max*	*min*	*max*	*min*	*max*
LAN	6.3	7	6.5	7.1	5.5	7.3	5.5	6.5
CBD	6.3	7	6.5	7.1	5.5	7.3	5.5	6.5
MPR	6.3	7	6.5	7.1	5.5	7.3	5.5	6.5
ACC	6.3	7	6.5	7.1	5.5	7.3	5.5	6.8
PCP	6.3	7	6.5	7.1	5.9	7.3	6.2	6.8
ALS	6.3	7.3	6.9	7.5	5.5	7.5	5.5	7
NDC	6.3	7.3	6.9	7.5	5.5	7.5	5.8	7
OBM	6.3	7.3	6.9	7.5	5.5	7.5	5.8	7

Table 4 : Mmax lower and upper bounds obtained by the different methods applied in this test.

The three alternative models for Mmax distributions are tested in the hazard calculation considering the logic tree for SM1. For model 2 and model 3 the same approach of the 2013 study is followed, i.e., a 100 random samples are drawn from each Mmax and used in the hazard calculation following a Monte Carlo approach.

Figure 37 shows the hazard curves, for PGA and PSA at 1s, obtained at the three sites considering the alternative distributions of Mmax. Table 5 summarizes the results of this test in terms of percentage differences with respect to spectral acceleration obtained in the 2012 study for three spectral periods and three return periods (475, 10000 and 100000 years).

As expected the difference between the four models increase with return period and is more evident for PSA at 1s than for PGA. In general, Model 1 provides the largest acceleration values. The 2012 SIGMA results are quite consistent with Model 1 except for Marseille site (low seismicity area) where Model 1 provides larger acceleration values by about 7% for PGA and 27% for 1s PSA. Model 3 provides the lowest acceleration values (about 15% lower than the 2012 results for PGA and 35% for PSA at 1s).

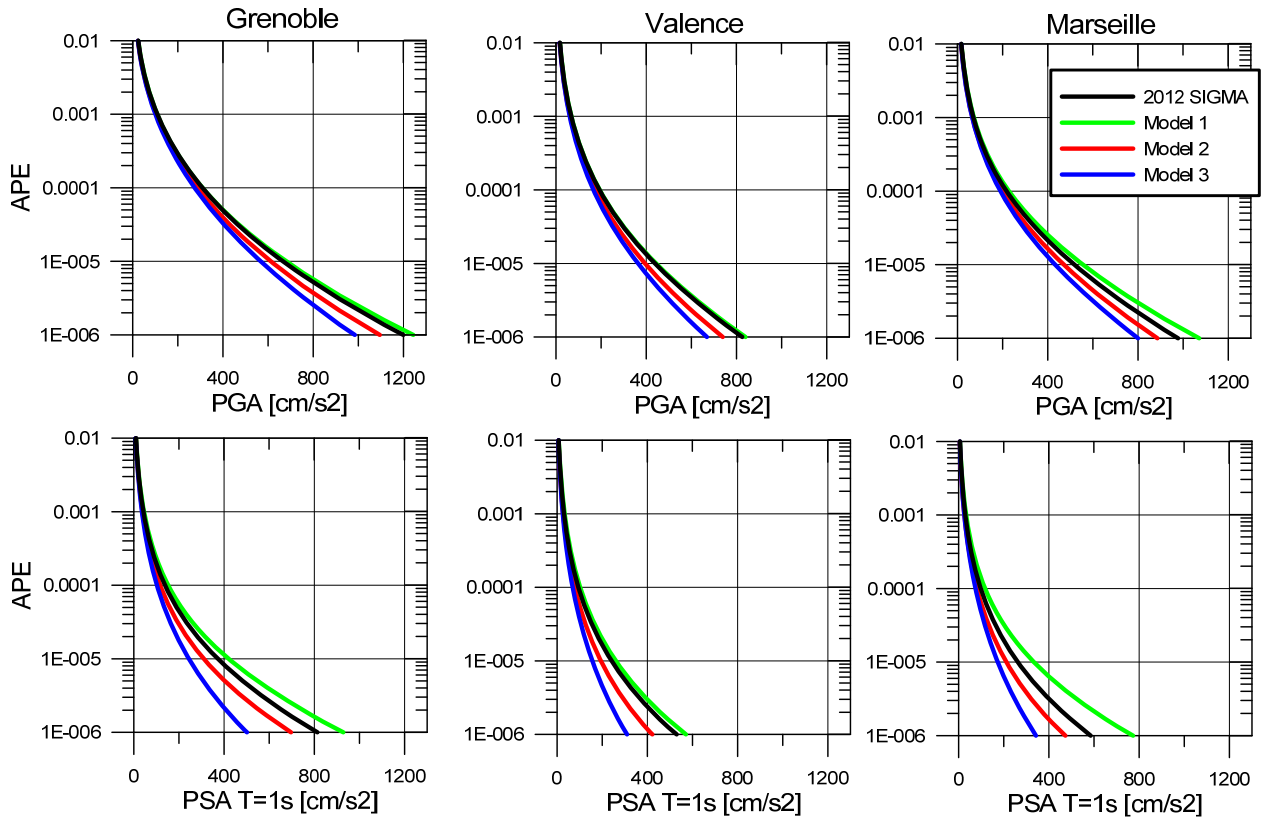

Figure 37 : Effect of the Mmax distribution on the PGA and PSA (T=1s) mean hazard curves for the three sites. Only SM1 is considered for this test.

	Model 1			Model 2			Model 3		
	GRENOBLE								
	RP475	RP10000	RP100000	RP475	RP10000	RP100000	RP475	RP10000	RP100000
PGA	-0.1 %	0.0 %	2.0 %	-5.0 %	-6.7 %	-8.1 %	-7.4 %	-11.0 %	-14.9 %
0.2s	0.7 %	1.0 %	3.4 %	-5.1 %	-7.4 %	-9.2 %	-7.5 %	-12.1 %	-16.4 %
1s	6.6 %	9.7 %	13.2 %	-9.2 %	-15.2 %	-16.8 %	-12.7	-25.8 %	-34.5 %
	VALENCE								
	RP475	RP10000	RP100000	RP475	RP10000	RP100000	RP475	RP10000	RP100000
PGA	1.2 %	0.4 %	1.1 %	-6.3 %	-8.9 %	-10.0 %	-8.7 %	-13.9 %	-17.0 %
0.2s	2.0 %	1.2 %	1.9 %	-6.5 %	-9.2 %	-11.4 %	-8.8 %	-14.3 %	-19.2 %
1s	7.9 %	8.4 %	7.7 %	-12.8	-16.9 %	-19.7 %	-16.5	-27.1 %	-35.3 %
	MARSEILLE								
	RP475	RP10000	RP100000	RP475	RP10000	RP100000	RP475	RP10000	RP100000
PGA	2.3 %	5.0 %	7.3 %	-5.9 %	-8.3 %	-9.2 %	-6.1 %	-12.8 %	-16.3 %
0.2s	2.8 %	5.8 %	9.4 %	-6.2 %	-8.7 %	-10.4 %	-6.3 %	-13.1 %	-18.6 %
1s	8.8 %	19.6 %	27.4 %	-13.1	-17.3 %	-19.3 %	-13.6	-23.8 %	-33.7 %

Table 5 : Percentage difference with respect to acceleration values obtained in the 2012 study for SM1.

Figure 38 shows the difference between the four Mmax models in terms of uncertainties. For this test, we selected only one GMPE (BA08) in order to avoid mixing uncertainties due to Mmax with those due to the use of several GMPEs. We note that the uncertainties due to the different Mmax models are quite different. The uncertainties in the hazard calculated with the different models are directly related to the uncertainties in the input Mmax. Model 1 provides the lowest uncertainties because the input Mmax distribution is quite narrow. On the other hand, Model 2 provides the largest uncertainties because the distribution of the input Mmax is quite large. Finally, as expected, the uncertainties are larger for spectral acceleration at 1 s than for PGA, because the scaling of ground motion with magnitude is stronger at low frequencies.

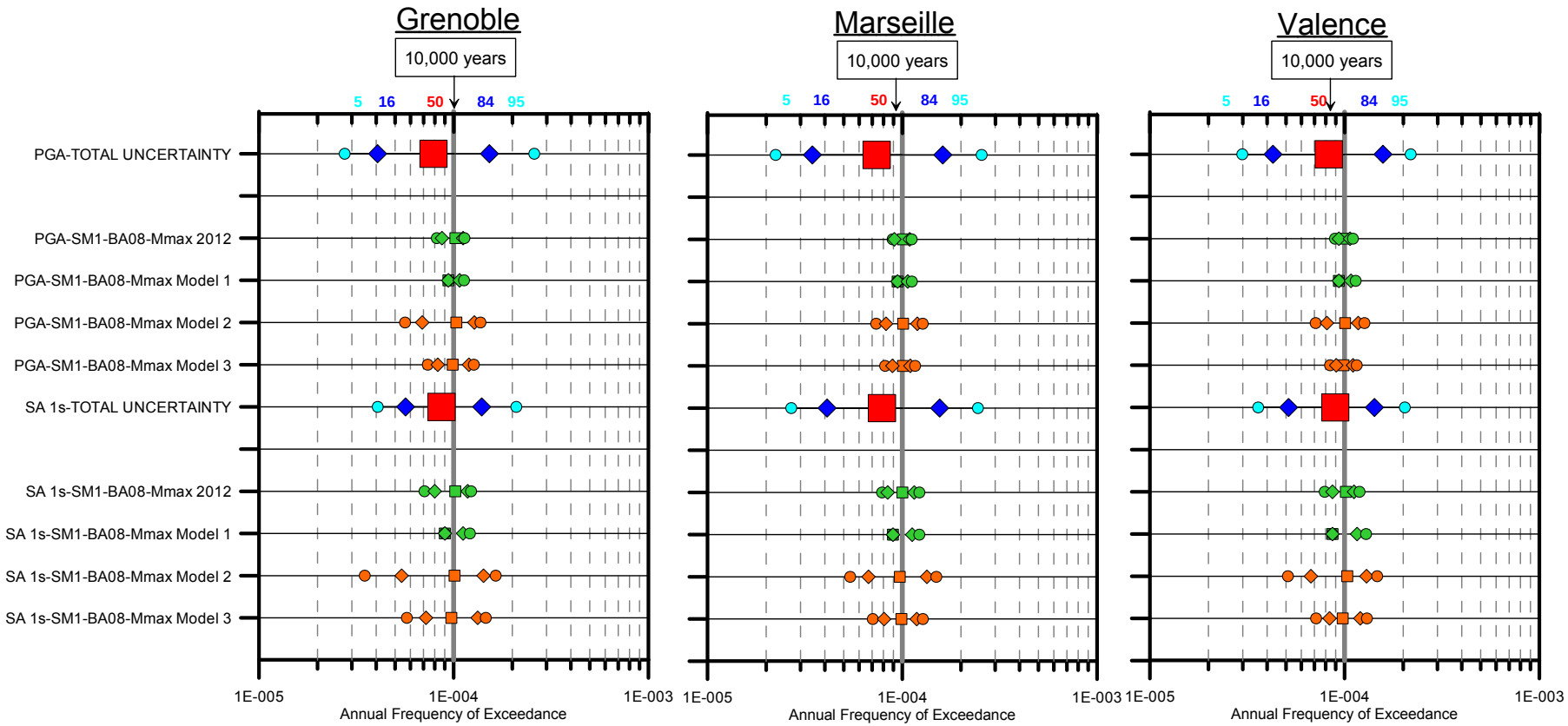

Figure 38 : Tornado diagrams at 10,000 years return period for the three sites showing, for Seismotectonic Model 1 and BA08 GMPE, the uncertainties due to the different Mmax models. The results are for two spectral periods (PGA and 1s).

6. SENSITIVITY TO DEPTH ALEATORY UNCERTAINTY

6.1 ALTERNATIVE DEPTH DISTRIBUTION BASED ON SI-HEX CATALOGUE

The Si-Hex catalogue represents the most recent and complete compilation of earthquakes for metropolitan France. A significant amount of work has been dedicated to relocate events and to better constrain the earthquakes depth, although this parameters remain poorly known for a large number of events. The 2012 SIGMA model considers a uniform distribution of earthquakes hypocenters with depth within the seismogenic layers of each of the considered seismotectonic model.

We performed a statistical analysis on earthquake depths for the Si-Hex catalogue, reported in Annex 3. The aim is to try to obtain some insight that may drive the choice of the aleatory distribution of depths used in the PSHA. As shown in Annex 3, due to the relatively small number of events for Mw larger than 3.5 – 4.0, in the last 50 years in metropolitan France, it is hard to draw any statistical conclusion on the distribution of earthquake depths for magnitudes of interest for PSHA. Anyway, in order to test alternative hypothesis with respect to the assumption of a uniform distribution in the 2012 SIGMA model we considered two alternative aleatory distributions of earthquake depths:

- A trapezoidal distribution with uniform probability down to the mean seismogenic depth and then a decreasing probability with increasing depths (Figure 39a);
- A triangular distribution centered on the mean seismogenic depth (Figure 39b).

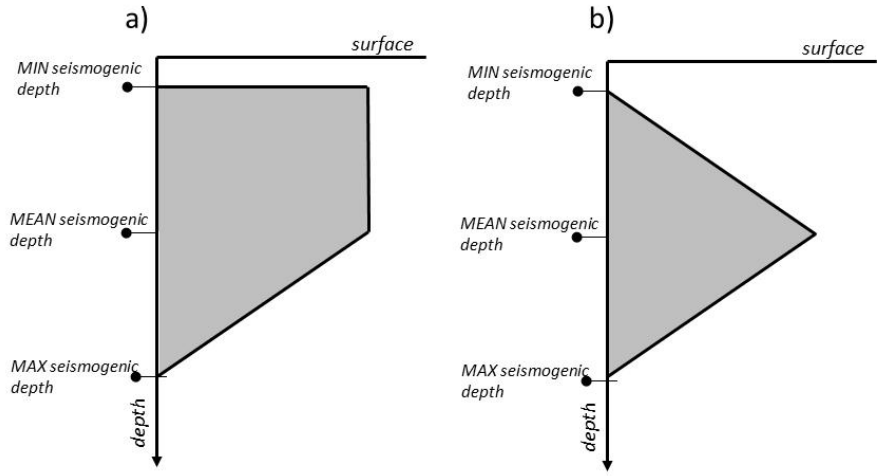

Figure 39 : Sketch of the alternative depth distributions considered in this test.

The results in terms of hazard curves obtained with the uniform, trapezoidal and triangular aleatory depth distributions are presented in Figure 40 and Figure 41 for the Grenoble and Valence sites respectively considering seismotectonic model 1. We did not consider the Marseille site in this test because the thickness of the seismogenic layer for the zone dominating hazard at this site is quite small and no significant changes are expected.

Note that the results of this test may depend on the considered GMPE. Here we used the Zhao et al., 2006 model which is based on rupture distance. It is evident that using a GMPE based on Joyner-Boore distance will result in no impact of the depth distributions on the calculated hazard.

Analysis of the results shows the following points:

- For the two sites analyzed and for the three spectral periods considered, mean hazard curves resulting from the uniform and the triangular distribution are similar while the mean hazard curves from the trapezoidal distribution are always slightly higher. This result can be explained by the fact that with the trapezoidal distribution, the majority of the earthquakes occurs in shallowest part of the seismogenic depth which leads to an increase in terms of ground motions levels;
- For Grenoble site, the differences with respect to the uniform distribution, for PGA at 100,000 years return period, is about 3% and 12% for the triangular and for the trapezoidal distribution, respectively. For Valence site, the differences are around 1% and 6% for the triangular and for the trapezoidal distribution, respectively.

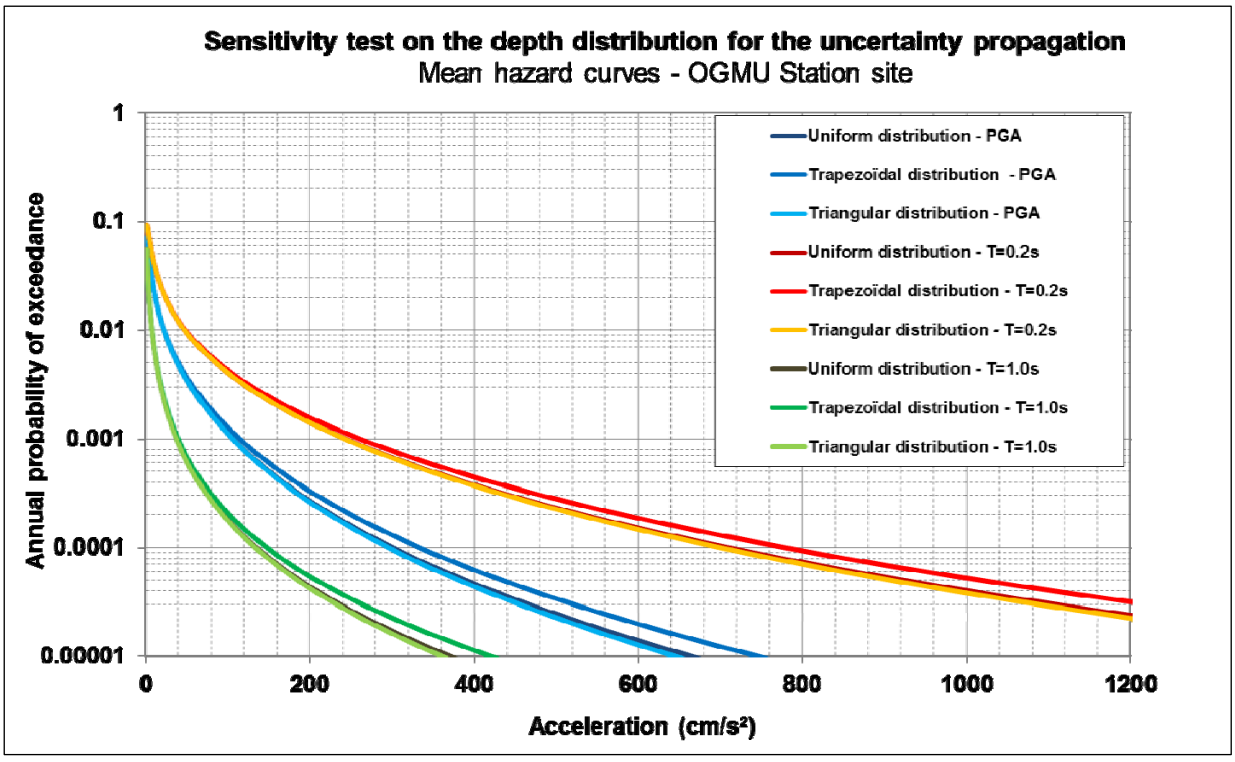

Figure 40 : Grenoble site - Impact of the alternative depth distributions for the uncertainty propagation in terms of mean hazard curves at three specific spectral periods (PGA, 0.2s and 1.0s)

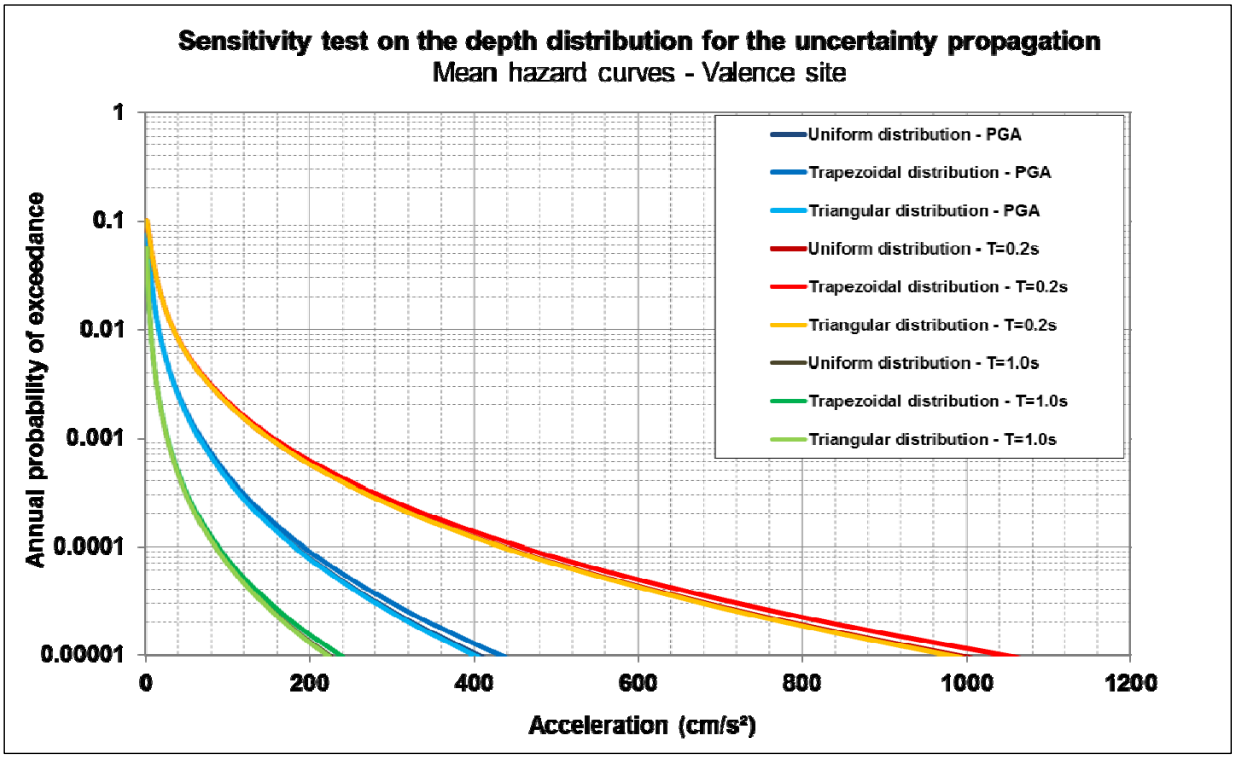

Figure 41 : Valence site - Impact of the alternative depth distributions for the uncertainty propagation in terms of mean hazard curves at three specific spectral periods (PGA, 0.2s and 1.0s)

6.2 MAGNITUDE-DEPENDENT DEPTH DISTRIBUTION

In this section, we test the effect of using a magnitude-dependent depth distribution of earthquake hypocenters within a source zone. The rationale behind this test is that the focal depth of large events is generally larger with respect to small events. This feature is not considered in the SIGMA 2012 model as a uniform distribution of hypocenters between the minimum and maximum considered seismogenic depths is used, regardless the earthquake magnitude.

We present a simple test performed for the Grenoble site in order to show the impact of the M-dependent depth distribution. For each site, we considered the areal sources that contribute to the hazard (see Table 1) and their minimum and maximum seismogenic depths. A new aleatory distribution of focal depths is defined in which the events with Mw < 6 are uniformly distributed within the whole seismogenic depth, whereas the largest events (M>=6) are uniformly distributed only at depth larger than 10 km (Figure 42).

The hazard is calculated using the Akkar et al. (2014) GMPE based on hypocentral distance in order to use point sources and thus to capture only the effect of the change in depth distribution without mixing the effect of rupture dimension modeling.

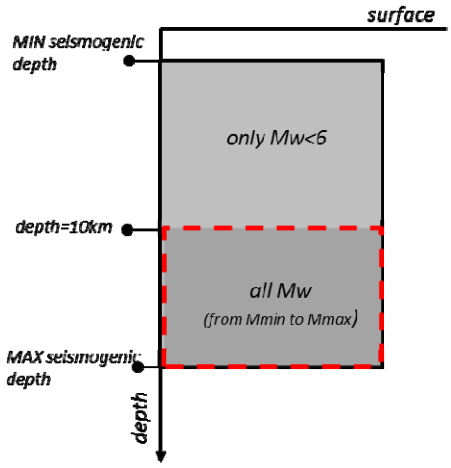

Figure 42 : Sketch of the Mw-dependent depth distribution considered in this study.

Figure 43 presents the hazard curves calculated at Grenoble for PGA and PSA at 1s considering the magnitude-dependent depth distribution. We presented the results for two alternative maximum magnitudes representing the mean and the maximum Mmax considered for the zones dominating the hazard at Grenoble. The M-dependent depth model produces lower hazard and the difference between the two depth models increases with decreasing APE. This is expected because at low APE the contribution of large magnitude events increases with respect to that of small magnitudes and in the M-dependent model the large magnitudes are confined to larger depths. The difference between the two depth models at APE=10^{-5} (100, 000 years return period) is of the order of 5% for PGA and smaller for PSA at 1s, considering the mean Mmax=6.7. The difference reaches 7% for PGA when considering the maximum Mmax= 7.3.

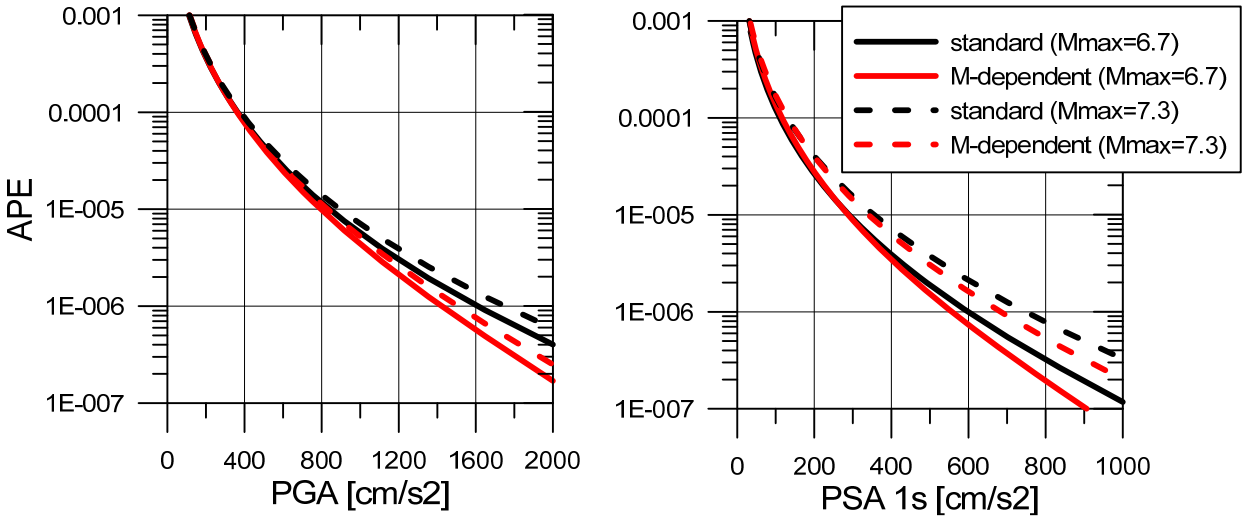

Figure 43 : Hazard curves at Grenoble for PGA (left) and PSA at 1s (right) obtained using the M-dependent depth distribution (in red) and the standard uniform depth distribution between the minimum and maximum seismogenic depths (in black). The hazard curves are calculated for two Mmax values. The results are obtained considering SM1 only.

7. SENSITIVITY TO THE SMOOTHED SEISMICITY APPROACH

In the 2012 study, the smoothed seismicity approach proposed by Woo (1996) was tested using the SIGMA catalogue and one single GMPE (Berge-Thierry et al., 2003). In this study, we completed the test on the smoothed seismicity approach by using the set of 4 GMPEs selected in the 2012 study. The aim is to provide a more meaningful comparison of the seismic hazard obtained using the classical approach based on seismotectonic zonation and the smoothed seismicity approach. A careful description of the performed sensitivity test and a discussion of the results are reported in Annex 5. Here we briefly summarize the main results.

Figure 44, Figure 45 and Figure 46 show the comparison of mean UHS calculated using the standard areal source zones approach and the smoothed seismicity approach at three return periods (475, 10 000 and 100 000 years) for the three sites. For the comparison, we considered the whole logic tree and for the smoothing approach the three different kernels (see Annex 5) are considered as different branches of the logic tree with equal weights.

In comparing the results we have to consider that in the standard smoothing approach by Woo (1996) the Mmax is limited to the maximum observed magnitude in the catalogue.

The results show that:

- The differences between the smoothing and zoning approach increases with return period, and the smoothing approach provides smaller spectral accelerations;
- Differences are larger for long spectral periods whereas at short spectral periods (T<0.1s) the two approaches are consistent (at least in Grenoble and Valence);
- The results of the two approaches in Marseille are quite consistent for all spectral periods (although the smoothing approach provides slightly larger values).

The main reasons for such differences are illustrated in Annex 5.

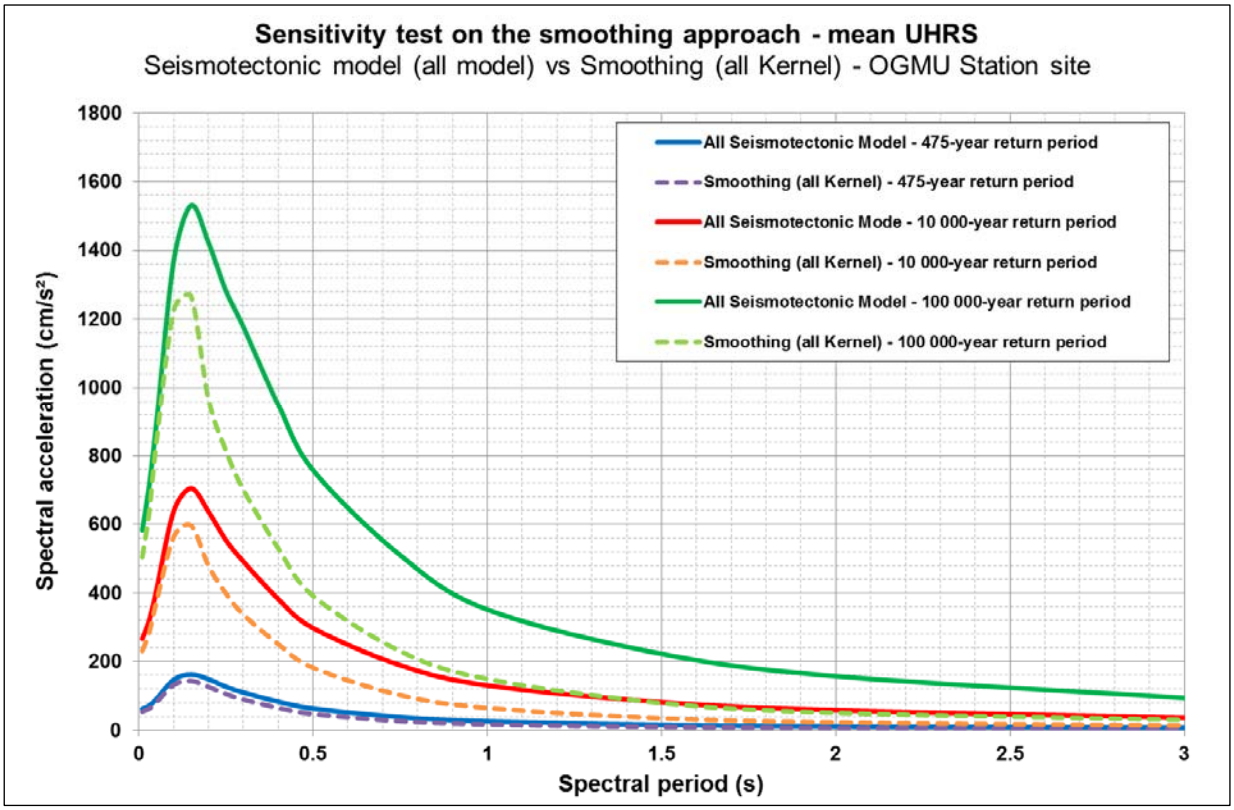

Figure 44 : Grenoble Site (OGMU RAP Station) –Comparison between the mean UHS calculated with the smoothing approach (dashed lines) and the classical zoning approach (solid lines) at three return periods: 475 years, 10 000 years and 100 000 years – Horizontal component, 5% damping

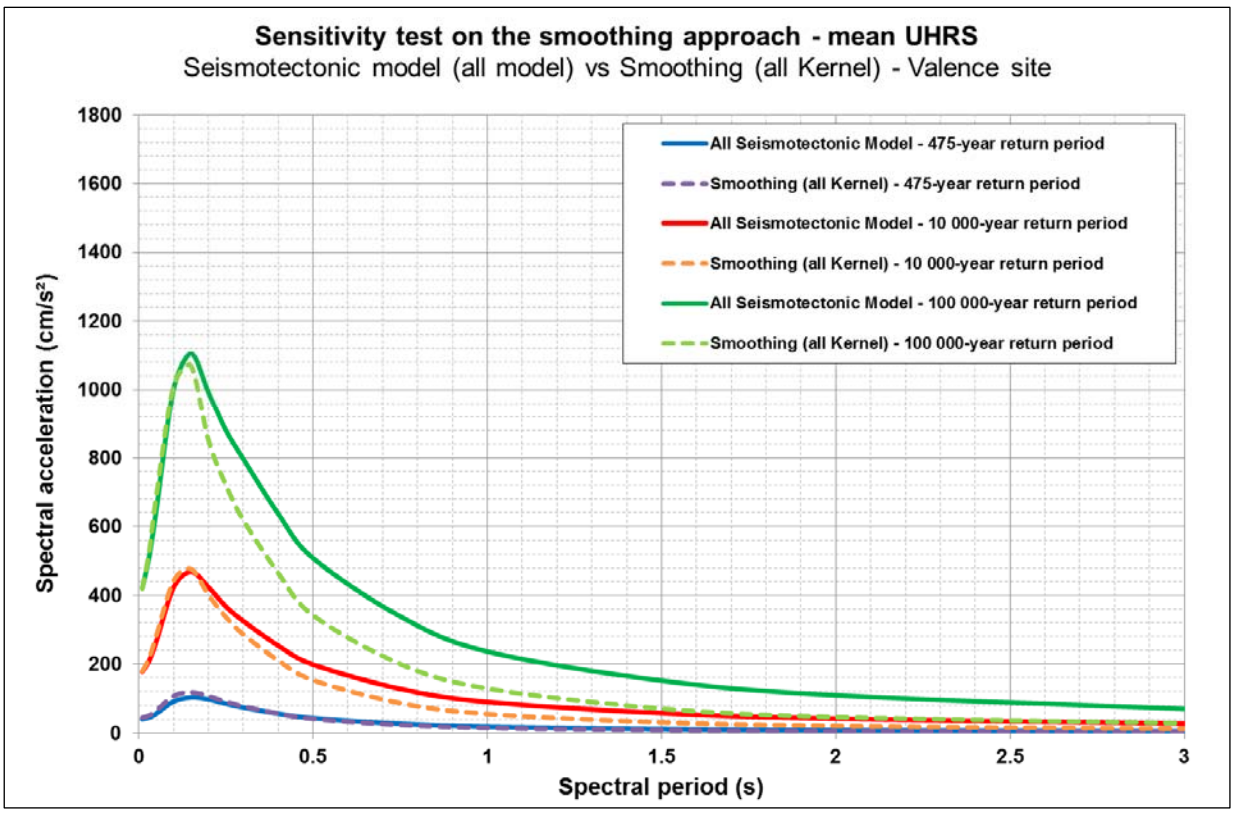

Figure 45 : Valence Site – Comparison between the mean UHS calculated with the smoothing approach (dashed lines) and the classical zoning approach (solid lines) at three return periods: 475 years, 10 000 years and 100 000 years – Horizontal component, 5% damping

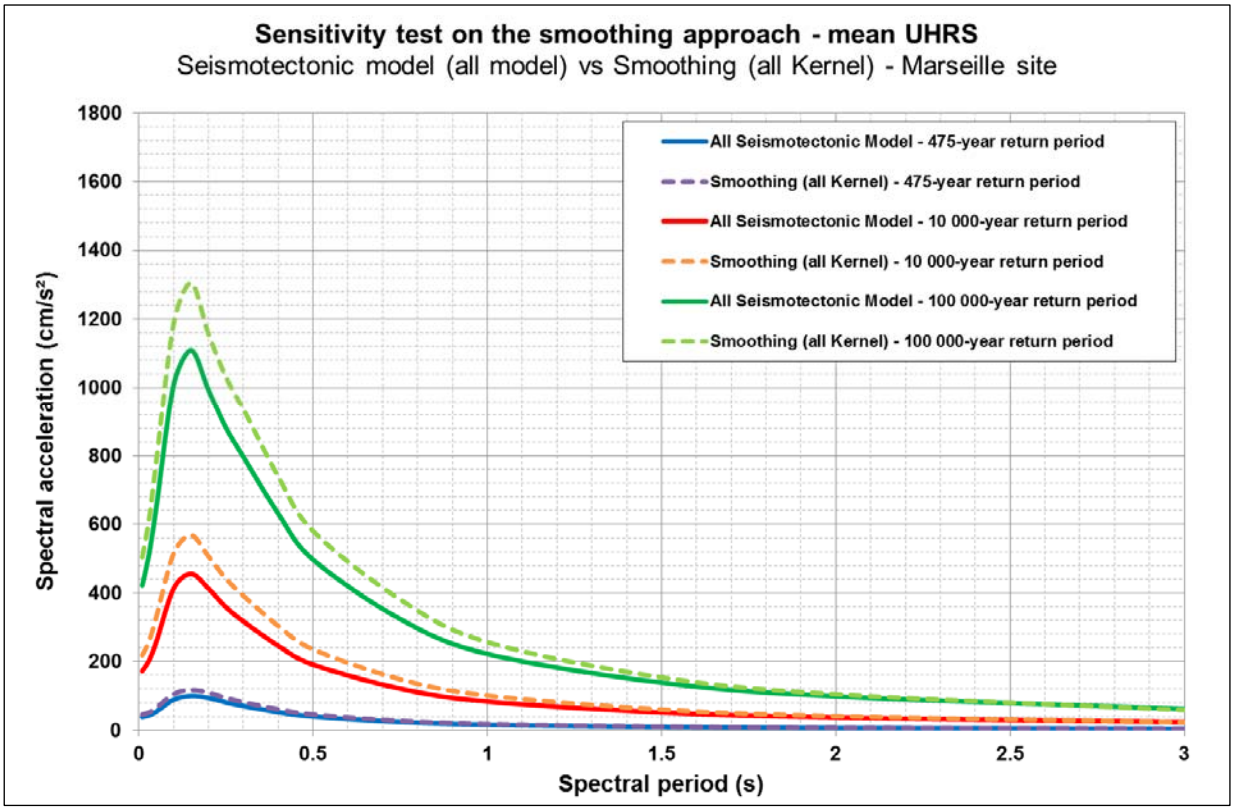

Figure 46 : Marseille Site –Comparison between the mean UHS calculated with the smoothing approach (dashed lines) and the classical zoning approach (solid lines) at three return periods: 475 years, 10 000 years and 100 000 years – Horizontal component, 5% damping

8. SENSITIVITY TO NEW GMPES

Several new GMPEs recently developed within the framework of international projects have been tested in the PSHA for the three considered sites. The aim is to assess the impact of the new GMPEs on the uncertainties on the mean hazard and to quantify the sensitivity of hazard to new GMPEs, compared to the ones used in the initial model.

The main characteristics of each new GMPEs are summarized below.

8.1 EMPIRICAL GMPES BASED ON RESORCE DATABASE

Within SIGMA WP2 a reference strong motion database for Europe and Middle East (RESORCE) has been developed. Several GMPEs have been derived using this common database (Douglas et al., 2014). These new models are all consistent in terms of input parameters (e.g., distance metric, magnitude definition, style-of-faulting). Among the derived GMPEs some of them (e.g., Akkar et al., 2014; Bindi et al., 2014) follow a standard parametric approach. Conversely, other models (e.g., Derras et al., 2014) are derived following a non-parametric approach. These models do not assume a specific functional form but rather let the data define the most suitable model. The advantage of these models is that potential bias related to the assumption of the fixed function form in standard parametric GMPEs is removed. The non-parametric GMPEs represent an alternative type of models with respect to standard parametric GMPEs.

8.1.1 Bindi et al. (2014) [Bindi14]

This GMPE model was developed using the RESORCE strong motion database for use in Europe and the Middle East. The model is considered valid for distances up to 300 km, hypocentral depth up to 35 km, and magnitudes from 4.0 to 7.6. Model coefficients were developed for both Joyner-Boore distance (R_{JB}) and hypocentral distance (Rhyp), as well as for site characterizations based on EC8 soil classification and on measured Vs30. The model supports four classes of style-of-faulting: normal, reverse, strike-slip, and unspecified (note that the unspecified style-of-faulting can only be used with site characterization based on EC8 soil classifications).

Specific application: the hazard calculations are performed considering the model based on R_{JB} and Vs30.

8.1.2 Akkar et al. (2014) [Akkar14]

This model corresponds to one of the most recent GMPEs developed for Europe and the Mediterranean region. It has been developed in the framework of SHARE and SIGMA projects. This GMPE is defined using 1041 records associated with 221 crustal earthquakes. The seismic database contains earthquakes with moment magnitudes from 4.0 to 7.6 for distances lower than 200 km. This GMPE allows consideration of nonlinear site effects as a function of PGA and Vs30, focal mechanism, and uses different distances (Joyner-Boore, epicentral and hypocentral distances). The predicted values correspond to the geometric mean of the horizontal components. This model can be considered as an evolution of the Akkar & Bommer (2010) GMPE.

Specific application: the hazard calculations are performed considering the model based on R_{JB}.

8.1.3 Derras et al., 2014 [Derras14]

This study makes use of the Artificial Neural Network method (ANN) for the derivation of predictive ground-motion models from a subset of the RESORCE (Reference database for Seismic ground-motion prediction in Europe). The derived model is completely data-driven and no a priori assumption is made in terms of functional form describing the magnitude, distance and site scaling. Only shallow earthquakes (depth smaller than 25 km) and recordings corresponding to stations with measured Vs30 properties have been selected. Five input parameters were selected: the moment magnitude Mw, the Joyner–Boore distance R_{JB}, the focal mechanism, the hypocentral depth, and the site proxy Vs30. The ground motion is predicted in terms of PGA and PSA at 62 periods from 0.01 to 4 s.

The used dataset contains 1088 records from 320 earthquakes, with mainly Italian and Turkish origins, covering a magnitude range 3.6–7.6 and a distance range 1-547 km. The range of validity recommended by the authors is defined by Mw [4–7], R_{JB} [5–200 km] and Vs30 [200–800] m/s.

Specific application: the hazard calculations are performed considering a fixed depth=10km for all the sources. This is in overall agreement with mean depth of the most contributing sources (see Table 1).

8.1.4 Ameri 2013 (SIGMA-2013-D2-92)

This model is developed within the framework of the WP2 of SIGMA project, using an updated version of the RESORCE database (detailed in SIGMA-2013-D2-91). The updated version includes French and Swiss data and thus the dataset used for the GMPE derivation is different with respect to the ones used in the GMPEs detailed above, especially for the moderate-magnitudes range. The base GMPE is derived as a function of Mw, distance (R_{JB} and epicentral), style-of-faulting and site class (EC8 soil types). Moreover, a regional model for France is introduced in order to explain the dependency of the residuals to the stress-parameter available for a substantial number of French events. The stress-parameter model is active for magnitudes smaller than 5 and then tapers to zero (i.e., no stress

dependency) for larger magnitudes. The dataset contains about 1700 records from 300 earthquakes. The range of validity for this model is Mw [3–7.2], R_{JB} [1–200 km].

Specific application: the hazard calculations are performed considering two different models. In the first case, the stress-parameter model is used and a value of 10 bars is assumed based on the average stress drop obtained by Drouet et al.(2010) for the French Alps. In the second case, no stress drop model is used and the ground motion is predicted from the generic model without considering regional features.

8.2 STOCHASTIC GMPE FOR FRANCE

An alternative to the use of records from past earthquakes comes from the advances in understanding the earthquake source and wave propagation processes. Simple numerical techniques, based on point-source or finite-fault stochastic simulations, can be used to calculate the ground motions for PSHA. A dataset of simulated ground motions is constructed for a variety of magnitude and distances (and other parameters). The simulation approach is usually relatively simple (e.g. SMSIM, Boore 2003) and the main input parameters of the model are derived by analysis of records from small events. This data set is then used to derive synthetic GMPEs in a similar way as done for empirical GMPEs.

In the framework of SIGMA, stochastic GMPEs have been proposed for France (SIGMA-2013-D2-71). The stochastic GMPEs developed for France-Alps region are used in the hazard calculation at the three selected sites and the results compared with those obtained using other empirical GMPEs and with the set of GMPEs used in the SIGMA preliminary hazard study.

The stochastic GMPE for France has been developed considering several models of the stress parameter ($\Delta\sigma$), including or not magnitude dependency of the stress parameter. Uncertainties in the $\Delta\sigma$ model, should be addressed in a logic tree framework. In any case, in report SIGMA-2013-D2-71, the different models have been tested against observed data and the results showed that the models with the magnitude-dependent stress parameter are leading to better results than the models with constant stress parameter. Moreover, better fit with the data is obtained for the model with a stress parameter for large events of 5 MPa (50 bars).

Specific application: the hazard calculations are performed considering two different stress-parameter models. In both cases the stress parameter is magnitude dependent and the two model differ for the stress values assumed for large-magnitude events. In the first case, a value of 50 bars is used for the large Mw events, whereas, in the second case a value of 100 bars is assumed.

8.3 EMPIRICAL GMPES FROM PEER NGA-WEST2 PROJECT

Within the framework of the PEER NGA-West2 project, a new global dataset has been compiled and used to derive several GMPEs. These GMPEs are intended to replace the models that were derived in 2008 within the NGA-West1 project and that were used extensively in several PSHA around the world. Five models have been derived and two of them are tested in the present progress report.

8.3.1 Abrahamson et al. (2014) [ASK14]

The Abrahamson et al. (2014) model is an update of the Abrahamson and Silva (2008) GMPE based on the PEER NGA-West2 database. The model is considered valid for distances up to 300 km, magnitudes from 3.0 to 8.5, and spectral periods from 0.0 to 10.0 seconds. As in the 2008 model, this model is sensitive to site conditions including Vs30 and depth to Vs = 1000 m/s ($Z_{1.0}$), however, nonlinear site effects in the ASK13 model are based on the spectral

accelerations at the period of interest rather than PGA. Source terms include style-of-faulting and depth to top-of-rupture (Ztor), and hanging wall effects include distance scaling off of the ends of fault ruptures based on source-to-site azimuth. The ASK13 model also includes regional distance and Vs30 scaling factors.

Specific application: the hazard calculations are performed by using the correlation equation between Vs30 and $Z_{1.0}$ proposed by the Authors to derive a value of $Z_{1.0}$. The Ztor parameter has been fixed to 10km.

8.3.2 Boore et al. (2014) [BSSA14]

The Boore et al. (2014) model was developed using the PEER NGA-West2 database following the methodology of the Boore and Atkinson (2008) model. The BSSA13 model is considered valid for magnitudes from 3.0 to 8.5 for strike-slip and reverse-slip events and from 3.0 to 7.0 for normal-slip events, distances up to 400 km, and site conditions with Vs30 from 150 to 1500 m/s and Z1.0 from 0.0 to 3.0 km. Model coefficients are provided for spectral periods from 0.0 to 10.0 seconds. The base-case model is the Boore and Atkinson (2008) model, with updated coefficients based on the new NGA-West2 data. BSSA13 includes optional adjustment factors for basin depth and regional path scaling that can be applied to the base-case GMPEs. BSSA13 also incorporates magnitude, distance, and site condition effects into the between-event and within-event components of standard deviation.

Specific application: the hazard calculations are performed by using the correlation equation between Vs30 and $Z_{1.0}$ proposed by the authors to derive a value of $Z_{1.0}$.

8.4 HAZARD SENSITIVITY TO NEW GMPES

The hazard results obtained using the new GMPEs are presented in this section and are compared to the ones obtained with the 4 GMPEs selected in the initial model. For the purpose of the sensitivity analysis, the test is performed using a single seismotectonic model (SM1) and a single earthquake catalogue (catalogue 1), assuming that the variation between the hazard curves calculated for the different GMPEs will essentially be similar for the three seismotectonic models (as a first approximation).

The hazard curves obtained at the three sites using the new GMPEs are presented for PGA and T=1s in the Annex 6.

The tornado diagrams for the three sites, the three spectral periods and for 475 and 10,000 years return periods are presented in Figure 47 and Figure 48, respectively. In each diagram, the hazard uncertainties obtained for SM1 in the initial PSHA model are also reported (considering all GMPEs), as a reference.

The main results are:

- For 475 years return period, the new GMPEs generate on average smaller hazard than the set of GMPEs initially selected. This is visible at the three sites and for the three considered spectral periods. For 10,000 years return period, the new GMPEs provide hazard values that are, on average, consistent with the previous GMPEs (slight larger hazard is obtained in Grenoble);
- The variability among the hazard obtained with the new GMPEs is smallest at T=1s and largest (and quite consistent) for the other two considered spectral periods;
- The largest hazard at both return periods is obtained, for PGA and T=0.2s, using the ASK14 GMPE. This results is largely sensitive to the adopted value of Ztor=10km. As a matter of fact, this parameter is related to the modeling of the fault plane and it is difficult to constrain it in case of areal sources of diffuse seismicity. The choice of Ztor=10km is in agreement with the average depth of the seismogenic layer. Although this

choice can appear too conservative (because the finite-rupture dimension implies a Ztor shallower than the depth of the zone), we stress that the controlling scenario for 475 years (but also for longer return periods) are characterized by magnitudes around 5, for which the point-source approximation applies;

- The smallest hazard at both return periods is obtained, for PGA, using the Ameri (2013) model considering a stress parameter $\Delta\sigma$=10 bars. This value is intended to be representative to the average stress parameter expected in the French Alps for future events with magnitude smaller than 5. As explained above, this value is consistent with the study by Drouet et al. (2010) that observed smaller high-frequency content in the source spectra of Alpine events with respect to other French region. Thus, the results obtained in terms of seismic hazard is expected because the high-frequency ground motion predicted in this case will be generally smaller than the ones derived from the other models that do not consider this feature.

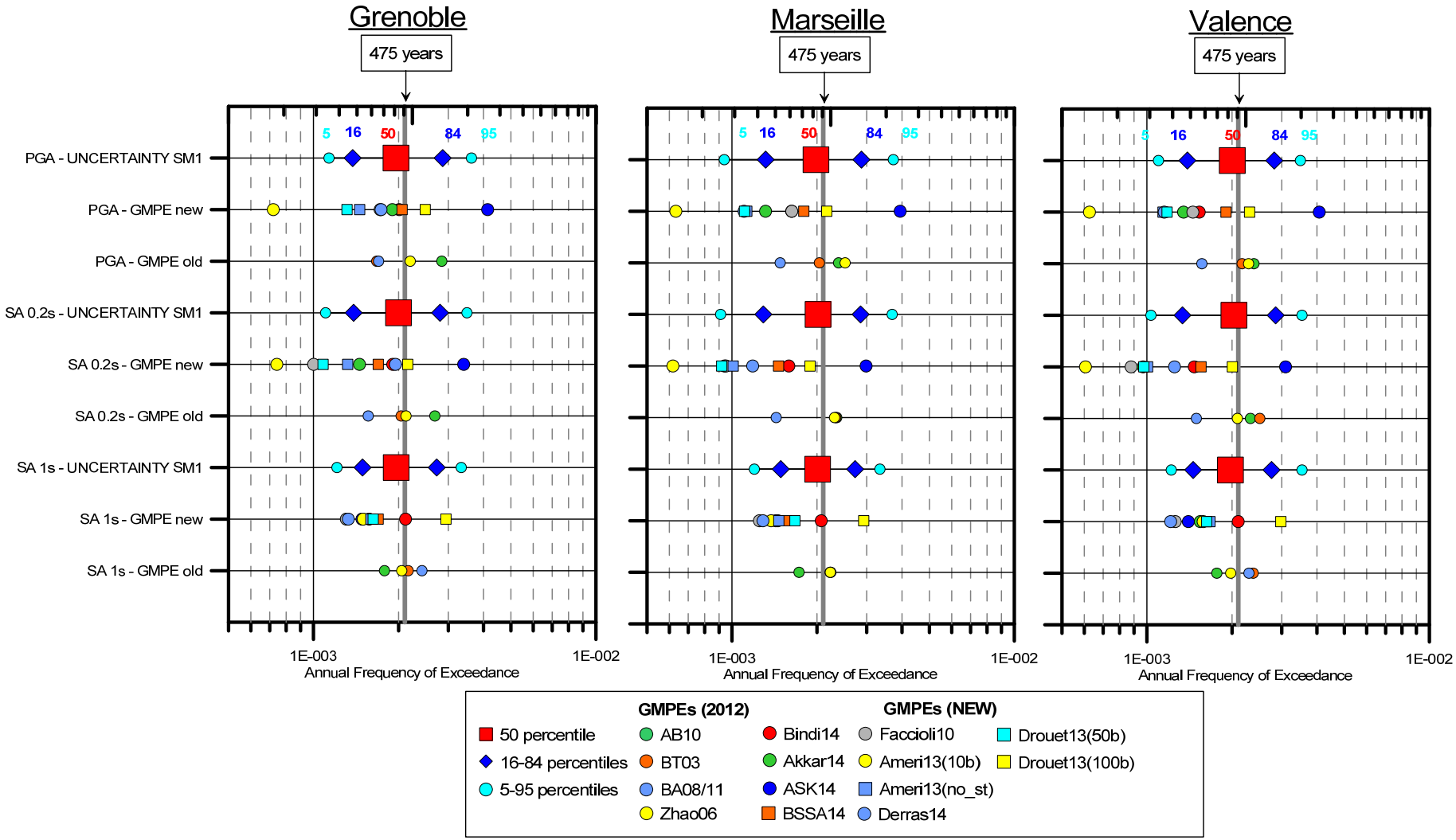

Figure 47 : Tornado diagrams at 475 years return period for the three sites showing the sensitivity of mean hazard to new GMPE at three spectral periods (PGA, 0.2s and 1s). The GMPEs used in the 2012 PSHA model are also shown for comparison. Note that only SM1 is used to illustrate sensitivity in this example.

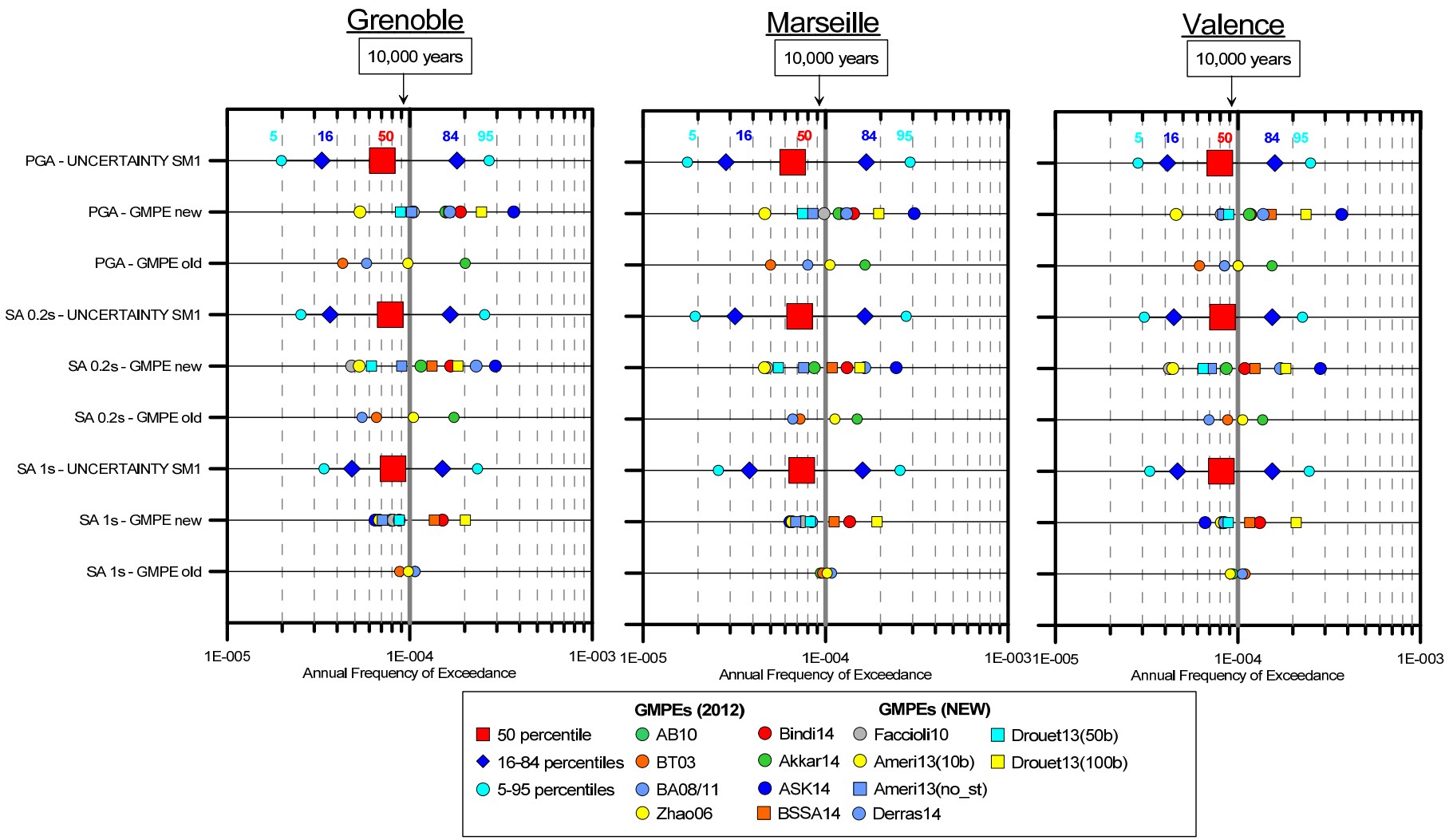

Figure 48 : Tornado diagrams at 10,000 years return period for the three sites showing the sensitivity of mean hazard to new GMPE at three spectral periods (PGA, 0.2s and 1s). The GMPEs used in the 2012 PSHA model are also shown for comparison. Note that only SM1 is used to illustrate sensitivity in this example.

8.1 HAZARD RESULTS USING A NEW SET OF GMPES

Within the SIGMA project an initiative is devoted to perform a site-specific PSHA for few virtual sites in order to illustrate different methodological approaches (the so-called “integrated exercise”). Within this framework, a working group has been organized by the WP2 leaders in order to select a set of GMPEs and relative weights to be used in the integrated exercise. The selected GMPEs are:

- Boore et al., (2014) , weight=0.265;
- Faccioli et al. (2010), weight=0.265;
- Ameri (2013), no stress-parameter model, weight=0.265;
- Bora et al., (2014), weight=0.205;

Although this set of GMPEs and weights have been proposed for the integrated exercise, we believe that this set is a good candidate to replace the set selected for the 2012 study.

Figure 49 compares the mean hazard curves obtained by the 2012 PSHA model with the one obtained replacing the GMPEs (and the weights) with the new set illustrated above. The results clearly show that the new set of GMPEs provides smaller accelerations for return periods shorter than about 5000 years, with respect to the 2012 GMPEs. This is observed for the three sites and the three considered spectral periods. For longer return periods (10, 000 years and longer) the accelerations using the new set of GMPEs are similar to those obtained in the 2012 PSHA. The systematic differences in Figure 49 can be easily explained in terms of the underlying datasets used to derive the new GMPEs with respect to 2012 ones. Indeed, the new selected GMPEs use dataset that with minimum Mw of 3 or 4 (depending on the GMPE) whereas the former set of GMPEs rely on datasets with minimum Mw of about 5. The effect of such reduction in the minimum magnitude of the dataset is that the ground motion predicted for magnitudes around 5 is reduced (Bommer et al., 2007). Because the contribution to the hazard of Mw around 5 is important for relatively short return periods and for the level of seismic activity of the three considered sites, the hazard is reduced.

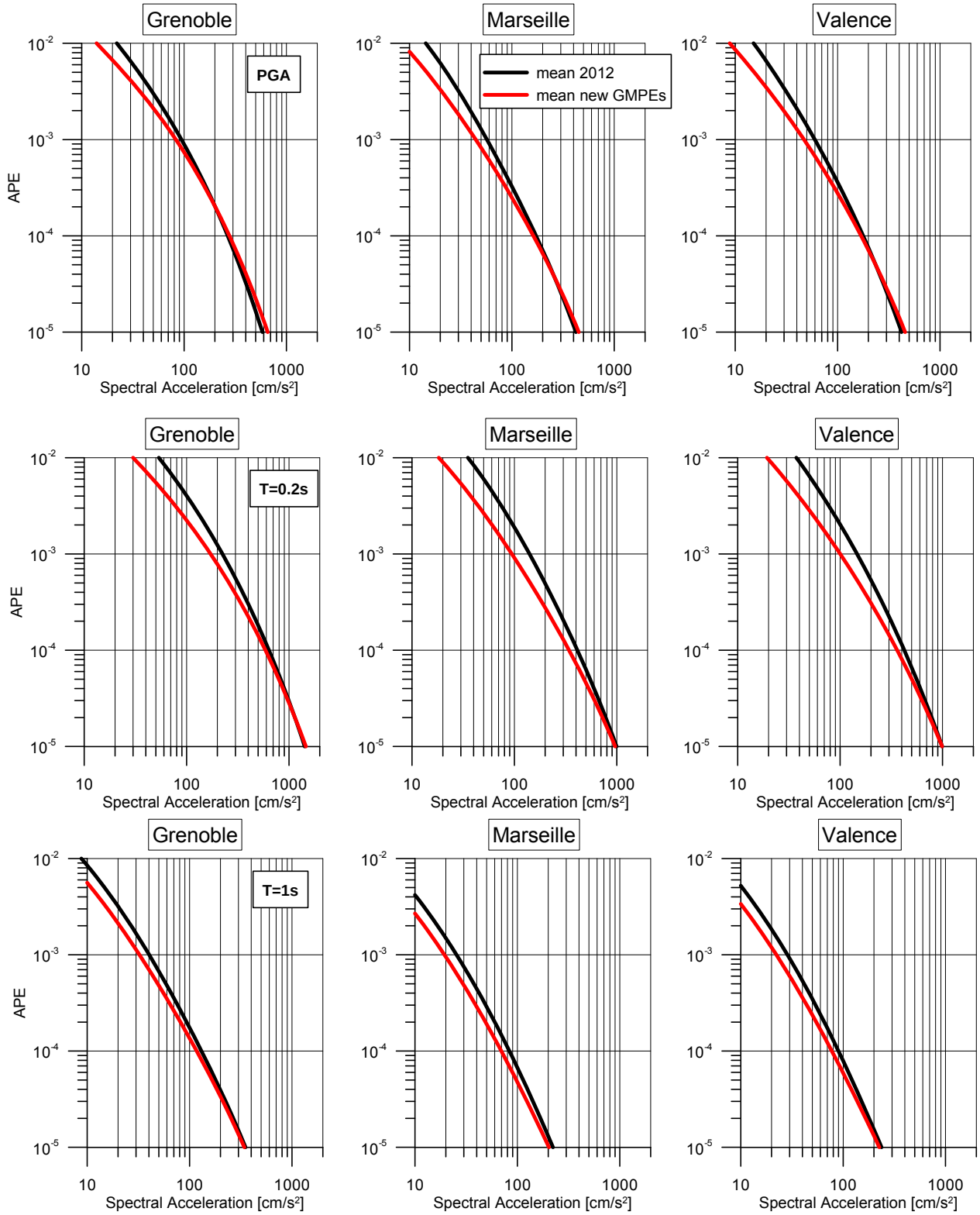

Figure 49 : Comparison of mean hazard curves calculated using the 2012 PSHA model and the new set of GMPEs and weights (see text for explanation). The results are presented for the three sites and considering three spectral periods.

9. SENSITIVITY TO STANDARD DEVIATION (SIGMA) MODEL

In this sensitivity test, we compare the results using two different models for the standard deviation (sigma) of the GMPEs:

- the sigma of each selected GMPE is used as it was published in the relative papers;
- the concept of single-station sigma, SSS (Rodriguez-Marek et al., 2013). This is typically used in site-specific PSHA, where local site amplification and its uncertainty are taken into account in a detailed way. For this reason, the part of the total sigma of the GMPEs that is due to site-to-site variations among sites characterized by the same site parameterization (e.g., Vs30 value) should be removed because these variations are not present when considering a single site. Note, For the purpose of this test we just want to measure the impact of the single-station sigma model on the hazard at specific return periods but formally this approach should only be used in the framework of a site-specific PSHA.

The single station sigma (SSS) model by Rodriguez-Marek et al. (2013) is used in this study as decided within WP2. This single station sigma (σ_{ss}) is defined as follows.

$$\sigma_{ss} = \sqrt{\phi_{ss}^2 + \tau^2}$$

Where τ is the event-to-event variability and ϕ_{ss} is referred to as the event-corrected single-station standard deviation. Rodriguez-Marek et al. (2013) compiled a large database of ground motions from multiple regions to obtain global estimates of these parameters. Results show that the event-corrected single-station standard deviation (ϕ_{ss}) is remarkably stable across tectonic regions. They proposed different model for ϕ_{ss}, a constant model (only function of spectral period), a magnitude-dependent and a distance-dependent model. In this study, we used the constant model reported in Table 6.

Period [s]	Constant ϕ_{ss} [ln]	Constant ϕ_{ss} [$\log_{10}$]
PGA	0.46	0.20
0.1	0.45	0.20
0.2	0.48	0.21
0.3	0.48	0.21
0.5	0.46	0.20
1	0.45	0.20
3	0.41	0.18

Table 6 : Constant model for ϕ_{ss} proposed by Rodriguez-Marek et al. (2013).

The other necessary ingredient for the calculation of σ_{ss} is the event-to-event variability (τ). One possible approach is to use the τ value defined in each GMPE. This way a σ_{ss} is defined for each GMPE. Another approach is to use one single τ value, believed to be the best representative of the event-to-event variability in the study area. This way one single σ_{ss} is defined and used for all GMPEs. This second approach has been used in a recent PSHA SHAAC Level 3 project for a NPP site in South Africa (Rodriguez-Marek et al., 2014; Bommer et al., 2014) and it is used in the present study. During the WP2 Workshop, it was decided to use the τ value of the Ameri (2014) GMPE because this model is the only one considering French events in the dataset.

Figure 50 shows the sigma values of the GMPEs selected for the IE, the ϕ_{ss} proposed by Rodriguez-Marek et al. (2013), the τ of the Ameri (2014) GMPE and the σ_{ss} model finally used in this study.

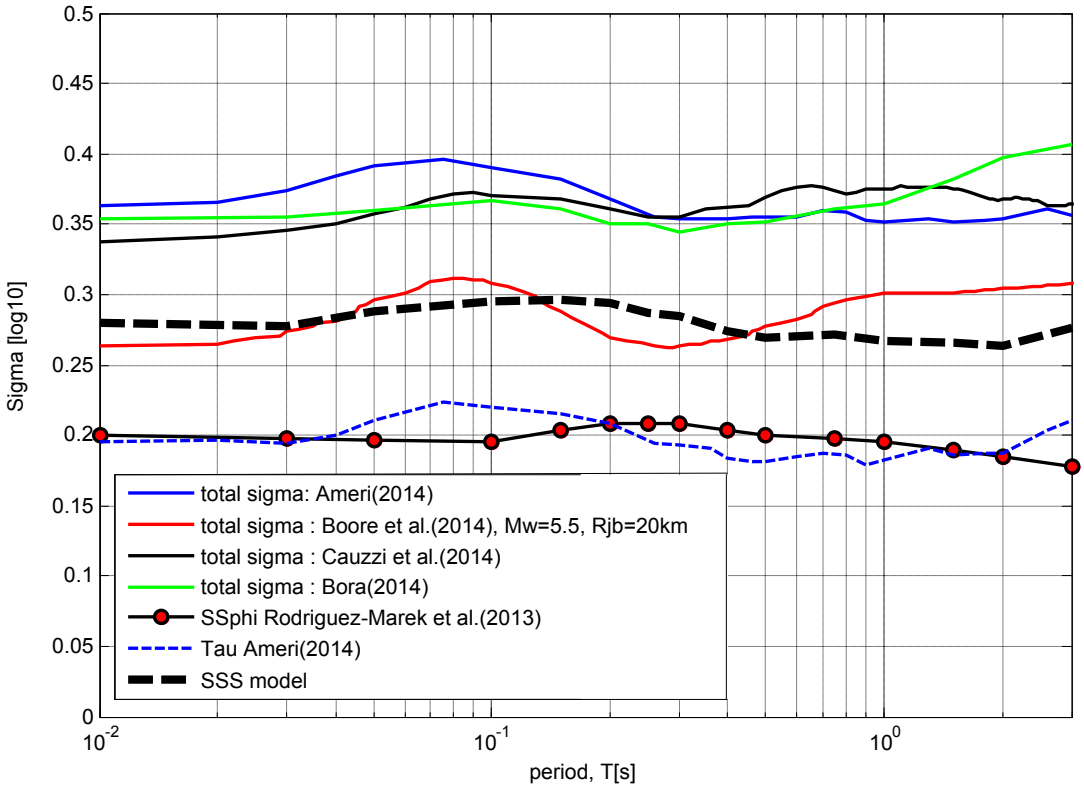

Figure 50 : Standard deviation (sigma) models as a function of spectral period used in this study. The single-station sigma (SSS) model is showed by the dashed black line.

9.1 RESULTS FOR GRENOBLE SITE

The results of the test are presented for the Grenoble site, which is characterized by highest seismic hazard among the three sites. We performed two different PSHA calculations:

- C1: using the sigma values of each selected GMPE;
- C2: using the SSS model as described in the previous section.

The obtained mean UHS for 10'000 years and 30'000 years return periods are presented in (Figure 51). In order to quantify the reduction of spectral accelerations obtained when using the SSS model we report in Table 7 the mean UHS obtained for C1 and C2 and their ratio. The use of SSS model leads to a reduction of the hazard estimates of about 20 to 30 % depending of the spectral frequency and return period considered. As expected, the differences increase with the return period.

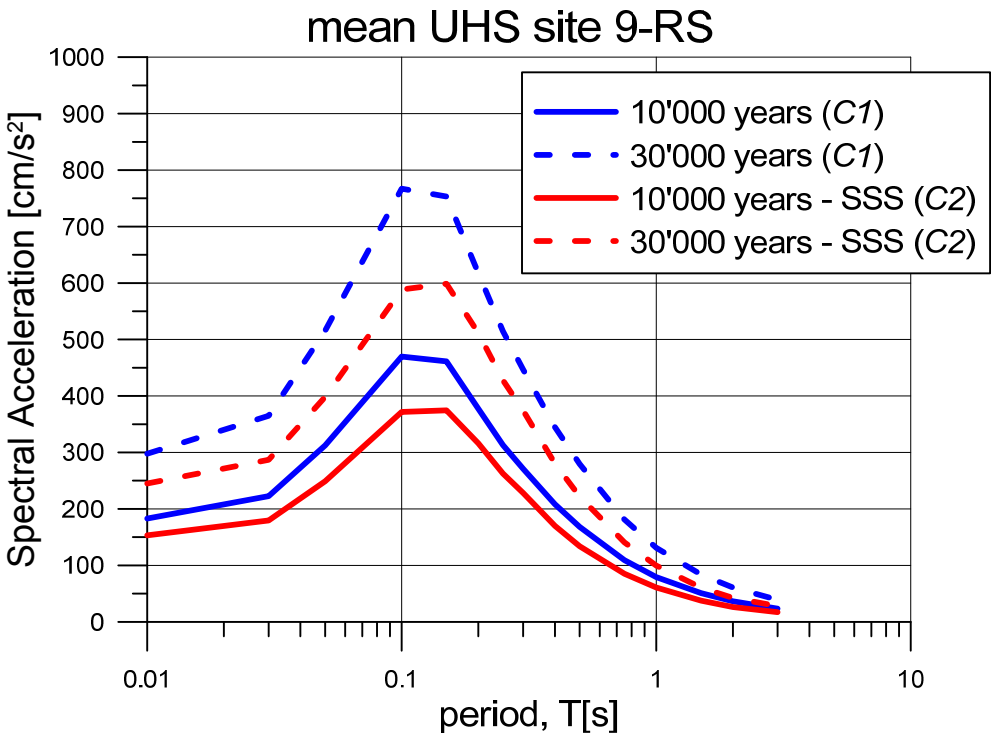

Figure 51 : Mean Uniform Hazard Spectra (UHS) for case 9-RS with a Vs30=800 m/s. UHS obtained from PSHA calculations C1 and C2 are presented for 10'000 years and 30'000 years return periods (continuous and dashed lines, respectively).

	C1 – UHS [cm/s^2]		C2 – UHS [cm/s^2]		Ratio C2/C1	
T[s]	10000 yrs	30000 yrs	10000 yrs	30000 yrs	10000 yrs	30000 yrs
0.01	183.09	297.74	153.34	244.91	0.838	0.823
0.03	222.65	365.03	179.68	286.93	0.807	0.786
0.05	312.53	515.81	249.06	398.50	0.797	0.773
0.1	469.69	767.13	371.75	588.64	0.791	0.767
0.15	461.19	753.29	374.60	598.67	0.812	0.795
0.2	377.37	617.55	316.07	511.35	0.838	0.828
0.25	313.17	514.51	262.67	427.99	0.839	0.832
0.3	271.04	446.89	228.43	374.35	0.843	0.838
0.4	208.29	344.88	169.79	280.05	0.815	0.812
0.5	168.26	279.72	134.00	221.94	0.796	0.793
0.75	109.14	181.35	85.06	140.71	0.779	0.776
1	79.25	131.16	60.66	99.54	0.765	0.759
1.5	50.78	83.73	37.48	60.54	0.738	0.723
2	36.43	60.66	26.23	42.35	0.720	0.698
3	23.26	38.95	17.27	27.81	0.743	0.714

Table 7 : Values of mean Uniform Hazard Spectra (UHS) for calculations C1 and C2 and spectral ratios (C2/C1) presented for 10'000 years and 30'000 years return periods

10. MAIN CONCLUSIONS AND RECOMMENDATIONS

This report presents the intermediate results of the sensitivity analysis on the SIGMA PSHA model. We exploited the 2012 SIGMA PSHA model in terms of sensitivity to different elements of the model: the earthquake catalogues, the seismotectonic models and the ground motion prediction equations (GMPEs). We tested the effect of several alternative hypotheses concerning the calculation of activity rates and their uncertainties, the assessment of the Mmax distributions, the aleatory variability of earthquakes depth, the consideration of the smoothed seismicity approach. The sensitivity of the mean hazard to the alternative models was assessed, as well as the contribution of the uncertainties within each element to the total hazard uncertainties. A deaggregation analysis was performed in order to identify the sources that contribute the most to the seismic hazard (i.e., whose uncertainties contribute most to the total hazard uncertainties). Finally, several recent GMPEs have been tested as alternatives to the set of GMPEs used in the initial model, and their impact on the seismic hazard at the considered sites is investigated.

The main conclusions that we draw from the sensitivity analysis concerning the 2012 model are:

- The uncertainties in the total hazard based on the initial SIGMA PSHA model increase with increasing return periods. The uncertainties for the Grenoble and Valence sites are comparable, whereas they are larger for Marseille;
- The mean hazard uncertainty for the initial SIGMA PSHA is controlled by Source Model and GMPE. The use of the alternative synthetic catalogue has a negligible impact on the mean hazard;
- The uncertainty within GMPE are similar over the different GMPEs considered in the logic tree. The same holds for the earthquake catalogues considered in 2012;
- The uncertainty within seismotectonic model is different for the three alternative models. In particular, it is larger for SM1 and SM2 and smaller for SM3 that is characterized by very large areal source zones. This is related to the uncertainties in the MFDs that are larger for zones with a small number of earthquakes (such as many zones in SM1 and SM2) and smaller in zones with a large number of earthquakes. The analyses we performed showed that a specific work on uncertainty estimation related to GR and their propagation through the logic tree is needed for future studies. A better characterization of uncertainties in the historical earthquake catalogue, possibly considering the specificity of each relevant event, is definitely worth pursuing.

Beside the analysis on the 2012 model, we tested a number of alternative hypotheses that are intended to represent plausible alternatives supported by the technical community. In Figure 52 and Figure 53, we attempt to summarize the tests we have shown in this study by comparing the effects of the different hypotheses on the mean hazard for 475 and 10, 000 years return periods and two spectral periods (PGA and T=1s).

The main conclusions from the sensitivity analysis of alternative hypotheses with respect to the 2012 PSHA are:

- The use of the Si-Hex catalogue to replace the instrumental part of the SIGMA 2012 catalogue has a minor impact on the hazards at the three sites;
- The use of alternative methods to estimate the GR parameters show a significant impact on the hazard. However, this effect is apparent as the minimum magnitude of the fit and the magnitude step are fixed to the reference values in the 2012 study. For the future we recommend to investigate each fitting method by using a range of minimum magnitudes, magnitude steps and completeness periods in order to compared the

results by each of the fitting methods in terms of mean values and standard deviations of each of the GR parameters.

- The tests on the different aleatory distributions of earthquake depths (either magnitude-dependent or not) showed a minor impact on the mean hazard

- The impact of the adopted Mmax distribution is a function of return period and spectral period. At 475 year return periods the impact is minor for PGA but become important (of the same order of GMPEs) for long spectral periods. At 10 000 years return period the impact is moderate for PGA and large for long spectral period (larger than the impact of the choice of the GMPEs). In terms of contribution to the hazard uncertainties, the uncertainties due to the Mmax distribution are directly related to the range of Mmax obtained by the different methods. In any case, the contribution of Mmax seems lower than that due to GR uncertainties.

- The smoothed seismicity approach shows a moderate impact on the mean hazard at short spectral periods and a large impact at long spectral periods. This is largely because in the classical Woo (1996) approach the Mmax is limited to the maximum observed magnitude in the catalogue which is significantly lower than the Mmax considered in the zoning approach. This is clearly visible for Grenoble site where the influence of large distant earthquakes (affecting the long spectral periods) is drastically reduced in the smoothed seismicity approach. Moreover, for Valence and Marseille sites the impact of the choice of the kernel function is large. These results suggest that the method applied in this study should be improved by account for Mmax larger than the observed one and by selecting kernel functions in an adaptive way based on seismicity density in the area of each grid point.

- The new proposed set of GMPEs show approximately the same influence on the mean hazard uncertainties as those selected in the 2012 PSHA. However, the new set clearly shows a decrease of the hazard levels at short return periods. At long return periods, the results are consistent with those obtained by the 2012 GMPEs.

- In order to test the impact of the aleatory variability (sigma) model of the GMPEs a test on the application of the single-station sigma approach is performed. Because a native empirical single-station sigma model is not available for the three considered sites we used the model by Rodriguez-marek et al., (2013) based on a data set from multiple countries. The test shows that the reduction of spectral acceleration and 10’000 and 30’000 years return period with respect to the standard (full sigma) approach is of the order of 20%-30%. We recall that, in the current practice of site-specific PSHA, the single-station sigma approach can only be applied if the site response is considered in details in the hazard calculations.

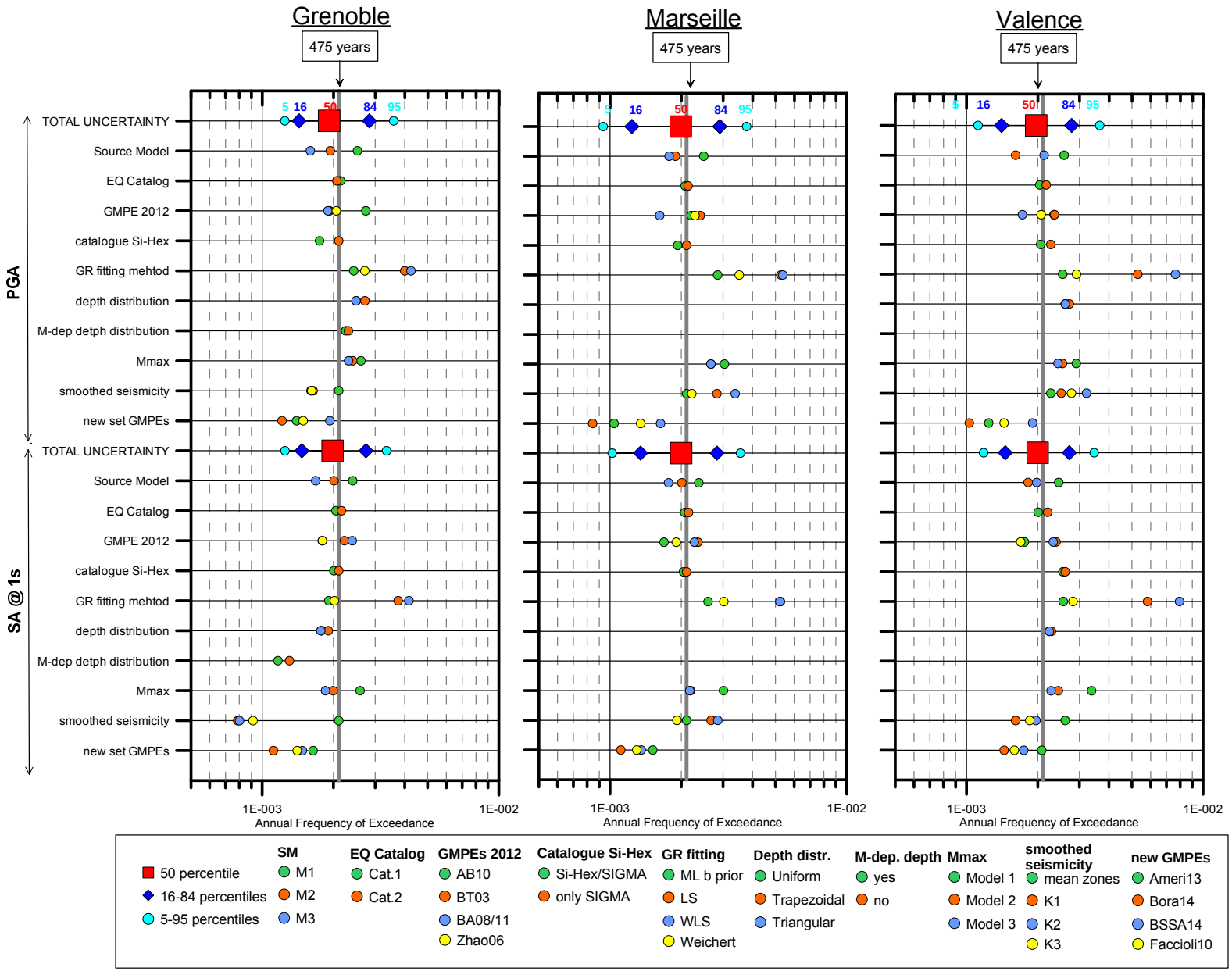

Figure 52 : Tornado diagrams at 475 years return period for the three sites showing the sensitivity of mean hazard to the elements tested in this study for two spectral periods (PGA and 1s).

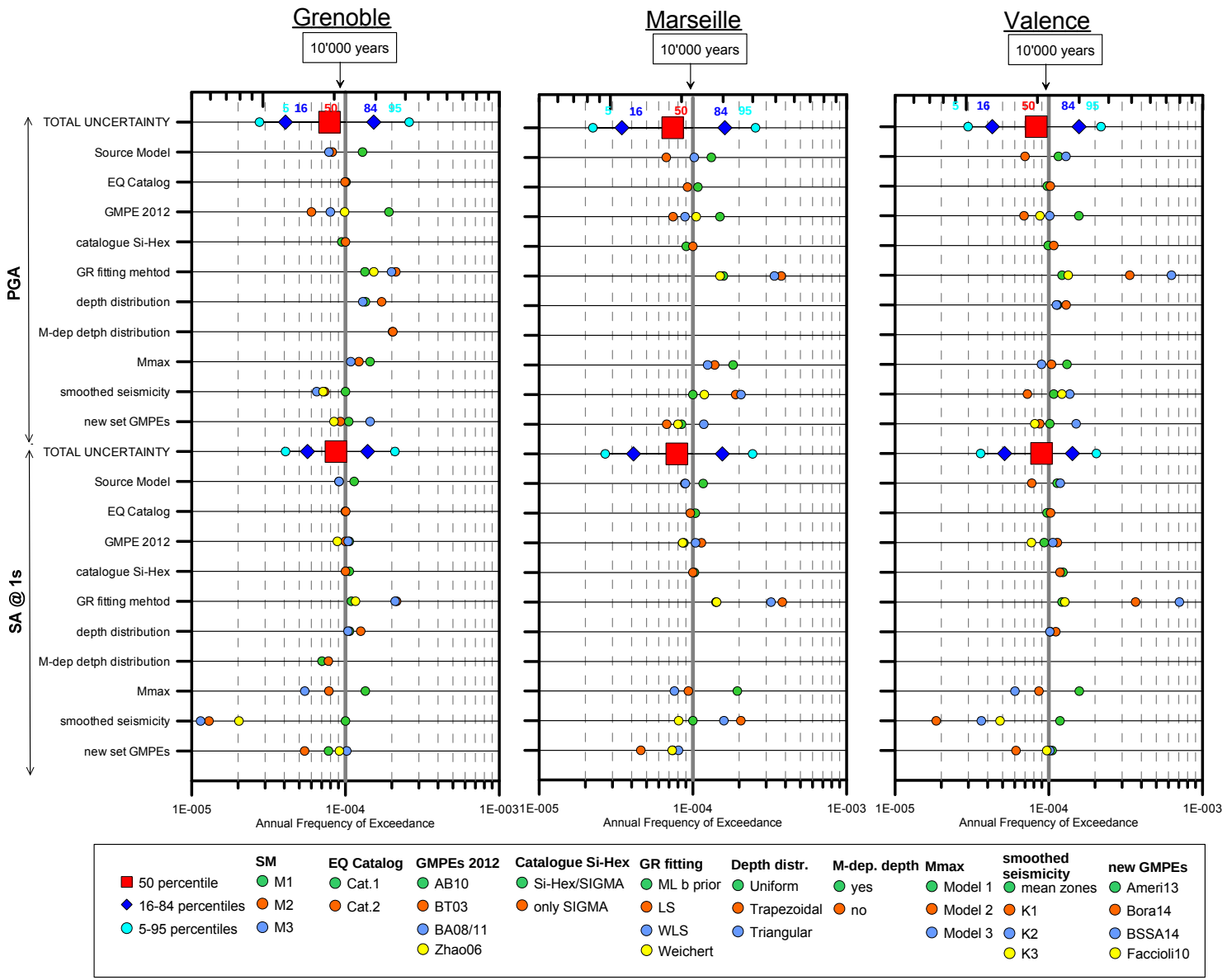

Figure 53 : Tornado diagrams at 10, 000 years return period for the three sites showing the sensitivity of mean hazard to the elements tested in this study for two spectral periods (PGA and 1s).

11. REFERENCES

ABRAHAMSON N. AND SILVA W. (2008). Summary of the Abrahamson and Silva NGA ground-motion relations. Earthquake Spectra, Vol. 24, n° 1, p. 67-97.

ABRAHAMSON N. , W. J. SILVA, AND R. KAMAI (2014). Summary of the ASK14 Ground-Motion Relation for Active Crustal Regions. Earthquake Spectra, (in press).

AKKAR S., M.A. SANDIKKAYA, AND J.J. BOMMER (2014). Empirical Ground-Motion Models for Point- and Extended-Source Crustal Earthquake Scenarios in Europe and the Middle East. Bulletin of Earthquake Engineering, 12, 1, pp 359-387

AKKAR, S. AND BOMMER, J.J. (2010). "Empirical equations for the prediction of pga, pgv and spectral accelerations in europe, the mediterranean region and the middle east," seismological research letters, 81, 2, 195-206.

ANDERSON, J. G., AND S. E. HOUGH (1984). A model for the shape of the fourier amplitude spectrum of acceleration at high frequencies, Bull. Seismol. Soc. Am. 74, 1969–1993.

ATKINSON, G & BOORE, D (2006). Earthquake Ground-Motion Prediction Equations for Eastern North America. Bulletin of the Seismological Society of America, Vol. 96, No. 6, pp. 2181–2205, December 2006.

ATKINSON, G.M., and BOORE, D.M. (2011). Modifications to existing ground-motion prediction equations in light of new data, *Bulletin of the Seismological Society of America,* 101, 1121-1135.

BEAUVAL, C., H. TASAN, A. LAURENDEAU, E. DELAVAUD, F. COTTON, Ph. GUEGUEN and N. KUEHN (2012), On testing ground-motion prediction equations against small magnitude data. Bulletin of the Seismological Society of America, Vol. 102, n° 5, p. 1994-12007, October 2012.

BERGE-THIERRY C., CUSHING E., SCOTTI O. AND BONILLA F. (2004). Determination of the Seismic Input in France for the Nuclear Power Plants Safety: regulatory context, hypothesis and uncertainties treatment. Proceedings of the CSNI Workshop on seismic input motions, incorporating recent geological studies, Tsukuba, Japan 15-17 November 2004.

BEYER, K., AND J. J. BOMMER (2006). Relationships between median values and aleatory variabilities for different definitions of the horizontal component of motion. Bulletin of the Seismological Society of America 94 (4A), 1,512–1,522,

BINDI D., MASSA M., LUZI L., AMERI G., PACOR F.,PUGLIA R. AND P. AUGLIERA (2014) Pan-European Ground-Motion Prediction Equations for the Average Horizontal Component of PGA, PGV, and 5%-Damped PSA at Spectral Periods up to 3.0 s using the RESORCE dataset. *Bulletin of Earthquake Engineering*, 12, 1, pp 391-430

BOMMER J.J., DOUGLAS J., SCHERBAUM F., COTTON F., BUNGUM H. and FAH D. (2010). On the selection of ground-motion prediction equations for seismic hazard analysis. Seismological Research Letters, Vol. 81, n° 5, p. 783-793.

BOMMER, J.J., AKKAR, S. and DROUET, S. (2012), Extending ground-motion prediction equations for spectral accelerations to higher response frequencies, Bull. Earth. Eng., 10, 379-399.

BOORE D.M. and ATKINSON G.M. (2008). Ground-motion prediction equations for the average horizontal component of PGA, PGV, and 5%-damped PSA at spectral periods between 0.01 and 10s. *Earthquake Spectra, Vol. 24, n° 1, p. 67-97*.

BOMMER, J. J., K. J. COPPERSMITH, R. T. COPPERSMITH, K. L. HANSON, A. MANGONGOLO, J. NEVELING, E. M. RATHJE, A. RODRIGUEZ-MAREK, F. SCHERBAUM, R. SHELEMBE, P. J. STAFFORD, AND F. O. STRASSER (2014). A SSHAC level 3 probabilistic seismic hazard analysis for a new-build nuclear site in South Africa, Earthq. Spectra doi: 10.1193/060913EQS145M (in press).

BOORE, D.M., J.P. STEWART, E. SEYHAN, AND G.M. ATKINSON (2014). NGA-West 2 equations for predicting PGA, PGV, and 5%-damped PSA for shallow crustal earthquakes, Earthquake Spectra, (in press).

CAUZZI C. & FACCIOLI E. (2008). Broadband (0.05 to 20 s) prediction of displacement response spectra based on worldwide digital records. Journal of Seismology, Vol. 12, n° 4, p. 453-475

CAUZZI C., FACCIOLI E., VANINI M. et BIANCHINI A. (2014). Updated predictive equations for broadband (0.01 to 10 s) horizontal response spectra and peak ground motions, based on a global dataset of digital acceleration records. Bulletin of Earthquake Engineering, 13(6).

DERRAS, B., BARD P.Y., AND F. COTTON (2014) Towards fully data driven ground-motion prediction models for Europe*. Bull. Earthquake Eng.*, 12:495–516

DROUET S., COTTON, F,. AND GUÉGUEN P. (2010). VS30, kappa, regional attenuation and Mw from accelerograms: application to magnitude 3–5 French earthquakes. *Geophysical Journal International* 182(2), 880–898.

DOUGLAS J., S. AKKAR, G. AMERI, P-Y. BARD, D. BINDI, J. J. BOMMER, S. S. BORA, F. COTTON, B. DERRAS, M. HERMKES, N. M. KUEHN, L. LUZI, M. MASSA, F. PACOR, C. RIGGELSEN, M. A. SANDIKKAYA, F. SCHERBAUM, P. J. STAFFORD AND P. TRAVERSA (2014) Comparisons among the five ground-motion models developed using RESORCE for the prediction of response spectral accelerations due to earthquakes in Europe and the Middle East, *Bulletin of Earthquake Engineering* 12, 1, pp 341-358.

EFRON, B., 1979. Bootstrap methods, another look at the jacknife, *Ann. Stat.* 7, 1–26.

FACCIOLI E, BIANCHINI A, VILLANI M (2010) New ground motion prediction equations for t > 1 s and their influence on seismic hazard assessment. In: Proceedings of the University of Tokyo Symposium on Long- Period Ground Motion and Urban Disaster Mitigation, March 17–18, Tokyo, Japan

RODRIGUEZ-MAREK A., F. COTTON, N. A. ABRAHAMSON, S. AKKAR, L. AL ATIK, B. EDWARDS, G. A. MONTALVA, AND H. M. DAWOOD (2013) A Model for Single-Station Standard Deviation Using Data from Various Tectonic Regions, Bulletin of the Seismological Society of America, Vol. 103, No. 6, pp. –, December 2013, doi: 10.1785/0120130030

RODRIGUEZ-MAREK, A., RATHJE, E.M., STAFFORD, P.J., SCHERBAUM, F., AND BOMMER, J.J., 2014. Application of single-station sigma and site response analyses in a probabilistic seismic hazard analysis for a new nuclear site, Bulletin of the Seismological Society of America, 104:1601-1619.

WHEELER, R.L. (2009), Methods of Mmax Estimation East of the Rocky Mountains, U.S. Geological Survey Open-File Report 2009–1018, 44 p.

ZHAO J.X., ZHANG J., ASANO A., OHNO Y., OOUCHI T., TAKAHASHI T., OGAWA H., IRIKURA K., THIO H.K., SOMERVILLE P.G., FUKUSHIMA Y. AND FUKUSHIMA Y. (2006). Attenuation relations of strong ground motion in japan using site classification based on predominant period. Bulletin *of the Seismological Society of America*, vol. 96, n° 3, p. 898-913.

WOESSNER J. , GIARDINI, D. AND THE SHARE CONSORTIUM (2012), Seismic Hazard Estimates for the Euro-Mediterranean Region: A community-based Probabilistic Seismic Hazard Assessment, in proceeding of the 15th World Conference on Earthquake Engineering , Lisbon.